+

Republic of Iraq

Ministry of Higher Education & Scientific Research

University of Kerbala

College of Engineering

Civil Engineering Department

Behavior of Steel Column of Sandwich Cross Section with Opening Under Concentric Loading

A Thesis Submitted to the Council of the Faculty of the College of the Engineering/University of Kerbala in Partial Fulfillment of the Requirements for the Master Degree in Civil/Infrastructure Engineering

Written By:

Layth Ghanem Mahdi

Supervised By:

Prof. Dr. Sadjad Amir Hemzah

February 2022   Rajab 1444

Republic of Iraq

Ministry of Higher Education & Scientific Research

University of Kerbala

College of Engineering

Civil Engineering Department

Behavior of Steel Column of Sandwich Cross Section with Opening Under Concentric Loading

A Thesis Submitted to the Council of the Faculty of the College of the Engineering/University of Kerbala in Partial Fulfillment of the Requirements for the Master Degree in Civil/Infrastructure Engineering

Written By:

Layth Ghanem Mahdi

Supervised By:

Prof. Dr. Sadjad Amir Hemzah

February 2022   Rajab 1444

بسم الله الرحمن الرحيم

يَرْفَعِ اللَّهُ الَّذِينَ آمَنُوا مِنكُمْ وَالَّذِينَ أُوتُوا
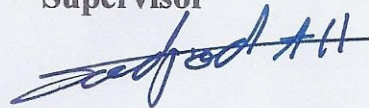الْعِلْمَ دَرَجَاتٍ

صدق الله العلي العظيم

(المجادلة: من الآية ١١)

Examination committee certification

We certify that we have read the thesis entitled "**Behavior of Steel Column of Sandwich Cross Section with Opening Under Concentric Loading** " and as an examining committee, we examined the student "ayth Ghanem Mahdi" in its content and in what is connected with it and that in our opinion it is adequate as a thesis for the degree of Master of Science in Civil Engineering.
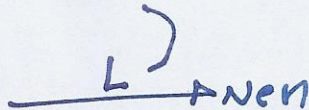
Supervisor

Signature:

Name :. Prof.Dr. Sadjad Amir Hemzah

Date: /   / 2022
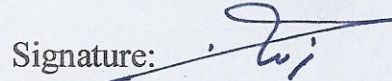
Member

Signature:

Name :. Assist Prof.Dr. Luay M.Abass Al-Shather
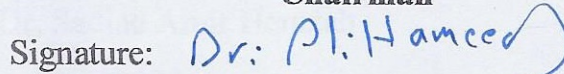
Date: /   / 2022

Member

Signature:

Name :.   Assist Prof.Dr.

Zainab Muhammad Ridha Abdul Rasoul

Date: /   / 2022

Chairman

Signature: Dr: Pl:Hameed

Name :. Prof.Dr. Ali Hameed Naser Al-Mamoori

Date: /   / 2022

Signature:

Name : Prof.Dr. Sadjad Amir Hemzah

Head of the Department of Civil Engineering

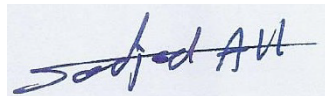Date: /   / 2022

Signature:

Name :Prof.Dr.Laith Sh. Rasheed

Dean of the Engineering College

Date: /   / 2022

Supervisor certificate

I certify that the thesis entitled "**Behavior of Steel Column of Sandwich Cross Section with Opening Under Concentric Loading**" was prepared by "Layth Ghanem Mahdi" under our supervision at the Department of Civil Engineering, Faculty of Engineering, the University of Kerbala as a partial of fulfilment of the requirements for the Degree of Master of Science in Civil Engineering.

Signature:

Prof.Dr. Sadjad Amir Hemzah

 Date: /   / 2022

Linguistic certificate

I certify that the thesis entitled "**Behavior of Steel Column of Sandwich Cross Section with Opening Under Concentric Loading**" which has been submitted by "Layth Ghanem Mahdi" has been proofread and its language has been amended to meet the English style.

Signature:

Dr Muhammad Abdulredha

Date: /   / 2022

Undertaking

I certify that research work titled "**Behavior of Steel Column of Sandwich Cross Section with Opening Under Concentric Loading**" is my own work. The work has not been presented elsewhere for assessment. Where material has been used from other sources it has been properly acknowledged / referred.

Signature:

Layth Ghanem Mahdi

Date: /   / 2022

Dedication

To the dearest of people and the closest to my heart … My precious father and mother, who were my help and support for me and their prayers had the greatest effect on the journey of the research ship until it anchored in this picture,

To my beloved spouse was the most important person in my life, who supported me and walked with me through the tough times.

To my daughter, Jomana, and my son Mostafa have been a source of joy and encouragement.

Signature:

Layth Ghanem Mahdi

Date: /   / 2022

Acknowledgements

In the name of ALLAH, the most compassionate, the most merciful.

First, all thanks to **Almighty Allah,** who enabled me to achieve this work.

I would also like to express my sincere gratitude toto my supervisors: **Prof.Dr. Sadjad Amir Hemzah** for his valuable assistance and guidance throughout the research.

Great thanks are also to the **dean**, **head** and **staff** of the Civil Engineering Department- Infrastructure / College of the Engineering / University of Kerbala and the Kufa University for their assistance throughout this study.

Signature:

Layth Ghanem Mahdi

Date: 25 / 6 / 2022

Abstract

The development in the science of construction and the increase in the height of the buildings showed the need for structural members with higher bearing capacity with less dimensions. Concrete-filled double steel tubular columns (CFDST) are an example of this development in the past twenty years.

CFDST columns have many advantages, such as high bearing capacity (more elevated than those of reinforced concrete columns (RCC) as well as higher fire resistance),in this research, the following factors were taken into consideration: the type of concrete used in this type of column, normal concrete (NC) or plastic fiber concrete (PFC), the number of openings in one model, and whether these openings are from one side or two opposite sides. The researchers made (14) models, (seven) filled models with normal concrete and (seven) with plastic fiber concrete and compared the experimental results of (14) models with the results of similar finite element models obtained from the Abaqus software for accuracy.   Columns models were tested using a central load, and the axial load was applied incrementally. The fourteen test samples were examined with different variables in the parametric study. The properties of normal concrete and plastic fiber concrete are necessary for the numerical analysis to provide working conditions similar to the laboratories.

Using PFC instead of NC resulted in a 17.80 percent increase in the column's bearing capacity compared to NC, and the larger the number of opneings on one side, the lower the column's bearing capacity, with a ratio ranging from 14.03 % to 19.23 %. Moreover, making opneings through opposite sides weakens the columns by 14.81% - 28.00%. When using the specified elements, the results were less than those in the experimental study,

I

where the percentage ranged in the normal concrete models from 0-12.22%, while in the plastic fiber concrete 1.29%-10.52%.

The rate of difference between the results of laboratory models and numerical models in normal concrete was (-7.40), while in concrete models made of plastic fibers the rate was (-5.73) and therefore there was convergence between the two studies, so it is possible to rely on finite elements to form more complex models.

Table of Contents

III

IV

List of Tables

List of Figures

VIII

List of Abbreviations

CFST	Concrete filled steel tube
CFDST	Concrete filled double skin tube
CFMST	concrete-filled multi-skin tube
NC	Normal concrete
PFC	Plastic fiber concrete
HSC	High-strength concrete
ABAQUS	Finite element package
ANSYS	Finite element package
ACI	American concrete institute
ASTM	American society for testing and materials
BS	British standard
CHS	Circular hollow section
SHS	Square hollow section
et al.	Others
CFRP	Carbon fiber reinforcement polymer
FEA	Finite element analysis
MPa	Mega Pascal (N/mm^2)
No.	Number
mm	Millimetre
ECC	Engineered cementitious composite
RC	Reinforced concrete

RCC	Reinforced concrete column
CDP	Concrete damaged plasticity

List of Symbols

Ag	The cross-sectional area of a section (mm^2)
Ac	The cross-sectional area of the concrete (mm^2)
As	The cross-sectional area of steel reinforcement (mm^2)
E_c	Concrete modulus of elasticity (GPa)
E_s	Steel modulus of elasticity (GPa)
f_{cu}	Concrete compressive strength (MPa)
f_y	Yield strength of steel reinforcement (MPa)
f_{sy}	Strength of steel reinforcement (MPa)
f_{su}	The ultimate strength of steel reinforcement(MPa)
f_{st}	Splitting tensile strength of concrete(MPa)
W	The total length of column (mm)
B	Total width of column (mm)
db	Dimeter of steel reinforcement
t	Tube thickness
P	Maximum applied load (kN)
P_u	Ultimate load (kN)
ϕ	Size of bar diameter (mm)

Chapter One: Introduction

Chapter One

Introduction

1.1 Background

Concrete-filled double steel tubular columns (CFDST) are becoming increasingly popular construction applications. This type of columns can offer many advantages, such as high strength, improved ductility, high load-carrying capacity, and a high construction speed . Moreover, the possibility of producing concrete grades with higher compressive strength today allows for leaner column design resulting in a larger floor area**(Yang et al., 2021)**.

1.2 Ingredients

The concrete-filled steel tubular columns (CFST) consist of a single hollow steel tube, and this cavity is filled with concrete **(X.-F. Yan et al., 2021).** There are several types of it:

A) Concrete-encased CFST.

B) CFST with additional reinforcement

C) Stiffened CFST.

This is shown in Figure (1-1).

(a) Concrete-encased CFST

(b) CFST with additional reinforcement

(c) Stiffened CFST
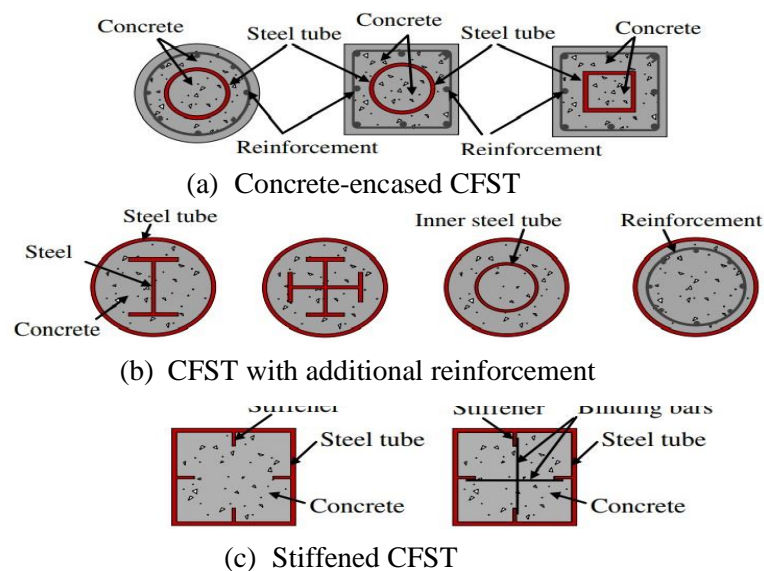
*Figure 1-1: CFST types (*Yang et al., 2021*)*

1

CFDST columns are an upgraded type of CFST, consisting of two concentric steel tubes separated by a concrete filler and the inner tube is hollow, while the previous type CFST was a single tube filled with concrete without any cavity **(Ipek & Güneyisi, 2019).**

Figure (1-2) shows the most commonly used types of CFDST columns.
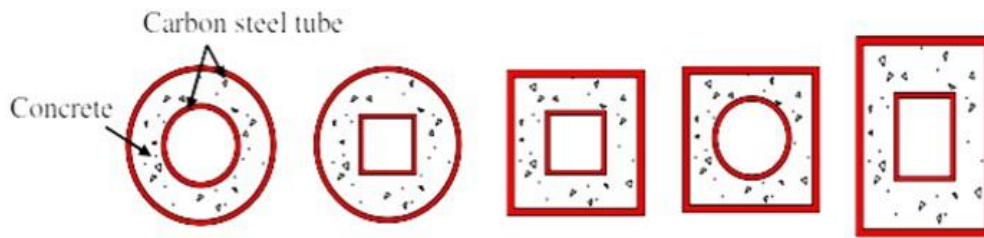
*Figure 1-2: Typical CFDST cross-sections (*Han et al., 2014*)*

In both types, the thickness of the steel pipes is less than 40 mm **(Zhang et al., 2020)** , which facilitates the process of manufacturing, transporting and installing this type of columns. The pipes are made of carbon iron or stainless steel (in special cases due to their high cost).

1.3 Advantages and disadvantages

1.3.1 Concrete-filled steel tubular Columns (CFST)

1-The CFST column, a composite element consisting of a steel tube and a concrete core, works together like a well homogeneous mass.

2-The steel tube fulfils two primary purposes: longitudinal reinforcement and transverse reinforcement. Therefore, it bears all the forces that affect it in different directions (perpendicular or parallel to its longitudinal axis) as well as in inclined directions at different angles concerning its longitudinal axis because the reinforcement is considered uniform over the entire length of the element, which helps in its stability**(Zhang et al., 2022)**.

3- The strength of the concrete core increases approximately twice because the mineral casing surrounds it, as the concrete is subjected to triaxial stresses.

4- Concrete deformations within the tube resulting from shrinkage and flow are much less than it is because the concrete core is not exposed to the effects of the surrounding medium (heat, moisture, toxic gases...) because the metal shell forms an insulating layer for the core and secures good conditions for concrete work under the influence of loads, and it prevents cracks from appearing.

5- At the same time, the steel pipe filled with concrete shows very high resistance against collapse in case of loss of the overall or local stability of the structure **(Ipek & Guneyisi, 2021)**.

6- Filling the steel pipe with concrete increases its resistance against rust on the one hand and, on the other hand, reduces the thinness of the element, which leads to an increase in the durability of the pipe wall and thus increases its resistance **(Xiong et al., 2017).**

1.3.2 Concrete-filled double skin steel tubular columns (CFDST)

1- The CFDST column, also a composite element, consists of two concentric steel tubes, and the space between them is filled with concrete. These materials work together as a homogeneous mass well**(Ouyang & Kwan, 2018b)**.

2- CFDST columns optimally combine the advantages of CFST concrete-filled steel tubular shown in Figure (1-3) and sandwich shape resulting in:

- Higher flexural rigidity.
- Enhanced stability under external stress.
- Improved damping properties.
- Improved performance.
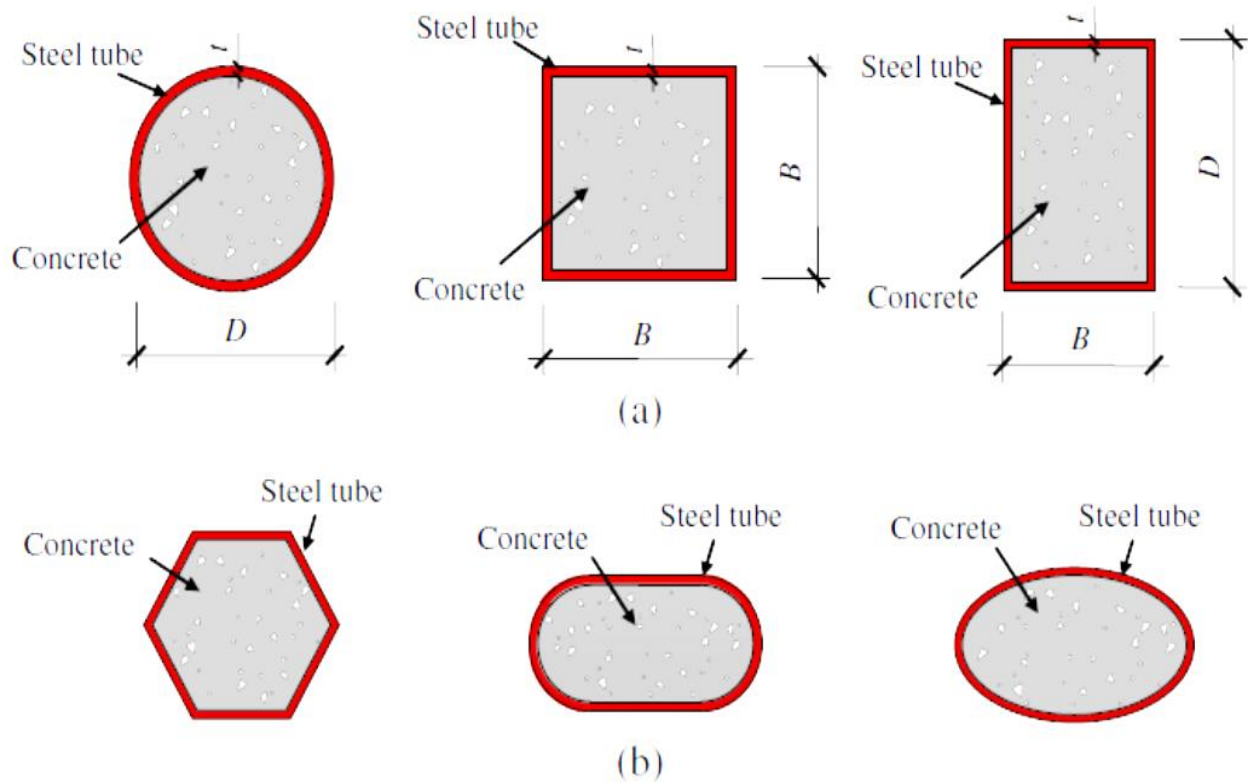
*Figure 1-3: Typical CFST cross-sections (*Ibanez et al., 2021*)*

It can also effectively delay or prevent the buckling of domestic steel pipes in several ways, which improves their efficiency and ability to bear additional loads. As rebar in concrete, steel tubes link to the concrete in an interconnected manner. As a result of this interconnection, the probability of column failure due to a single material failure is reduced, and column failure becomes dependent on the failure of 3 layers together, which saves time or gives an alert to address the problem **(Z.-B. Wang et al., 2017)**.

CFDST members are more economical compared to conventional reinforced concrete (RC) in terms of speed in construction, in addition to the absence of the need for a mold because the tubes work as a mold, saving a lot of time and money **(Li et al., 2014)**.

CFDST columns require a smaller cross-sectional area compared to RC columns (and for the same load), which saves space in the building as well as the lower weight of the structure and, therefore, the lower thickness of the foundations and greater economic feasibility presence of concrete between two layers of steel, one internal and the other external, increases the life of the concrete and reduces the need for its maintenance **(Farajpourbonab, 2017).**

1.4 Applications

The uses of CFST members are not new. They have been in use in China for more than 50 years, as they were used as carrier columns in the Beijing subway station, built-in 1966, and in the buildings of electric power stations **(Han, Ma, et al., 2018).**

The seventies of the last century witnessed a great development in the uses of these members. They were used as the main bearing members in buildings, bridges and other facilities due to their high bearing capacity and ability to withstand various conditions. Figures (1-4) and (1-5) illustrate the use of CFST in transmission towers of electric **(Alhalaby & Wang, 2017).**
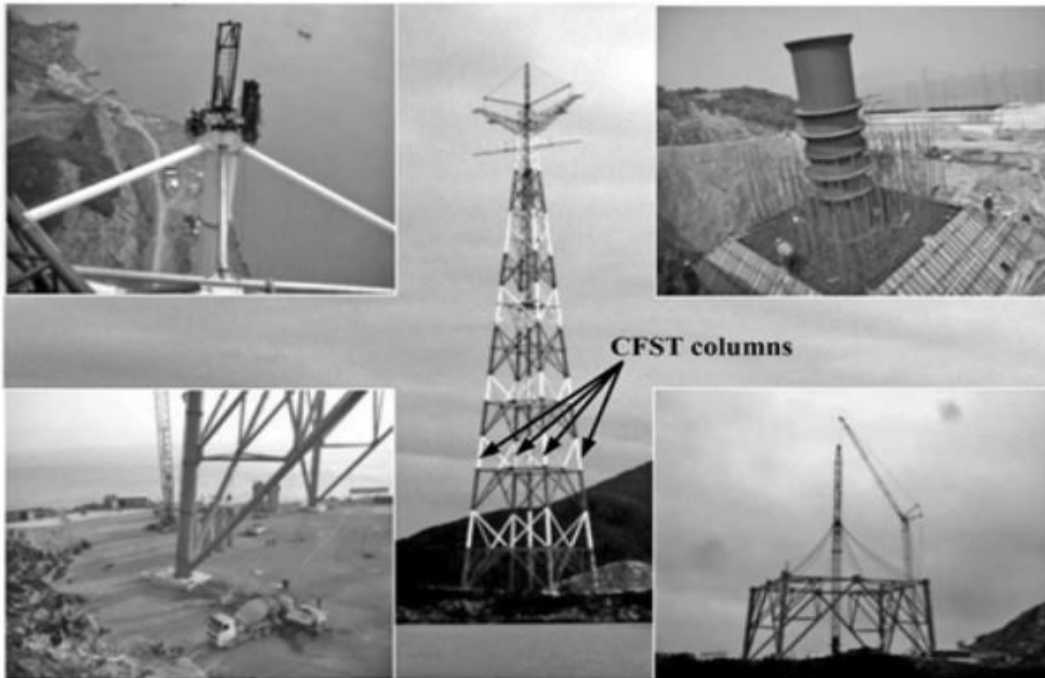
*Figure 1-4: An electrical transmission tower in Zhoushan, China (*Ou, 2013*)*

*Figure 1-5: Shows the use of CFST in the construction of tall buildings in China (*Han, Lam, et al., 2018*)*

Figures (1-6) and (1-7) illustrate the use of CFST in constructing bridges in China.
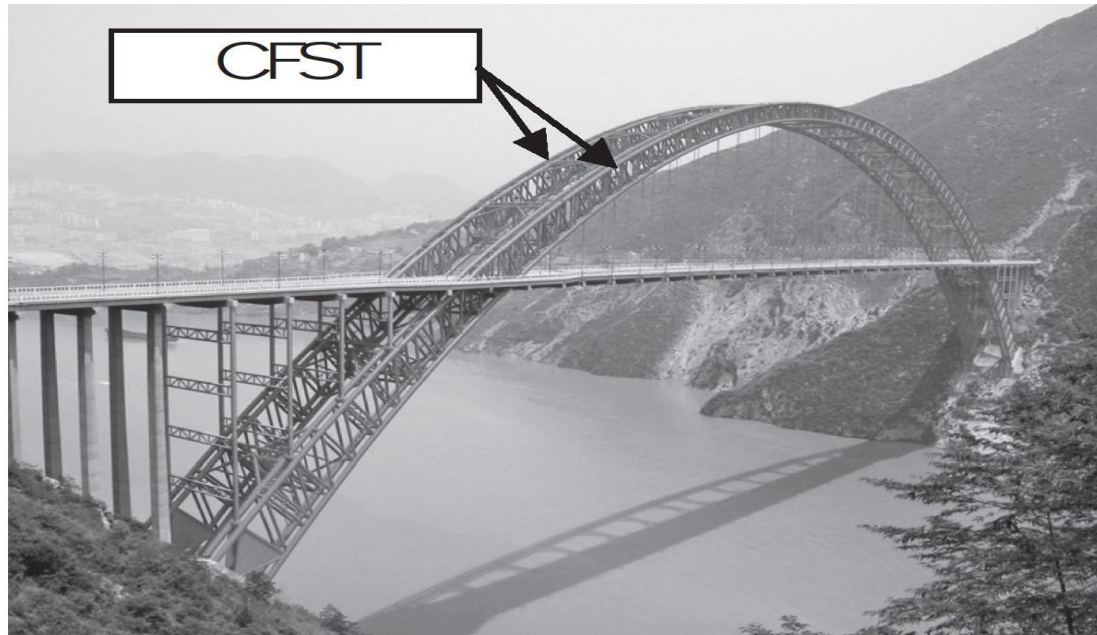
Figure 1-6: Wuhan Yangtze River Bridge, Chongqing, China(Han, Lam, et al., 2018*).*
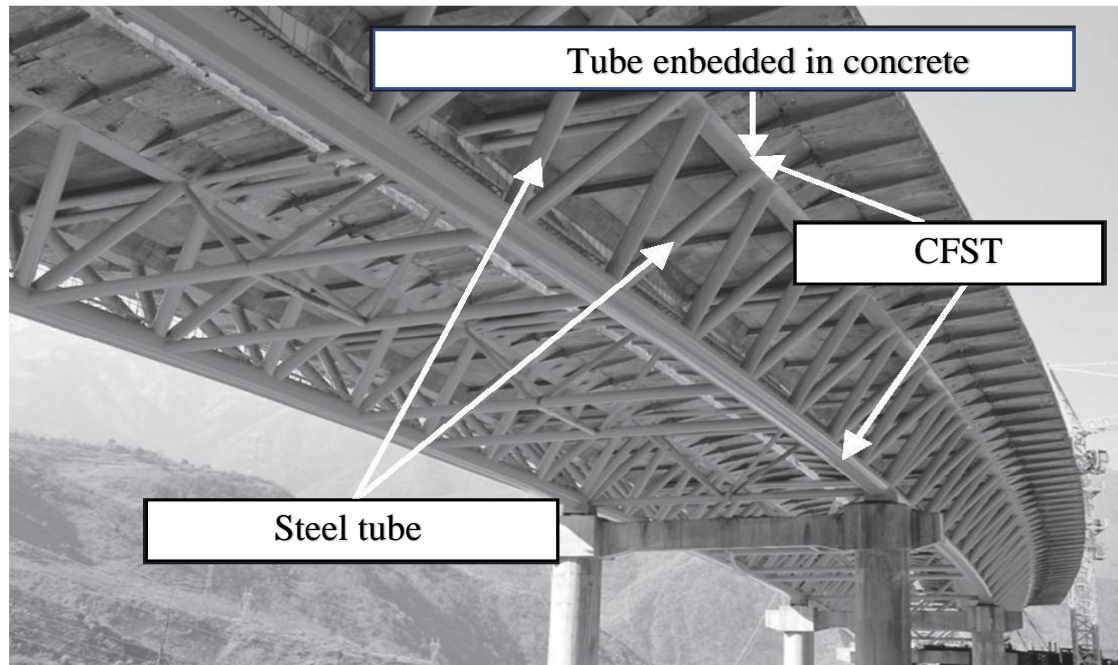
*Figure 1-7: Ganhaizi Bridge, Yaan, Sichuan Province, China (***Qian et al., 2016***)*

In Europe, CFST members have been widely used in new urban housing projects, as shown in Figures (1-8) and (1-9).

*Figure 1-8: Fleet Plate House, London, UK (*Kalemi, 2016*)*

*Figure 1-9: The campsite column used in Fleet Plate House, London, UK (*Kalemi, 2016*)*

The use of CFST members in the United States is relatively recent compared to its past. However, research on this topic has seen significant development, and its design limitations have been included in the 2010 AISC Code .Figure (1-10) shows the use of this type of column in the designs of high-rise buildings.

*Figure 1-10: Gateway Tower, Seattle, U.S (*Han, Lam, et al., 2018*).*

1.5 Objective of Study

The main objectives of this research are to study the bearing capacity and deformation of CFDST column (calculated from a standard model) and compare it with the cases if there are 1, 2 or 3 openings on the front side of the columns or the same openings are on the front and back sides of the columns. It is also comparing the bearing capacity of the columns and their deformation for the same openings shown above in the case of using plastic fiber concrete instead of normal concrete

1.6 Layout of Thesis

This thesis contains the following chapters:

Chapter One: contains an overview of the research vocabulary problem and
objective.

Chapter Two: some previous studies related to the research that was

reviewed.

Chapter Three: deals with the materials used to prepare the models and

methods for preparing the practical models.

Chapter Four: includes the practical study conducted in this research.

Chapter Five: includes computer models and their analysis using numerical
analysis methods using Abaqus 2019 program and discusses
those results.

Chapter Six: summarizes previous chapters' results and recommendations for
future work.

Chapter Two: Literature Review

Chapter Two

Literature Review

2.1 General

This chapter talks about the latest research on CFST columns in the past five years, and it was found from this research that steel tubular columns filled with concrete have become popular in composite columns, especially in modern buildings, because of their high strength, rigidity and fire protection features **(Imani et al., 2015).**

Other forms of these columns have emerged, such as concrete-filled twin-tube steel tubular columns (CFDST), and more recently concrete-filled multi-shell steel tubular columns.

CFDST poles are a relatively new form of CFST poles, and recent studies in this chapter have shown that CFDST poles can retain all the advantages of traditional CFST poles, in addition to the fact that the inner steel tube in poles (CFDST) poles offer advantages Other good including:

• The column has less weight

• Energy absorption is higher than (CFST) columns.

• High hardness and therefore higher resistance to bending.

• High ability to resist lateral loads.

• The absence of a vacuum between the inner and outer tubes as a result of filling this space with concrete helped delay the heat transfer to the inner tube, which in turn leads to more time for fire resistance**.**

2.2 Concrete Filled Steel Tubular (CFST) Columns

(Y. Wang et al., 2017) made 36 models shown in Figure (2-1) , and the sample diameters ranged from 150 to 460 mm, while the steel ratios ranged from 4.0 to 10.0%; the failure test was carried out by subjecting models to axial pressure, to examine the effect of column size (CFST). The axial stress, complex modulus of elasticity, modulus of plasticity and the impact of change in column size (of CFST) on these factors were studied. Through the test results, it was shown that the axial stress, the upper axial strain and the modulus of elasticity generally decrease in value with the larger the diameter of the section, and the elastic modulus remained practically constant when the diameter of the model examined was increased. This indicates that the effect of changing the size in the composite modulus of elasticity is not clear.

Meanwhile, the effect of volume change is about 4-10% of the peak axial stress of steel. Moreover, the size impact would generally diminish as the steel proportion expanded.

*Figure 2-1: tested models(*Y. Wang et al., 2017*).*

(Ouyang & Kwan, 2018a) the researchers realized that the confining property of concrete within the steel tube in CFST columns could greatly increase the strength and elastic properties of concrete columns. This increase is equal in circular (CFST) columns. Still, in non-circular (CFST) columns, the stresses are usually different and not uniform. This makes it difficult Perform structural analysis and design and make necessary the use of finite element (FE) models, taking into account the effect of both lateral expansions, and the triaxial lateral behaviour of confined concrete as well as the plastic behaviour of steel tube.

Ninety-two square models were made of CFST columns and bearing them axially Figure(2-2) shows some of these models. The concrete used in these models had a compressive strength ranging from 24 to 110 MPa. The yield stress of the steel pipes ranged from 262 to 835 MPa, and the ratio of the depth of the steel pipe to its thickness was from 18 to 102.

The results of the FE analysis showed load-strain curves in good agreement with the experimental results. Through FE models, a barometric study was made on the effect of the corner radius, where it was found that increasing the radius would provide better confinement in the post-peak phase. This leads to The behaviour of CFST square columns improving in the post-peak phase.

(a) C30 specimens   (b) C50 specimens

*Figure 2- ٢: Checked models(*Ouyang & Kwan, 2018a*).*

Other researchers **(Cai et al., 2018)** studied CFST columns. The first case is CFST columns coated with engineered cementitious composites (ECC), and the second case is concrete-filled (CFST) columns.

Made six models of CFST columns, four models of CFST columns were coated with ECC, and the remaining two models were coated with concrete; the mechanical behavior of these columns was studied by applying an axial load on these models.

The test results showed that the durability and flexibility are higher in ECC-coated CFST columns than in the second model.

The influence of the thickness of the steel tube and the ratio of the column models' longitudinal strength are discussed. And a new method was made

to calculate the bearing capacity of ECC-coated CFST columns and verify it with practical experience.

Other researchers **(Dey et al., 2019)** conducted a limited analysis of the elements, and the purpose was to understand the cross-sectional behaviour of the various CFST column models. Moreover, through the ABAQUS program, the numerical models were generated and analyzed, the results are shown in the Figure(2-3), and the bearing capacity of the column models was calculated using the American code ACI-318.

The results of the numerical analysis were in good agreement with the calculated design results, and the results showed that it is necessary to take into account the geometric characteristics of the circular column in the design, and the numerical results showed the predictability of failure modes in this type of columns.

(a)   (b)
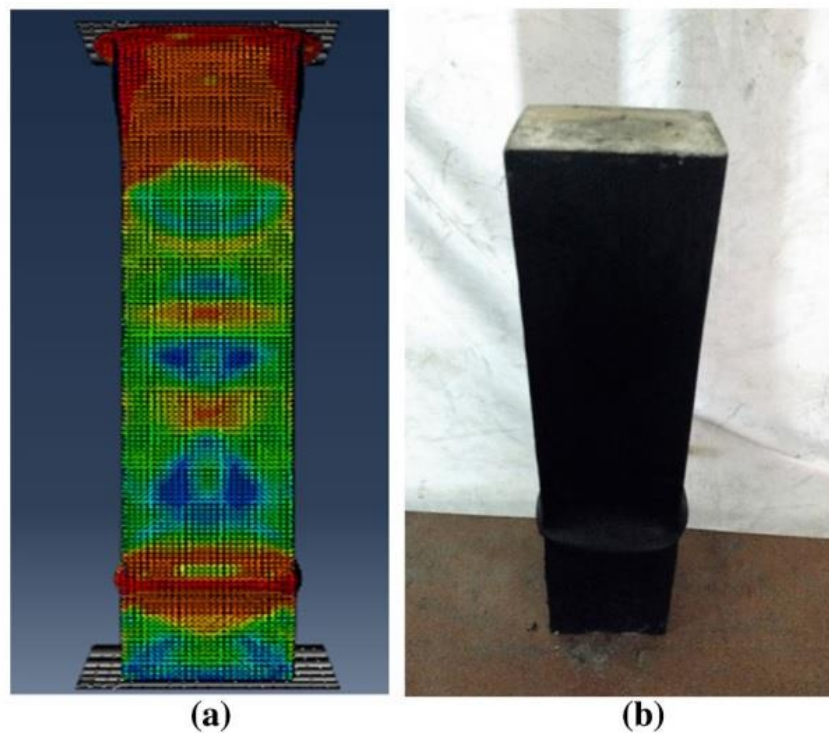
*Figure 2-3: The results of the analysis process (*Dey et al., 2019*)*

(**Hossain & Chu, 2019**) presented the effect of the type of concrete used to fill CFST columns on the geometric properties of these columns. 42 models made of different shapes (round, rectangular, and square) and of varying thinness. Six types of concrete were used to fill these models: regular concrete, rubber concrete, self-concrete compaction, lightweight concrete, and high-strength concrete, in addition to the geometrically designed cement composite. Using the models in the lab, the model's failure mechanisms and bearing capacities were examined, along with the stress, strain, and displacement characteristics.

The current analytical models to estimate the confined strength of concrete showed that its performance was better for CFST columns filled with normal concrete (within 125% of the experimental values), while the performance of the columns was filled with the rest of the concrete types used in the research. Concrete confining models that assumed a direct proportionality between concrete confining strength and cylinder compressive strength did not perform well (up to 233% of the experimental value)**.**

(**Li et al., 2020**)discussed the effect of initial self-strain in concrete and steel fiber on the compressive behavior of CFST columns. Models were made of 36 CFST columns with compressibility ranging between 3.31 MPa and 6.66 MPa, and the volume ratio of steel fibers went between (0.6% - 1.2%) under axial pressure. Thicknesses of 2.5 mm and 3.5 mm, and 4.25 mm were used in the pipes steel to achieve different confining hardness.

The compressive strength grades of screening concrete were multiple (C40, C50 and C60) to obtain the results of various deformations in the failure mode. Through the laboratory results, the samples showed that the failure was in the shear, while the self-compression or steel fibers did not have a clear role in affecting the loss. The final load of CFST columns ranged between 9.8% -27.6% and this percentage

contributed to the concrete's self-stress, which at the same time significantly reduced its susceptibility to deformation.

The addition of mineral fibers should increase the closing load and enhance the behaviour of CFST columns in terms of ductility and self-strain. Based on the results of this examination and the literature, the most efficient subjective stress level (ratio of radial subjective stress and urban strength) of 0.10 has been suggested.

(Y. Yan et al., 2021)tested reinforced CFST columns using high-strength carbon-fiber-reinforced polymer (CFRP) and carbon-fiber-reinforced cement (ECC).

Thirty test samples were made, including three unstrengthened models used for comparison purposes and 27 reinforced test samples. The main parameters in this paper are the compressive strength of concrete, the ratio of the pipe diameter to thickness as well as the number of layers used for CFRP mesh.

The experimental results showed that the carbon fiber-reinforced plastic samples had a better reinforcing effect than the non-reinforced ones, and the reinforced samples also showed higher bearing capacity.

Researchers **(Nguyen et al., 2021)** made six models of CFST columns consisting of a square tube welded with high-strength materials and these six models of different thicknesses; through laboratory tests, the performance of these models was evaluated based on the failure condition, the final bearing capacity and also the evolution of the stress condition.

Numerical models were also made using the finite elements method (FEM), and these models are similar to laboratory models. Through the experimental results, the mechanical properties of CFST columns were deduced, and FEM was used to check the equation Australia-New Zealand Composite structures - steel-concrete code (AS/NZS 2327) and deduce a parameter that can predict the bearing capacity of CFST columns.

Researchers **(Gupta et al., 2022)** discussed the high bearing capacity of CFST columns and, therefore, their use in structures with high loads, such as tall buildings and bridges, and because concrete is confined within the steel tube, it gives concrete higher strength.

The researchers made models of CFST columns filled with two types of concrete, M15 and M20. These models were subjected to an axial compressive load, where the load was applied in two ways, the first on the entire model and the second on the concrete part with only three samples.

Twenty-four samples of CFST columns are made for each model of cylindrical concrete. Half of these samples are examined after 14 days, and the other half after 28 days. The effects of the tensile test of the steel tube are also recorded, and the results of the axial stress of the columns are recorded. Similar numerical models are made using ABAQUS and ANSYS to compare the results and behaviors between the laboratory and numerical models. The results were similar between numerical and experimental studies.

Researchers **(Kothari et al., 2022)** discussed the economic aspects of CFST composite columns due to their high bearing capacity and thus the possibility of erecting taller buildings with smaller column dimensions than usual.

To verify these columns' bearing capacity, laboratory models of CFST columns were made to study the stress-strain behavior and the local bending of steel tubes and concrete for different model lengths and cross-sections. The results showed the convergence of laboratory and digital results, thus, the possibility of benefiting from numerical models to estimate the ability to bear the various shapes of these columns.

2.3 Concrete-Filled Steel Tube Reinforced by Double Layers of Steel Tube (CFDST) Columns.

(Hassanein et al., 2018)studied the structural behaviour of short CFDST columns to which a central load was applied.

The samples investigated by the researchers consist of two tubes, the outer is a hollow circular tube (CHS), the inner tube is a hollow square (SHS), and the space between the two tubes is filled with concrete. Experimental tests are conducted on the samples, and to ensure the accuracy of the modelling for these samples, numerical models are made using the ABAQUS program shown in Figure (2-4), and the results obtained from the numerical analysis are compared with the experimental results to verify the accuracy of the results. Various stress-strain curves were made for concrete and steel, and the best curves were selected from them, which will be used in the barometric study.

The study aimed to examine the effect of different ratios of diameter to thickness (Do/to) and the ratio of width to thickness (Bi/ti). The research essential important conclusions about CFDST short columns.
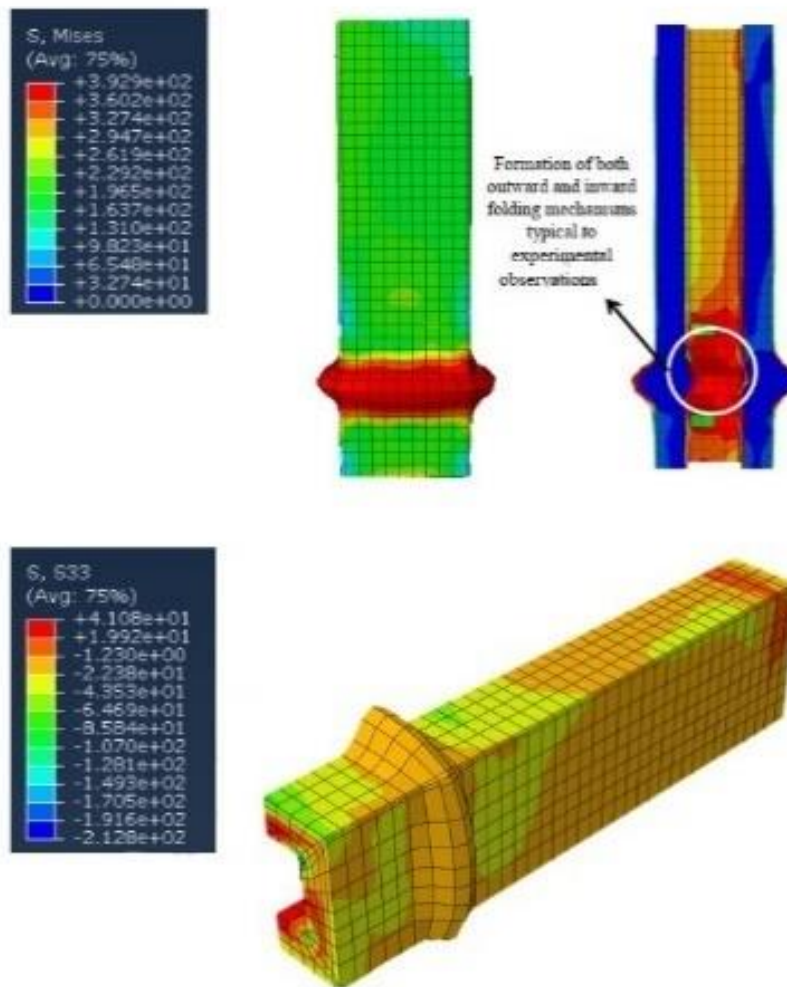
*Figure 2-4: The analytical model in the Abaqus program (*Hassanein et al., 2018*)*

Researchers **(Ekmekyapar & Hasan, 2019)** discussed the role of the inner tube in CFDST columns in stress-bearing and improving the structural performance of this type of column. The researchers made 21 models using these models used two types of normal concrete and high-strength concrete shown in Figure (2-5), in addition to using two different ratios of D / t. A failure test was conducted for sixteen samples. The results showed that better performance in CFDST columns could be achieved when an appropriate steel inner tube is used; in addition, the inner tube in CFDST

20

columns works harmoniously with concrete and reduces its failure even when using high-strength concrete (HSC).
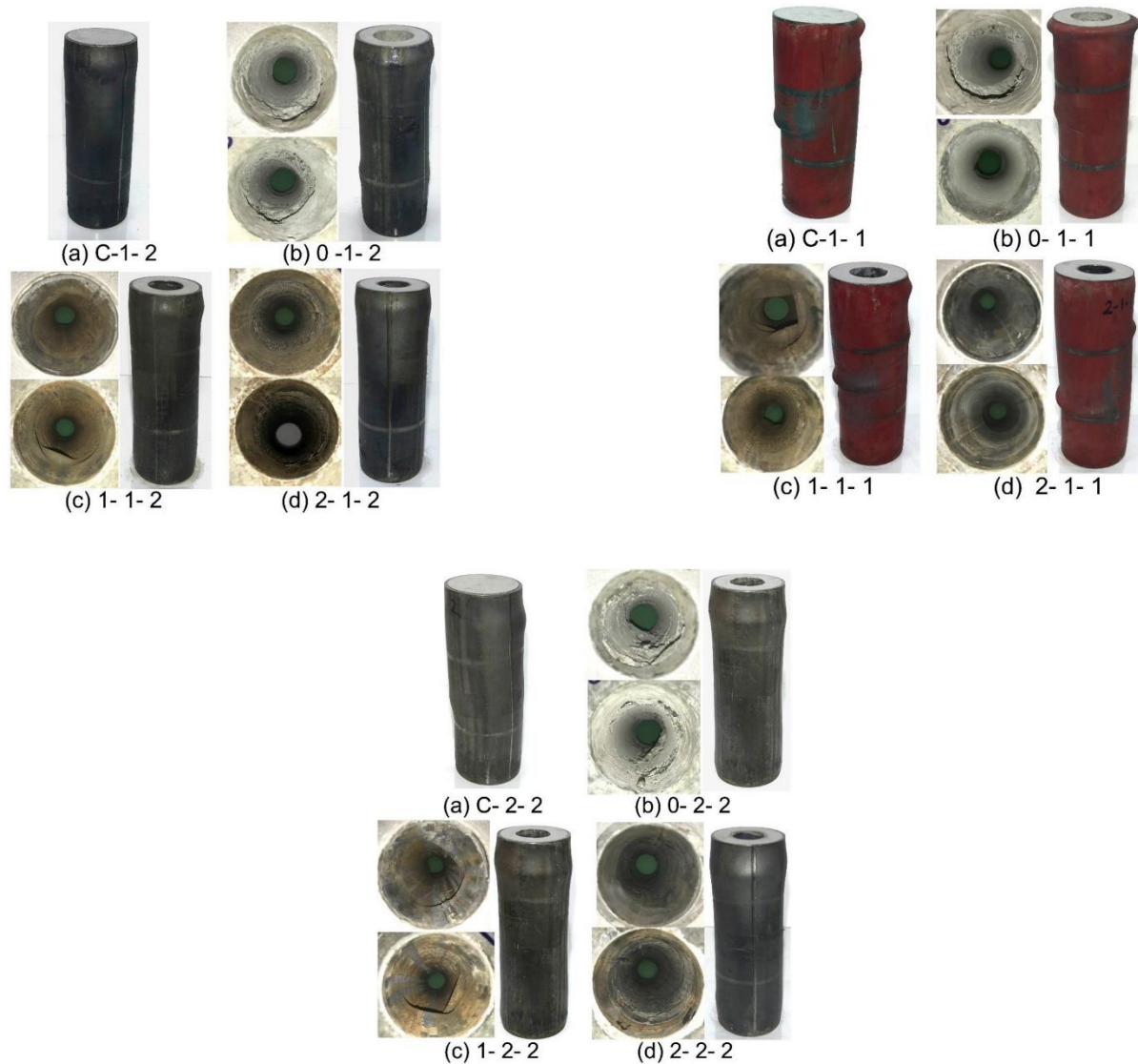
*Figure 2-5: Failure modes of te columns in Set 1(*Ekmekyapar & Hasan, 2019)

Other **(Ekmekyapar & Hasan, 2019)** presented a study on CFDST columns in which the inner and outer tubes are circular. These columns are more durable and ductile because of the concrete trapping in the round tubes' geometries. In this research, the structural performance of this kind of column is examined about

variables such as the inner and outer tube thickness, the confined concrete thickness, and the production pressure of the outer tube.. The numerical analysis was performed using the ABAQUS software, and the results obtained from the software were compared with the experimental results.

In the parametric study, the best materials models were used to examine the effects of several factors on the load-displacement relationships in CFDST columns.

(Fang et al., 2020)studied some properties of CFDST columns, such as ductility, wear resistance, and localized stability. Twenty-one models were made using normal and corrugated pipe wall shown in Figure (2-6).

The test was carried out by applying different axial loads, and the results showed that these columns have good properties in positional stability.

It was also found that the axial bearing capacity is higher due to the presence of the inner tube in the CFDST columns. The corrugated walls of the tubes provide all-concrete confinement and obtain better ductility.

Four tested models were selected to rely on them to predict the bearing capacity of CFDST columns.

(a) CFDST with vertical corrugated steel plates   (b) Concrete-filled double corrugated steel walls   (a) Square annular CSP

(d) CFDST with an inner CSP   (e) CFCST   (f) CFCST-S   (g) CFDST with an external CSP   (h) CFDST with inner and outer CSPs
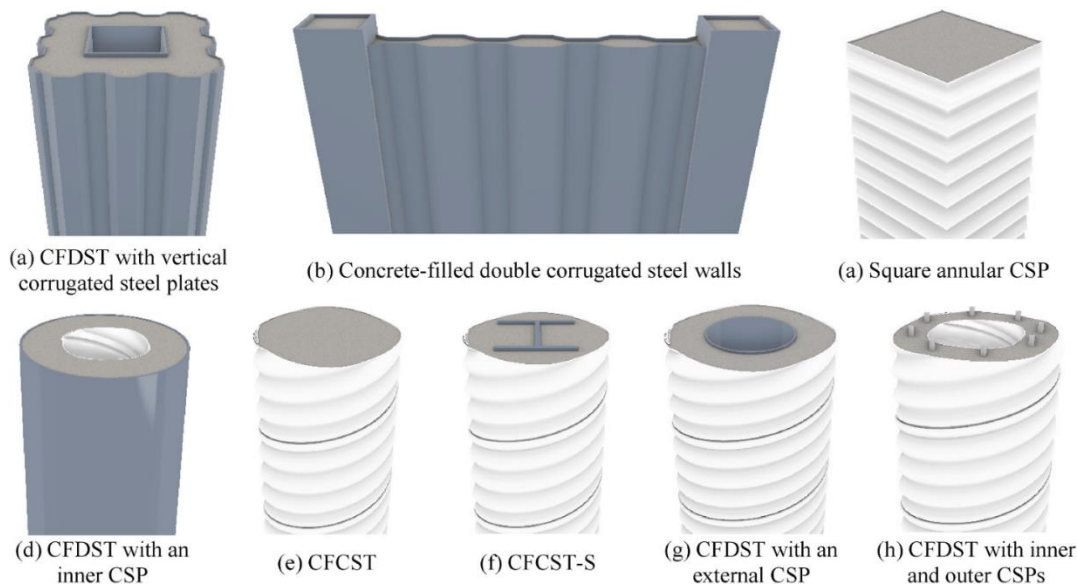
*Figure 2-6: Comparison of the similar components (*Fang et al., 2020*)*

(Ayough et al., 2020) studied CFDST columns' properties, consisting of a square outer column and a hollow circular inner column, by performing a series of nonlinear FEM tests.

The main criteria for this study were ductility, final stiffness, energy absorption capacity, and performance of CFDST columns.

Through the nonlinear FEM results, it is clear that confining the concrete core in a circular inner tube is unsuitable due to the difference in determining mechanism from that of the square outer tube, and neglecting the confining effects can lead to conservative results. Hence, it is necessary to consider the limiting effect of concrete when making calculations. It was also found that the performance of the CFDST columns is affected by the material properties and dimensions of the tubes that compose these columns; thus, a new design equation was deduced that predicts the final strengths of short and axial load CFDST columns.

An experimental investigation conducted by **(Hassan & Bhat, 2021)** between CFDST columns with analogs of conventional reinforced concrete column (RCC). Columns CFDST consist of two hot-rolled square tubes; these two tubes are concentric, the outer tube has a cross-section of 100 mm, the inner tube is 30 mm, and the space between the two tubes is filled with normal concrete of compressive strength M-25, as well as two other members of RCC with an amount of reinforcement equal to the amount of steel in CFDST columns.

The test was carried out on these bars, and the results were compared with the numerical models obtained from the ABAQUS program.

It was found that the bearing capacity of CFDST was 30% higher than that of RCC columns, and the performance of CFDST was better than that of RCC.

(Ci et al., 2021)in this search is entered circular concrete-filled double steel tubular column (CFDST) with a square hollow section (SHS) as an inner tube is introduced as a new form of a composite column. A series of axial compression tests that are carried out on this new type of composite column is reported in this study. Three-dimensional models based on the finite element (FE) program ABAQUS are also developed for such columns employing a modified confined concrete constitutive model for the core concrete. The accuracy of the model is verified by comparing the FE model with the experimental results. The effects of various parameters on the load-axial strain response of CFDST short columns are studied by using the validated FE model. The suggested formulas based on the confined concrete model for calculating the bearing capacity of CFDST short columns are proposed.

(Bhatia & Tiwary, 2022) talked about the used portion of the concrete core in CFST and CFDST columns due to unused core portions. The numerical models of the (CFST) and (CFDST) columns were made using the ABAQUS program. The numerical analysis was performed, the results were extracted, and compared with the results of the experimental models. The bearing capacity of the column models extracted from the numerical analysis was compared with the expected results using Eurocode 4 and the American Building Institute specifications. The D / t ratio was taken into account as a result of the compressive behavior of CFST columns, while the effect of this ratio decreases in CFDST columns, and the results showed that the hollow inner tube, when it is small, can better confine the concrete.

(Witteck et al., 2022) the researchers conducted an experimental studyon the performance of innovative Concrete-filled double steel tube (CFDST) columns with high-performance building materials under monotonic and cyclic loading. In total six stub CFDST-columns and two conventional stub concrete-filled steel tubes (CFST) were tested at Ruhr-Universität Bochum under a constant axial load with

either a monotonic or a cyclic increase of lateral displacement.This research focuses on comparing the characteristic behavior of the sample such as hysterical behavior, ductility and energy dissipation. The experimental investigations have shown that the resistances, ductility and energy dissipation of innovative CFDST is increased compared to conventional CFST-columns. The use of a high-strength inner tube did show the most benefits in terms of the resistances, while at the same time a configuration with normal-strength core materials showed better results in terms of the energy dissipation and ductility.

The research concluded that enlarging the inner tube increases the resistance, while improving the quality of the filling concrete contributes to an increase in energy dissipation and ductility.

2.4 Concrete-Filled Multi-Skin Tube Columns (CFMST)

Researchs **(Salim & Al-Khekany, 2021)**investigated a hollow composite column consisting of several layers of concentrated united steel (for the circular and square types) filling the void between them with concrete. This type of composite column is called concrete-filled multi-skin tube (CFMST), and an experimental part included 55 composite columns were examined , tested and exposed to a pivotal load. In laboratory and digital models, some engineering variables were studied, such as thickness, cross-sectional area, the number of steel layers, and quality of steel used, in addition to other variables and the extent of their impact on the flexural limits, both for laboratory models and computer-designed models using ABAQUS, and the following results were reached through this research:

- The maximum resistance of the column decreases with increasing height.

- It was found that in the case of increasing the thickness of the walls of the steel bars from (0.5 to 1 to 2) within the limits of Slenderness, it increased by 191% for the square and 293% for the circular.

- When the number of steel layers is increased, there is an improvement in the Slenderness limits and the column's resistance. Experiments have shown that increasing the number of steel layers to 4, improves the limits of thinness by 60% for the circular and 3.55% for the square.

- The circular sections had less resistance than the square sections and had the same external dimensions. As shown earlier, the heights required to find the Slenderness limits were higher in the square than in the circular shape, indicating that the square section is more solid than the circular shape.

2.5 Summary

A wide range of research methods are covered in this section, both for columns CFST and CFDST in terms of the effect of the type of concrete filling, as well as the influence of thickness of internal and external pipe dimensions and other determinants.

However, this research did not address the effect of openings in the composite columns of the CFDST type despite the importance of these openings for the passage of services (such as communications, electrical installations and plumbing), so this study was adopted.

CHAPTER THREE: EXPERIMENTAL WORK

Chapter Three

Experimental Work

3.1 Introduction

In structural applications, the main function of a column is the ability to carry and transfer loads (vertical and lateral) from structures to foundations; however, due to the development of building sciences and the emergence of new service systems such as communications, as well as the development of health services. The need arose for the possibility of the column playing another role in passing these services through the openings in the composite columns, demonstrating the need to enter into this study to show the effect of the openings on the main function of the composite column, which is the transfer of loads. This chapter discusses the practical program for producing laboratory models of a concrete-filled double steel tube (CFDST) and also includes a description of the equipment used in CFDST tests.

Because of the COVID-19 pandemic-related downtime, laboratory models of CFDST columns have been housed off-site at the College of the Engineering / University of Kufa.

The practical program of the study includes a description of all samples of materials used in the formation of CFDST, whether normal concrete or plastic fiber concrete, as well as steel tubes.

In addition, the compressive strength at the end of the curing phase (after 28 days) for both normal concrete and plastic fiber concrete has been calculated, as well as the yield stress of steel pipes used in the manufacture of CFDST models.

3.2 General Description of Samples

Fourteen specimens of composite CFDST columns were designed, manufactured and tested as part of a full pilot program to study the effect of service openings in CFDST columns on their bearing capacity. Seven of the samples are of normal concrete and seven other samples are of plastic fiber concrete as shown in Figure (3-1).
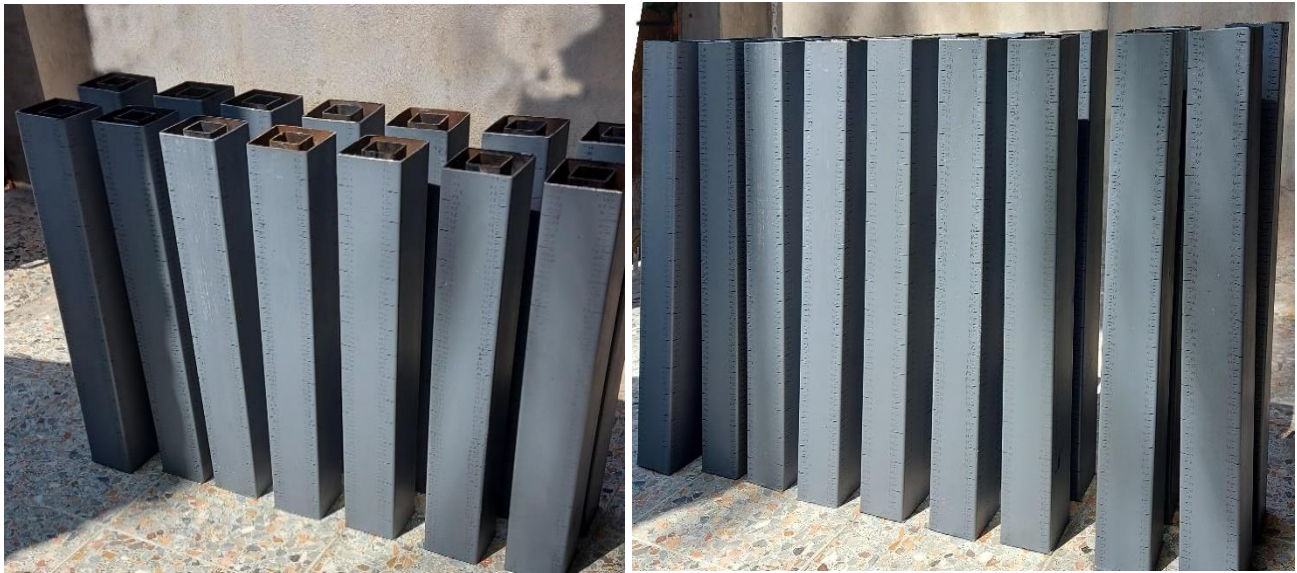
Figure 3-1: the test samples before casting

The main experimental parameters of CFDST columns studied in this study are the type of concrete used to fill the columns, , the number of opneings in the steel tubes, and whether these opneings are one-sided or two-sided. As shown in Figure (3-2), all authorized samples have a set height of 800mm and a cross-section with many opneings that vary from column to column. Figure (3-2) also shows whether the opneings are on one or both sides Figure (3-3). The graph in Figure (3-4) lists the basic details of sample patterns and symbols for each test sample.

First, an exterior layer with dimensions D = W = 100mm was employed, followed by an inner layer with dimensions D=W =50mm .

These samples are divided into two groups according to the concrete used, whether normal concrete or plastic fiber concrete. Each set consists of 7 models, one of which is without opening and certified as a load gauge, and the remaining six are hollow with different side openings. All samples have the same thickness for all layers of the steel tube (t = 2 mm).
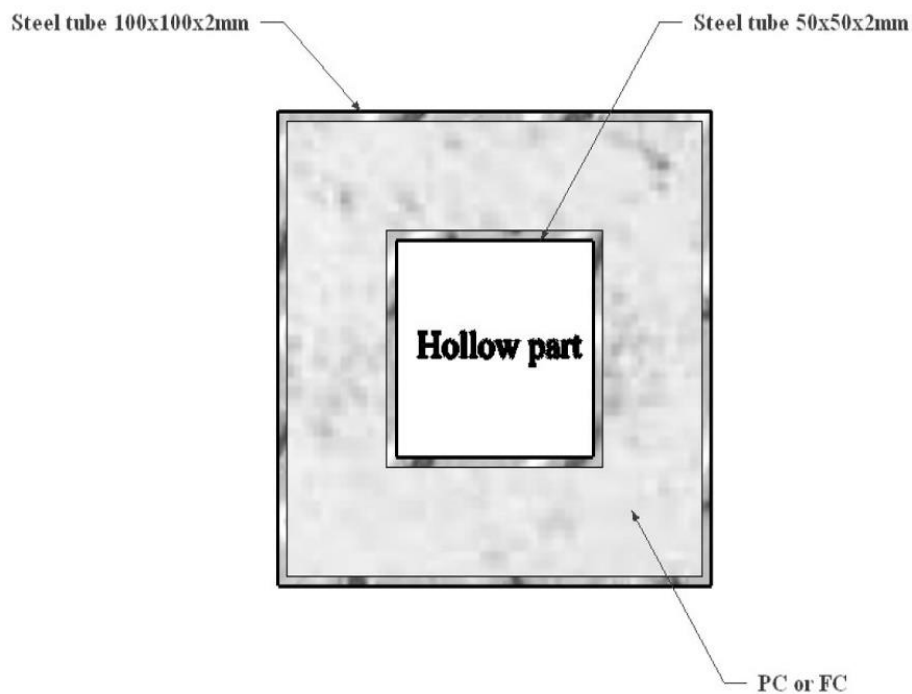
Figure 3-2: Sections of the test samples
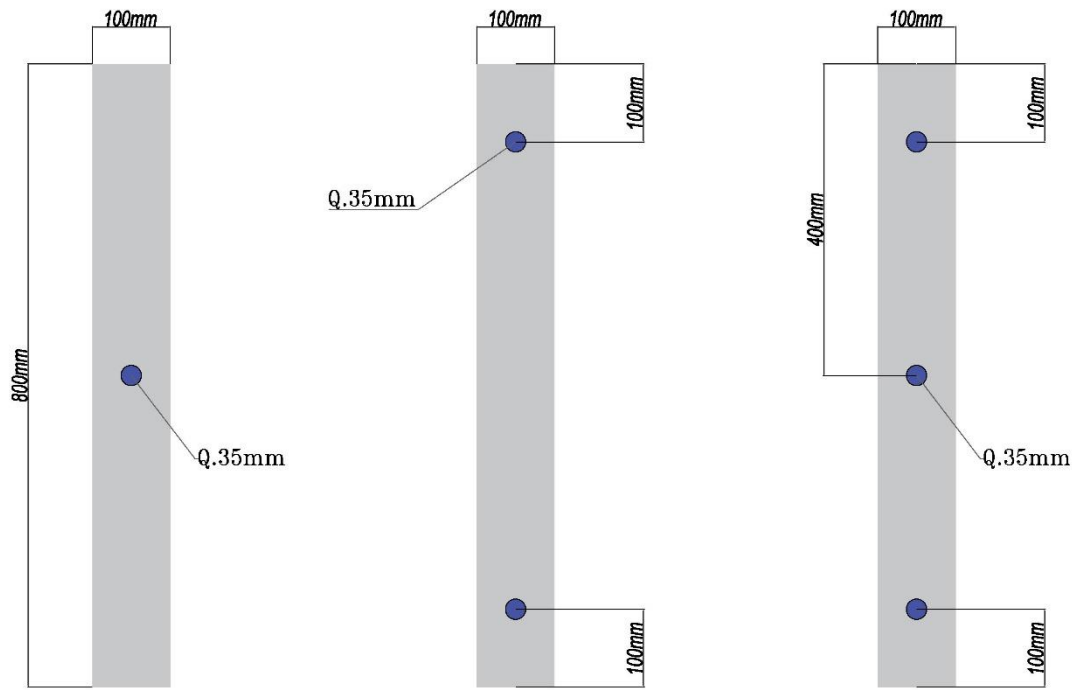
Single-sided opening test models
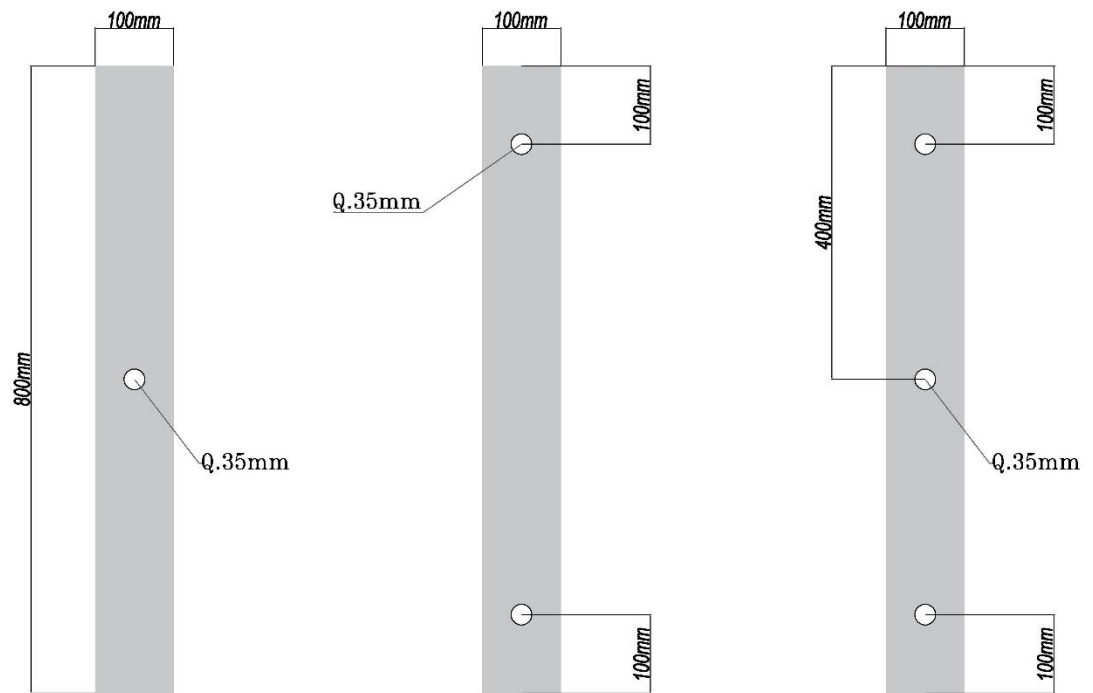
Test models with openings on opposite sides

Figure 3-3: Number and locations of openings in test models
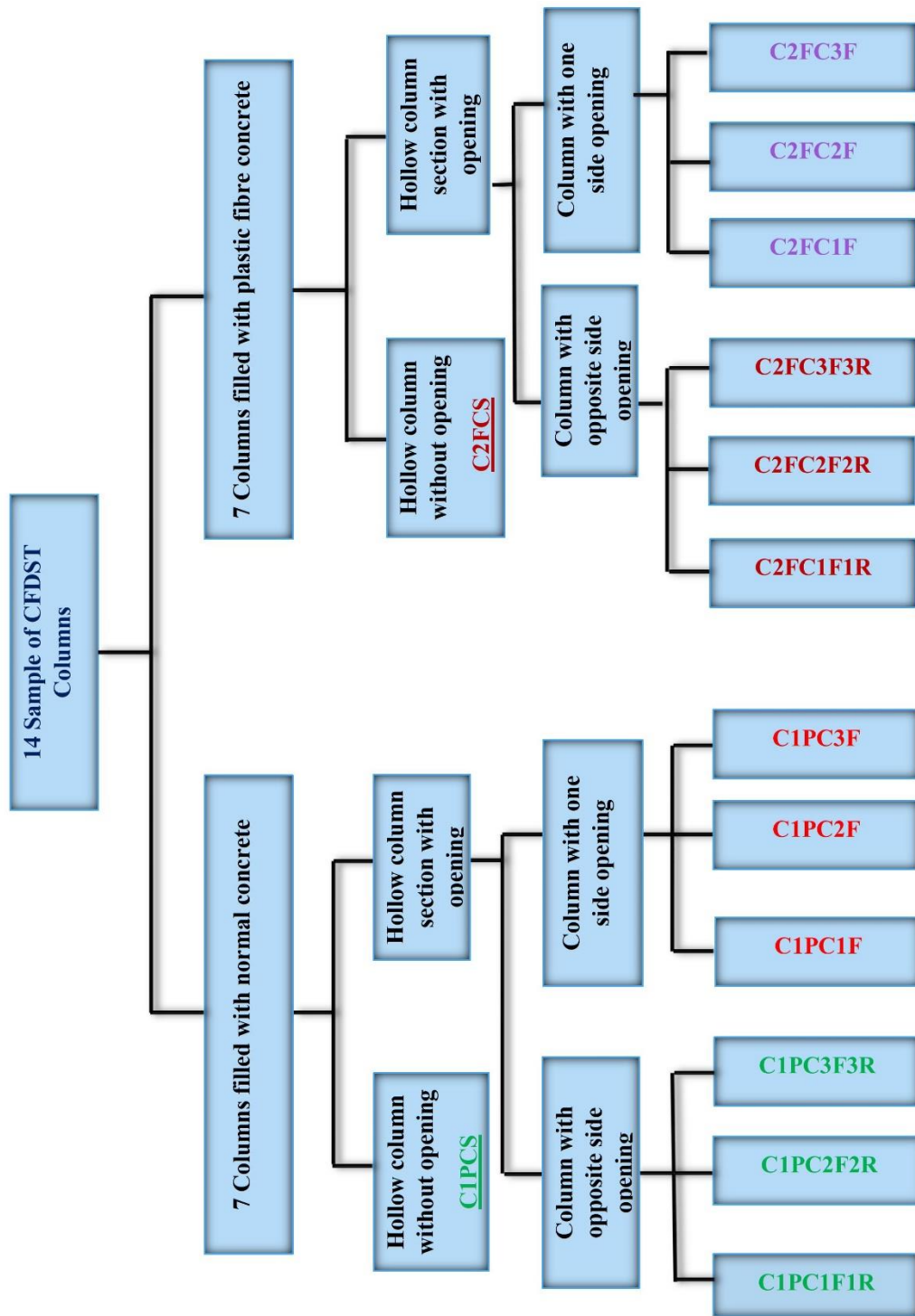
Figure 3-4: Distribution of test columns and their forms

To determine the test pattern, each sample was given a unique designation and according to the following classification system:

➢ The symbol C1 refers to a group 1, while the symbol C2 indicates a group 2.

➢ The second symbol indicates the type of fill concrete. NC represents normal concrete, and FC represents plastic fiber concrete.

➢ The third symbol contains the following cases:

- S indicates that the column is solid.

- 1F means that the column has one front opening, 2F means that the column has two front openings, and 3F means that the column has three front openings.

- 1R means that the column has two opposite openings, 2R means that the column has four opposite openings, and 3R means that the column has six opposite openings.

3.3 Adopted Experimental Parameters

The experimental program included studying the various factors that affect the bearing capacity of CFDST columns, and these parameters are:

➢ The difference in the bearing capacity of the CFDST column when it is solid compared to when it is hollow.

➢ The effect of the type of concrete filling for CFDST columns.

➢ The effect of the number and locations of openings in CFDST columns on the bearing capacity.

3.4 Materials Preparations

3.4.1 Concrete

This study uses normal concrete and plastic fiber concrete, which is normal concrete with a percentage of plastic fibers added.

Normal concrete requires mixing aggregates and binders; the aggregates used are coarse and fine aggregate, and the adhesive consists of water and cement. Therefore, fine aggregate, coarsed aggregate, cement, water, and plastic fiber are the basic materials that make up normal concrete and plastic fiber concrete. The above materials were tested in the Consulting Services Office, College of Engineering, University of Karbala laboratories according to the required standards.

3.4.1.1 Plastic Fibers

Plastic fibers are polypropylene fibers, synthetic fibers, and a product of the petrochemical industries. It can be produced in a single pack of capillary fibers or larger diameters.

Plastic fibers are used in several ways to strengthen concrete. Recent studies have shown an improvement in the mechanical specifications of concrete to which this type of fiberis added. In this study, the weight of the plastic fibers added was 1% of the weight of the cement used in preparing laboratory samples for fiber concrete. Sika's plastic fibers have been used, distinguished by their quality. Figure (3-5) shows the packaging used, while Table (3-1) shows the properties of the material

Figure 3-5: Plastic fiber (Sika fiber PPM-12)

Table (3-1) Properties for Sika Fiber PPM-12

No.	Paragraphs	Details
1.	Chemical Base	100% polypropylene
2.	Packaging	0.6 kg pulpable bag (carton box with 24 bags)
3.	Appearance / Color	Transparent fibers
4.	Storage Conditions	Storage temperatures between +5°C and +30°C. Store in a dry, covered place, protected from moisture, UV radiation, direct sunlight and frost.
5.	Density	~0.91 g/cm3
6.	Dimensions	32 microns
7.	Material	100% Virgin Polypropylene
8.	Ignition Point	365°C
9.	Surface	Coated for dispersion
10.	Design	Monofilament Fibre
11.	Fibre Length	Blended
12.	Thermal Conductivity	Low
13.	Electrical Conductivity	Low
14.	Acid Resistance	High

3.4.1.2 Cement

The cement used in pouring all the concrete samples in this study is Mass Cement R42.5, which is ordinary Portland cement (Iraqi Industry).

35

This cement conforms to the Iraqi Standard Specification (ISS) No. (5) for the year 1984 and as shown in Appendix(A)-Table (1).

The tests were conducted in the laboratory of the Engineering Consulting Office at the College of Engineering, University of Karbala.

3.4.1.3 Fine Aggregate

The natural sand used in this experimental work was provided from the quarries of Karbala. The tests on the sand used in manufacturing the test models showed that the sulfate content was within the Iraqi Standard No. (45) for the year 1984. The tests were conducted on the sand in the laboratory of Engineering Consulting Office at the College of Engineering, University of Karbala, as shown in Appendix (A)-Table(2).

3.4.1.4 Coars Aggregate

In this study, natural gravel with a maximum diameter of 10 mm (coarsed surface gravel) was used, which was prepared from Karbala quarries, where the coarsed aggregate was cleaned and washed repeatedly and then left to dry. The analysis of the sieve and the results of the tests shown in Appendix(A)-Table(3) showed that the sulfate content in the coarsed aggregate conformed to Iraqi Standard No. (45) for the year 1984.

These tests were carried out in the laboratory of the Engineering Consulting Office at the College of Engineering, University of Karbala.

3.4.1.5 Concrete Mixture Water

The water used in the concrete line must be free from all substances harmful to concrete, such as organic matter, acids, salts and alkali, because of the damage they cause to the concrete and the damage that these materials may cause to steel pipes. Therefore, tap water was used because it is free of the substances mentioned above and is suitable for such works.

4.4.2 The Steel Tube

In the pilot program of this study, samples were made of highly flexible steel tubes. The single tube comes in a standard length of 6 meters, then cut into pieces; the height of one model is 800 mm, the fixed height required for all samples used for examination. The tubes come in two models: the outer tube has dimensions (D=W=100mm), while the inner tube has dimensions(D=W=50mm), and a fixed thickness of all columns is (2) mm. The tensile test was performed on six samples, three for the outer tube and the same for the inner tube.

The tensile test was carried out in an internationally known test machine in the laboratory of the College of Engineering / University of Baghdad and is shown in Figure (3-6); tested according to ASTM A529- ASTM A36, the obtained examination results are shown in Table (3-2).

Figure 3-6: Steel tube testing machine

Table 3- 2: Tensile testing for steel tubes

Test type	Sample Lab. No.	Sec 48	Sec 48	Specification Limits			
	Trade Mark or field No.	Square steel tube 50x50 mm	Square steel tube 100x100 mm	ASTM A 36		ASTM A 529	
	Property	Test Results		Plate& bar	shape	Grade50	Grade55
Physical	Sample thickness(mm)	2	2	Not limited		Not limited	
Mechanical	Yield strength (MPa)	378.2	369.1	Min. 250		Min. 345	Min. 380
	Tensile strength (MPa)	466.4	425.5	400-550		450-690	485-690
	Elongation in 50 mm (%)	30	27.0	Min.23	Min.21	Min. 21	Min. 20

3.4.3 Molds

In this study, no molds were needed except for cube molds to find the compressive strength of concrete. After the concrete is poured into the cubes, it is left to dry for 24 hours, then the formwork is removed, and the concrete cubes are cured by placing them in water for 28 days, then they are removed from the tank and left to dry and then tested to determine the compressive strength of the concrete.

3.5 The Process of Mixing Normal Concrete and Plastic Fiber Concrete

In this study, it was depended that the required compressive strength of concrete (Normal and plastic fibers) is (25 MPa minimum) in (28 days). Before mixing, the mixer and its blades must be cleaned of any concrete residues resulting from previous concrete mixing work.

The concrete mixing process is summarized in the following paragraphs:

1- Aggregate materials (sand and coars aggregate) are added to the mixing machine and mixed for an appropriate period of not less than 3 minutes.

2- Cement is added to the mixture and mixed to achieve homogeneity, and the mixing time shall not be less than 3 minutes.

3- Water and plasticizer (Sikament®-221 N), whose properties are shown in Table(3-2) and Figure(3-7), were added, and the mixing process was continued for 5 minutes.

4- In the case of concrete made of plastic fibers, plastic fibers are added to the concrete mixture and mixed for an appropriate period of not less than 5 minutes.

5- The concrete is ready to pour test samples and test cubes.

Table (3-3) shows the properties of the plasticizer, while the Table (3-4)show the quantities of materials that make up the concrete mix.

Figure 3-7: Superplasticizer (Sikament®-221 N)

Table (3-3) Properties for superplasticizer (Sikament®-221 N)

No.	Paragraphs	Details
		PRODUCT INFORMATION
1.	Composition	Modified Mix of Naphthalene & Lignosulphonate Based product
2.	Packaging	Bulk Deliverie 1000 LTRs IBC 20 kg Pail
3.	Storage conditions	In dry conditions at temperatures between +5°C and +35°C. Protect from direct sunlight. It requires recirculation when held in storage for extended periods.
4.	Appearance and colour	Dark brownish liquid
5.	Specific gravity	1.220 ± (0.010) g/cm3
6.	pH-Value	5 - 7

No.	Paragraphs	Details
	TECHNICAL INFORMATION	
7.	Concreting guidance	The standard rules of good concreting practice, concerning production and placing, are to be followed. Laboratory trials shall be carried out before concreting on site, especially when using a new mix design or producing new concrete components. Fresh concrete must be cured properly and curing applied as early as possible
	APPLICATION INFORMATION	
8.	Recommended dosage	Recommended dosage for concrete: 1- For plastic Concrete (0.6 - 1 %) by weight of Binder (600 - 1000 gm) for 100 kg cement . 2- For Flowable Concrete (1- 2 %) by weight of Binder (1000 - 2000 gm) for 100 kg cement . 3- Optimum dosage should be determined by site trials. When adjusting the consistency , high water reduction property of the admixture must be taken in consideration , excessive water addition must be prevented .
9.	Dispensing	Sikament®-221 N is added to the gauging water or added with it into the concrete mixer. To take advantage of the high water reduction, a wet mixing time, which is depending on the mixing conditions and mixer performance, of at least 3 mins. per cubic meter after the admixture addition is recommended. Sikament®-221 N shall not be added to dry cement.

Table 3- 4: Quantities of components of normal concrete& plastic fiber concrete

No.	Type of Concrete	Ingredients	Weight
1.		Cement	350 kg/m3
2.		Coarse aggregate	1182 kg/m3
3.	Normal concrete	Fine aggregate	657 kg/m3
4.		Water content	160 L/m3
5.		Superplasticizer (Sikament®-221 N)	3 kg/m3

No.	Type of Concrete	Ingredients	Weight
6.		Cement	350 kg/m3
7.		Coarse aggregate	1182 kg/m3
8.	Plastic fiber concrete	Fine aggregate	657 kg/m3
9.		Water content	160 L/m3
10.		Superplasticizer(Sikament®-221 N)	٣ kg/m3
11.		Plastic fiber	150 g/ m3

3.6 Casting and Curing Procedure

In this study, 14 test samples were made, the samples were filled with concrete vertically, and the target force in concrete was 25 kN/mm2. During the casting process, a steel plate with dimensions of 100 * 100 mm was installed under each test sample; these samples were arranged in a vertical position to ensure their stability during the pouring process and as shown in the Figure (3-8), and all fourteen test samples were poured at one time to ensure that all samples were from one mixture.

Six cubes were poured into knowing the compressive strength of the concrete Figure (3-9); the samples were wrapped with plastic wrap to avoid drying the concrete during the curing period. After covering the top surface of the concrete, the CFDST column samples were left in the laboratory. The cubes were placed in a water tank for 28 days and then taken out for drying and examination according to the requirements of Iraqi Standard No. (52). The examination was conducted in the laboratory of the College of Engineering. / Baghdad University.

Figure 3-8: Test samples   *Figure 3-9: Six concrete cubes*

3.7 Mechanical Properties for Hardened Concrete

There are standard tests used to find the mechanical properties of concrete; these tests depend on standard samples (cubes with dimensions of 150x150x150 mm), where these cubes are used to find the compressive strength of the tested concrete. These samples are examined in a digital test device to find the compressive strength of concrete, as shown in Figure(3-10). Concrete's compressive strength was determined by the average values of three samples of each kind of concrete tested following ASTME8/E8M-11. Table (3-5) shows the study cubes' compressive strength results.

Figure 3-10: Concrete Tests Through Digital Testing Machine

Table 3-5: Compressive strength results of cubic samples

No.	Type of concrete	Compressive strength-28 Day (Mpa)	Average	Density (Kg/m3)
A-1		43.49		2406
A-2	Normal Concrte	32.99	36.95	2386
A-3		34.37		2368
B-1		40.37		2331
B-2	Plastic Fiber concrete	39.35	39.66	2332
B-3		39.26		2369

Where Fcu = 0.82 Fc⁻

3.8 Instruments and Structural Behavior Test Of Column

3.8.1 Columns Test Device

All samples of CFDST columns were examined using a hydraulic testing machine with a capacity of 500 kN, shown in Figure (3-11), which is located in the laboratory of the College of Engineering at the University of Kufa, where this machine applies an axial load that is applied to the test sample and the load path is from the bottom to top. This machine consists of a hydraulic actuator (located on the side of the machine) and high-strength steel plates with a thickness of 20 mm and dimensions (120 * 120) mm used to distribute the machine's load on the test sample. Pregnancy readings are linked to a computer program that records them for later analysis. A camera system is linked to the computer to record the process of applying the payload, and the video is recorded.

Figure 3-10: CFDST columns checking machine

3.8.2 Linear Variable Differential Transformer (LVDT)

In this stady, a 25 mm transducer was used to estimate the axial displacement of the examined sample Figure (3-12) shows where the LVDT is installed.The transducer records the readings resulting from the loading process, and these data are the approved results of the examined sample, which will be compared with the results of a similar model in the computer program later.
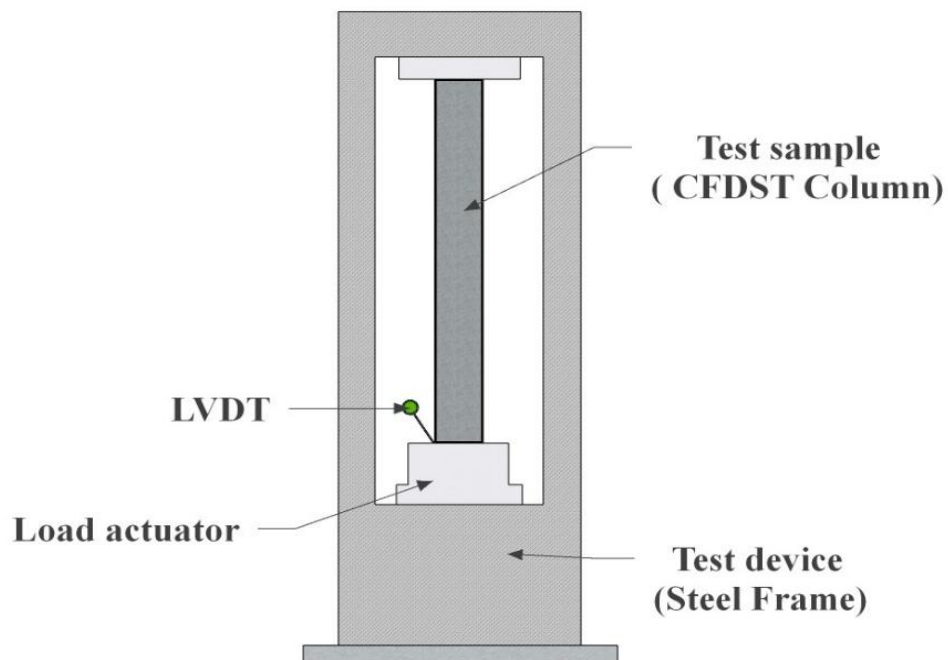
Figure 3-11: LVDT site diagram

3.9 Loading Procedure

The tests were conducted on two groups of composite columns (CFMST), each consisting of 7 columns. One of the seven columns in each group was adopted as the reference column, represented by the C1PCS column in the first group and C2FCS in the second group. Vertically, these samples were examined by subjecting them to an axial load, and transducers recorded the data.The test was carried out with an axial load of 1/12 of the maximum rated capacity of the test sample of 500 kN.

Each loading took about one and a half minutes to ensure that the axial load was transmitted to each column, and the loading process continued until the test sample reached failure. Since the device stops loading and the data is recorded, the data recorded is both the load and the displacement recorded by the transducer.Testing of each sample took about 30 minutes.

Chapter Four: Experimental Results and Discussion

Chapter Four
Experimental Results and Discussion

4.1 Introduction

In this chapter, the fourteen samples were tested in practice. Seven samples filled with normal concrete, the behavior of which is known by comparing the results of a standard sample of this type (without openings) and here we mean C1PCS with the remaining six models of the same type that have openings.

As for the second seven models, they are similar to the first seven, with the filled concrete replaced from normal concrete to plastic fiber concrete and the standard sample is here C2FCS

The behavior of these columns in terms of failure and endurance is studied depending on the following variables:

- Type of concrete filled: normal concrete or plastic fiber concrete.
- The number of openings in each model.

4.2 Mechanical Properties

The mechanical properties include the tested concrete samples' compressive strength and Young's steel modulus. The average was calculated for every three samples of concrete type (normal or plastic fibers) for representation.

4.2.1 Compressive Strength Results

One of the most important properties of hardened concrete is compressive strength, as this property effectively affects the behavior of the composite column **(Dundu, 2012)**. To know the effect of this property on the behavior of columns (CFDST), two types of concrete were used in this research work: normal concrete and plastic fiber concrete.

Table (3-5) shows the results of the standard compressive strength test of normal concrete and the plastic fiber concrete used in the research. The compressive strength value was calculated by taking the average value of three samples for each type of concrete used. The results indicate an increase in the compressive strength of the cube models by 7.34%, due to the use of plastic fibers in concrete.

4.2.2 Young's Modulus for steel

Young's modulus is an essential parameter in iron characterization because of its effect on the bearing capacity of iron pipes (internal and external) in CFDST columns as the endurance capacity increases with the increase in the value of this modulus.

4.3 Experimental results of columns

This part deals with the structural behavior of columns (CFDST) by applying a central compressive load on the tested models, and studying their behavior in terms of bearing capacity and types of failures in these models.

4.3.1 Control column (C1PCS)- Group one

The (C1PCS) column is the control column for a group (No.1), and this group consists of seven columns that are all filled with normal concrete.

The column is installed on the testing machine, and (LVDTs) are prepared in their respective Figure (4-1). The load is gradually applied to the control column until the column fails, as shown in the Figure (4-2).Through experience, it was found that this column failed at a load of 295 kN, shown in Figure (4-3) and the installed displacement of the device. LVDTs 4.37 mm.The failure of the C1PCS columns is due to the local buckling of the outer steel tube, the presence of concrete between the two tubes helping the failure not to reach the inner tube.The value obtained from this sample examination will be used to compare with the six models from the same group i.e. group (1) and these six samples are divided into:

- Three Columns with openings on one side.
- Three Columns with openings on opposite sides

Figure 4-1: C1PCS column test

Figure 4-2: C1PCS Column failure

Figure 4-3: Load-displacement curve - C1PCS column.

4.3.2 Columns with openings on one side

This group includes three columns, as shown in the Figure (4-4).

Figure 4-4: Columns with openings on one side

4.3.2.1 C1PC1F Column

This column specimen has a one-sided opening of 35 mm in diameter and 50 mm in depth; the center of the aperture is 100 mm from the top of the sample. The load is gradually loaded, as shown in the Figure (4-5), until the column fails, as shown in the Figure (4-6).

the model failed at 285 kN. The maximum displacement achieved was 7.84 mm. When comparing these results with the results of the standard column (C1PCS), it was found that the bearing capacity of this column decreased by 3.33%. This is normal because there is a opening that reduces the load-bearing capacity of this column.

Figure (4-7) presents a comparison of the load-displacement curve of the column (C1PC1F) and the standard column (C1PCS).

Figure 4-5: Load column gradually   *Figure 4-6: Column fails*
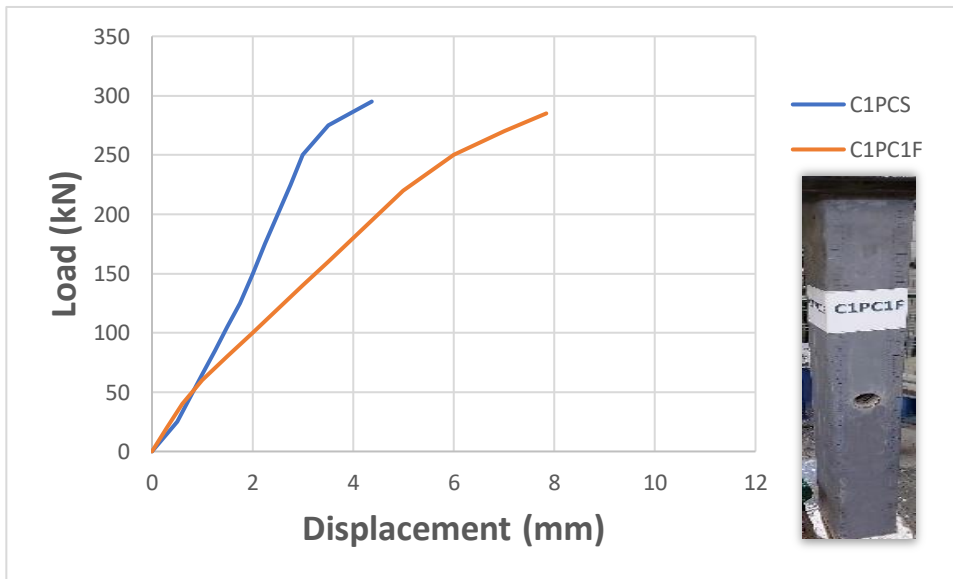
Figure 4-7: Load-Displacement curve - C1PCS&C1PC1F columns

4.3.2.2 C1PC2F Column

This column specimen contains two openings on one side, each opening 35 mm in diameter and 50 mm deep, filled the column with normal concrete.

The load is loaded gradually , as shown in the Figure (4-8), until the column fails, as shown in the Figure (4-9). the model failed at 275 kN; the maximum displacement achieved was 6.78 mm. When comparing these results with the results of the standard column (C1PCS), we find that the bearing capacity of this column decreased by 6.78%. This is normal due to the presence of the two openings, which reduce the carrying capacity of this type of column. Figure (4-10) presents a comparison of the load-displacement curve of the column (C1PC2F) and the standard column (C1PCS).

Figure 4-8: Load column gradually

Figure 4-9: Column fails.
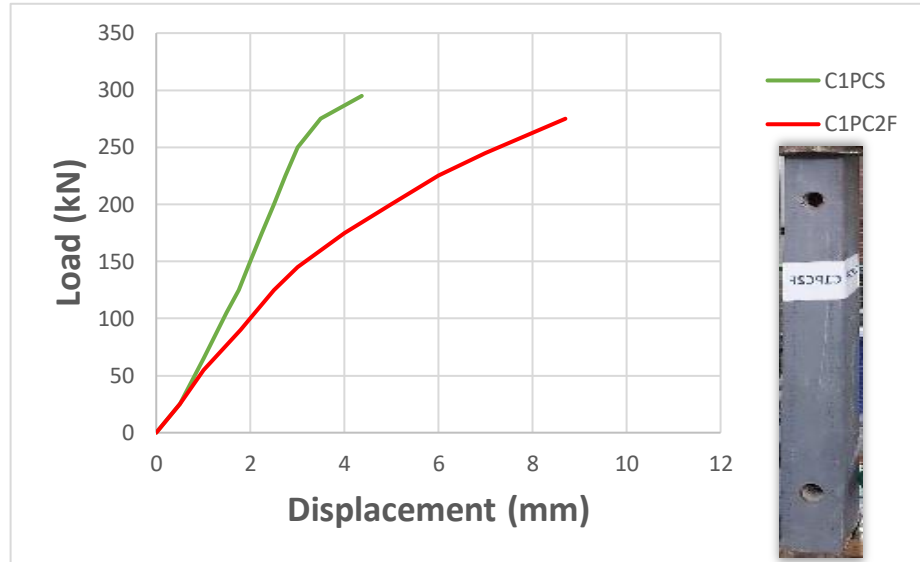
Figure 4-10: Load-displacement curve - C1PCS&C1PC2F columns

4.3.2.3 C1PC3F Column

His column specimen contains three openings on one side, each opening 35 mm in diameter and 50 mm deep, The openings are one in the middle of the model and one upper opening is 100 mm from the top edge of the model and the same is a third opening but at the bottom of the model.

The load is loaded gradually and as shown in Figure (4-11) until the column fails, as shown in the Figure (4-12). the model failed at 260 kN; the maximum displacement was 6.41 mm. When comparing these results with the results of the standard column (C1PCS),

The decline rate in this model was 11.86%, which is higher than the previous model (C1PC2F) which was the decrease 6.78%, and this is expected due to the increase in the number of openings in this model from two to three, and one of these three openings is in the middle, which is a weak area.

Figure (4-13) presents a comparison of the load-displacement curve of the column (C1PC3F) and the standard column (C1PCS).

Figure 4-11: Load column gradually

Figure 4-12: Column fails
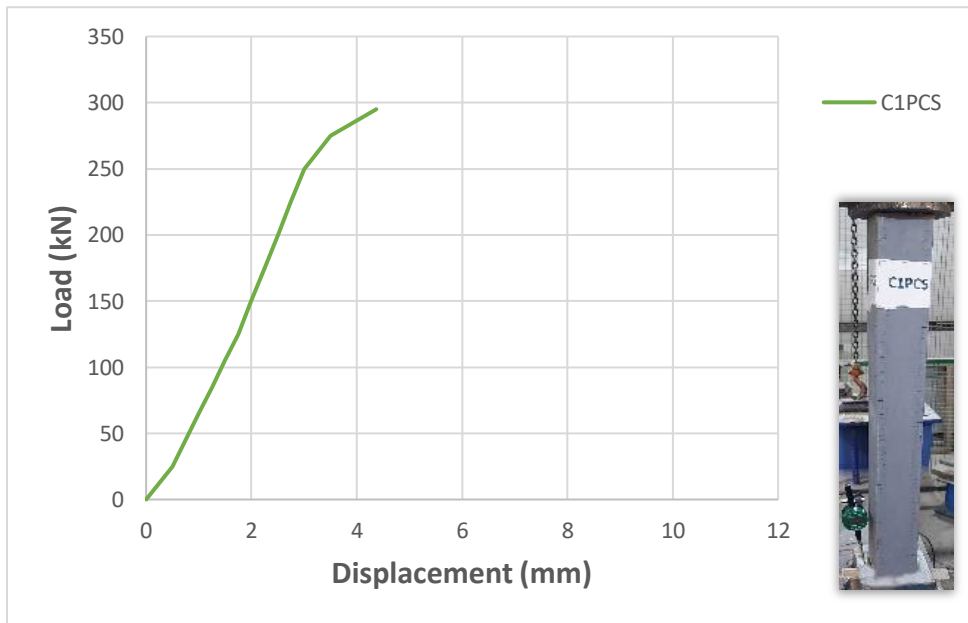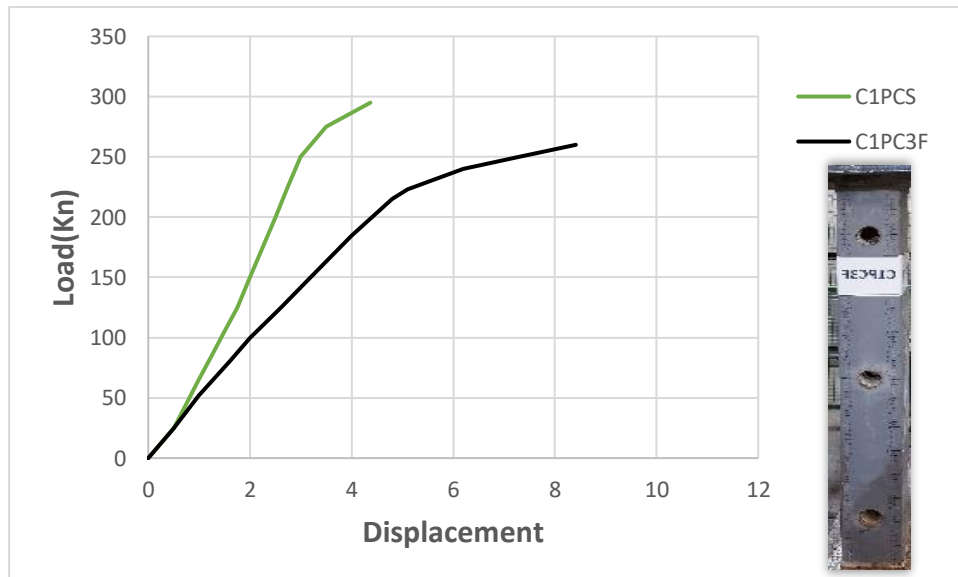

Figure 4-13: The load-displacement curve - C1PCS&C1PC3F columns

4.3.3   Columns with openings on two opposite sides

This group includes three columns, as shown in the Figure (4-14)

Figure 4-14: Columns with openings on opposite sides

4.3.3.1 C1PC1F1R Column

This column specimen has a opening through opposite sides of 35 mm diameter. The column is filled with normal concrete. The load is gradually loaded, as shown in the Figure (4-15), until the column fails, as shown in Figure (4-16).

The model failed at 270 kN; the maximum displacement achieved was 6.71 mm. When comparing these results with the results of the standard column (C1PCS), it was found that the bearing capacity of this column decreased by 8.47%.

Figure (4-17) presents a comparison of the load-displacement curve of the column (C1PC1F1R) and the standard column (C1PCS).

Figure 4-15: Load column gradually


Figure 4-16: Column fails
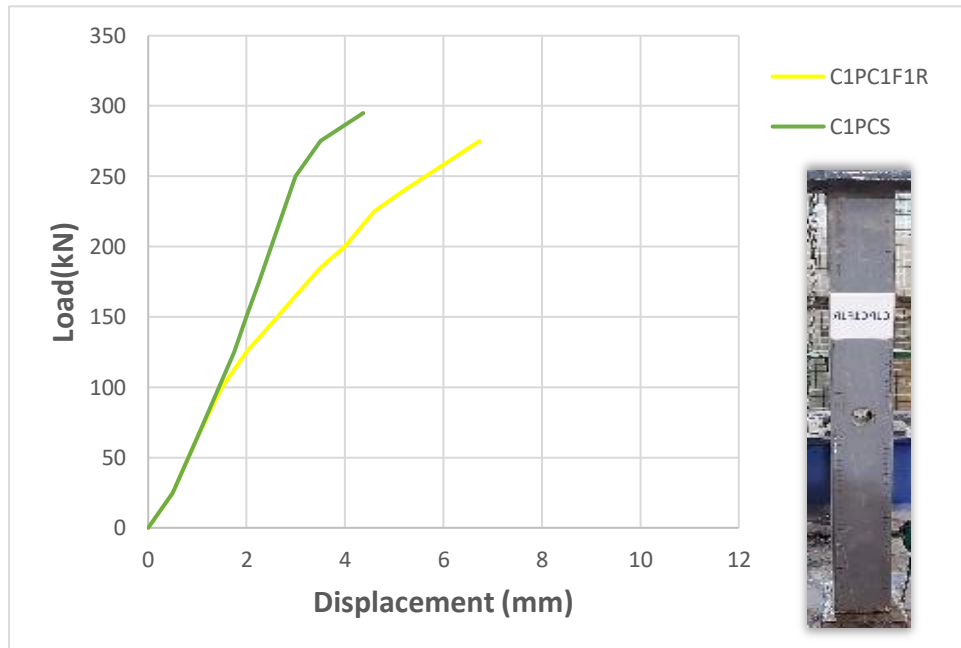
Figure 4-17: Load-displacement curve- C1PCS&C1PC1F1R columns

4.3.3.2 C1PC2F2R Column

This column specimen has two openings on opposite sides; each opening diameter is 35 mm. The column is filled with normal concrete. The load is loaded gradually and as shown in Figure (4-18) until the column fails, as shown in Figure (4-19). The model failed at 250 kN; the maximum displacement was 8.63 mm. When comparing these results with the results of the standard column (C1PCS), it was found that the bearing capacity of this column decreased by 15.25%. This ratio is increased due to the two openings on the sides, which reduces the load-bearing capacity.

Figure (4-20) presents a comparison of the load-displacement curve of the column (C1PC2F2R) and the standard column (C1PCS).

*Figure 4-18: Load column gradually*   *Figure 4-19: Column fails*
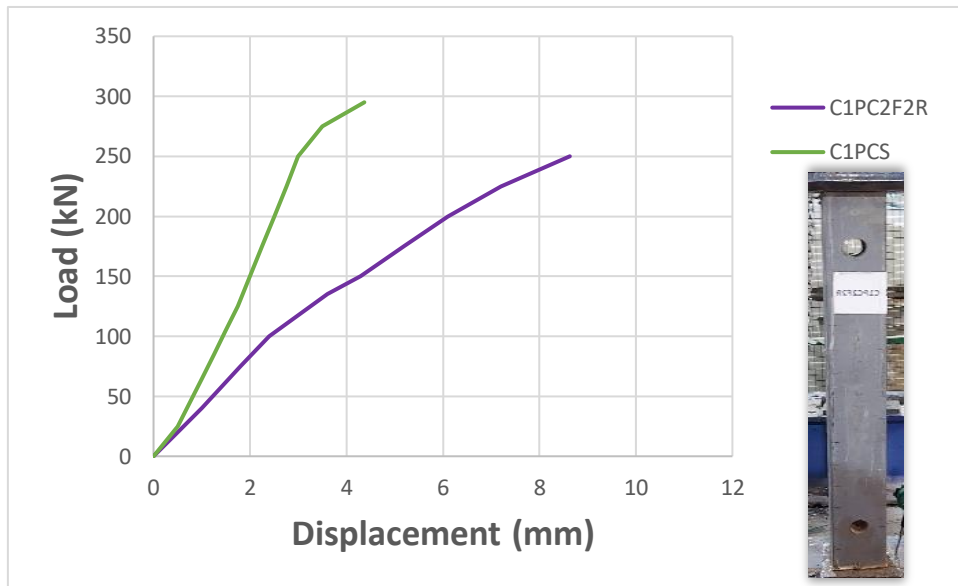
Figure 4-20: Load-displacement curve- C1PCS&C1PC2F2R columns

4.3.3.3 C1PC3F3R Column

This column specimen has three openings on opposite sides; each opening diameter is 35 mm. The column is filled with normal concrete.

The load is loaded gradually and as shown in Figure (4-21) until the column fails, as shown in Figure (4-22). The model failed at 240 kN; the maximum displacement was 8.40 mm. When comparing these results with the results of the standard column (C1PCS), it was found that the bearing capacity of this column decreased by 18.64%. The reason for a further decrease in the bearing capacity of the column (C1PC3F3R) was due to the increase in the number of openings to six openings (three on each side). Figure (4-23) provided a comparison of the load displacement curve of the column (C1PC3F3R) and the standard column (C1PCS).

Figure 4-21: Load column gradually


Figure 4-22: Column fails
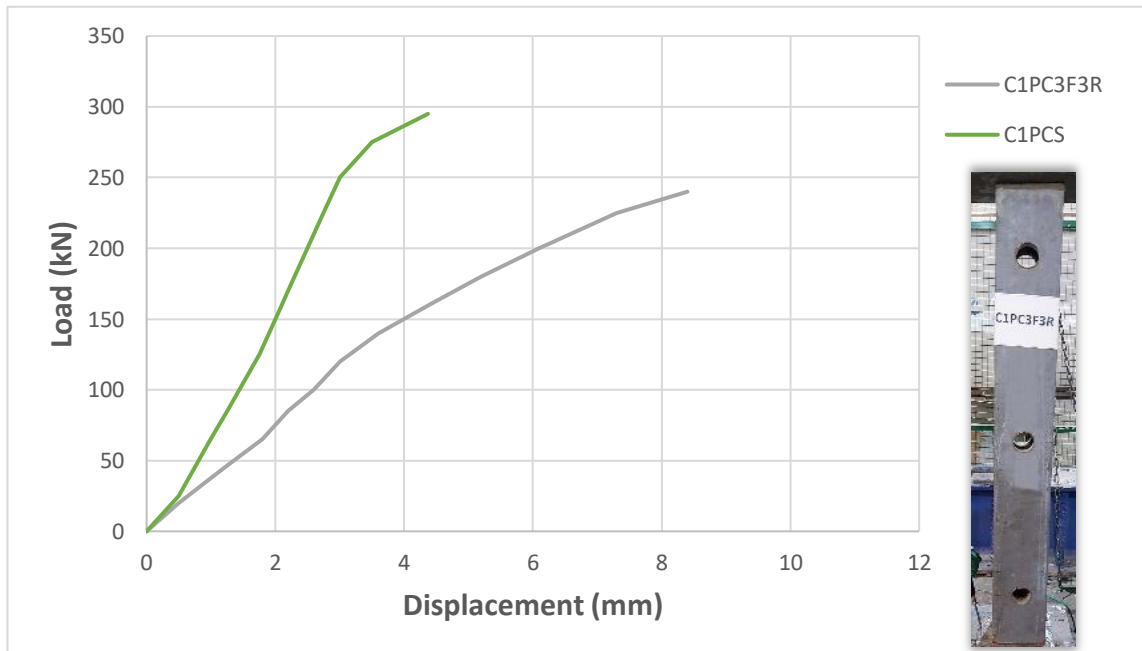
Figure 4-23: Load-displacement curve - C1PCS&C1PC3F3R columns

4.3.3.4 Load-Displacement Curve for All Group One

Figure (4-24) represents a combined case of the load-displacement curve for group one .
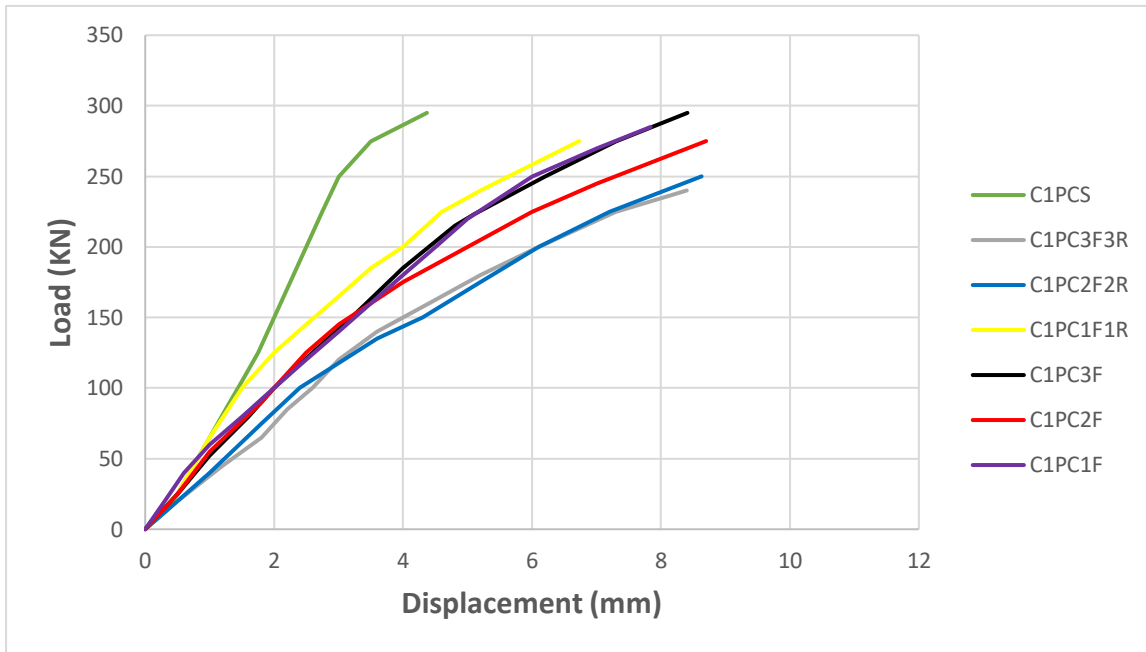
Figure 4-24: Load-displacement curve - all group one.

4.3.4 Control column (C2FCS)- Group two

The C2FCS column is the control column for a group (No.2), and this group consists of seven columns that are all filled with plastic fiber concrete. The column is installed on the testing machine, and LVDTs are prepared in their respective locations Figure (4-25). The load is gradually applied to the control column until the column fails, as shown in the Figure (4-26).

Through experience, it was found that this column failed at a load of 340 kN, as shown in Figure (4-27), and the installed displacement of the LVDTs is 8.22 mm.

Figure 4-25: C2FCS column test

Figure 4-26: C2FCS column failure
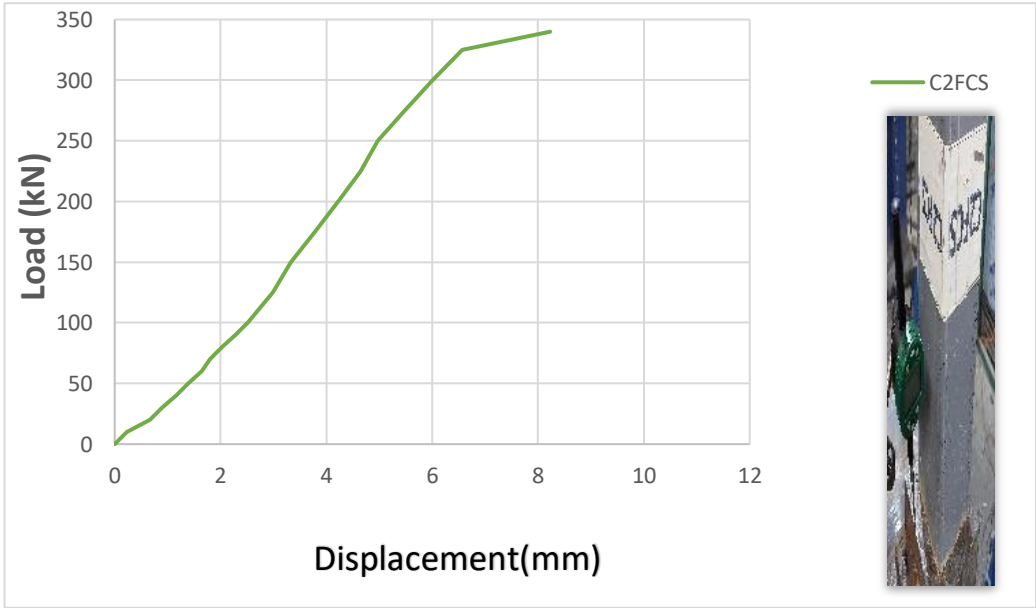
Figure 4-27: Load-displacement curve - C2FCS column

61

The failure of the C2FCS columns is due to the local buckling of the outer steel tube, the presence of concrete between the two tubes helping the failure not to reach the inner tube. The value obtained from this sample examination will be used to compare with the six models from the same group i.e. group (2) and these six samples are divided into:

- Three Columns with openings on one side.
- Three Columns with openings on opposite sides

4.3.5 Columns with openings on one side

This group includes three columns, as shown in Figure (4-28).
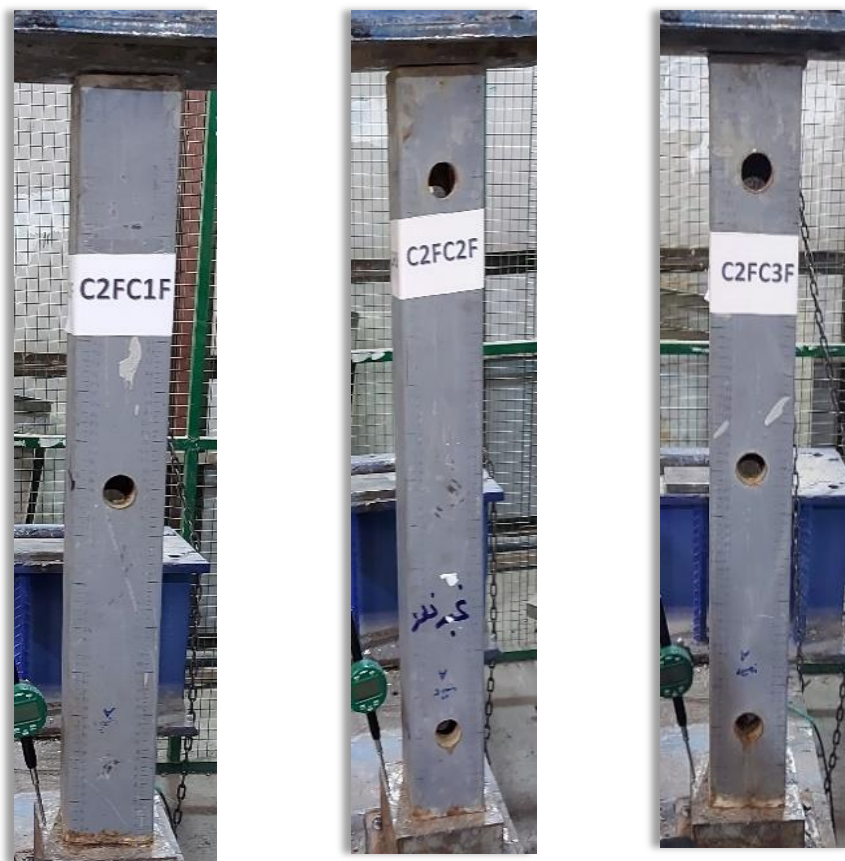
Figure 4-28: Columns with openings on one side

4.3.5.1 C2FC1F Column

This column specimen has a one-sided opening of 35 mm in diameter and 50 mm in depth, filled with plastic fiber concrete. The load is gradually loaded, as shown in Figure (4-29), until the column fails, as shown in Figure (4-30).

The model failed at 325 kN; the maximum displacement achieved was 10.75 mm. When comparing these results with the results of the standard column (C2FCS),it was found that the bearing capacity of this column decreased by 4.41%. This good result shows that the opening had little impact in this column. Figure (4-31) presents a comparison of the load-displacement curve of the column (C2FC1F) and the standard column (C2FCS).
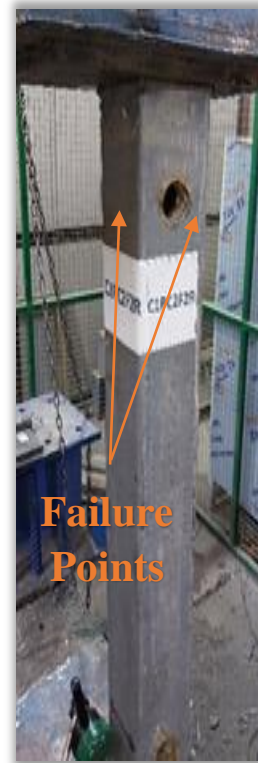

Figure 4-29: Load column gradually

Figure 4-30: Column fails

Figure 4-31: Load-displacement curve - C2FCS&C2FC1F columns

4.3.5.2 C2FC2F Column

This column specimen contains two openings on one side, each opening 35 mm in diameter and 50 mm deep, filled with plastic fiber concrete.

The load is loaded gradually as shown in Figure (4-32), until the column fails, as shown in the Figure (4-33). The model failed at 315 kN; the maximum displacement was 10.50 mm. When comparing these results with the results of the standard column (C2FCS), it was found that the bearing capacity of this column decreased by 7.35%. This is a good result because there are two openings in this column.

Figure (4-34) presented a comparison of the load-displacement curve of the column (C2FC2F) and the standard column (C2FCS).

Figure 4-32: Load column gradually


Figure 4-33: Column fails

Figure 4-34: The load-displacement curve - C2FCS&C2FC2F columns

4.3.5.3 C2FC3F Column

This column specimen contains three openings on one side, each opening 35 mm in diameter and 50 mm deep, filled with plastic fiber concrete. The load is loaded gradually as shown in Figure (4-35), until the column fails, as shown in Figure (4-36). The model failed at 310 kN; the maximum displacement was 8.63 mm. When comparing these results with the results of the standard column (C2FCS), it was found that the bearing capacity of this column decreased by 8.82%, meaning that the drop was greater than the previous model (C2FC2F), which was 7.35%, because this model contains more openings (three openings). Figure (4-37) presents a comparison of the load-displacement curve of the column (C2FC3F) and the standard column (C2FCS).

Figure 4-35: Load column gradually

Figure 4-36: Column fails
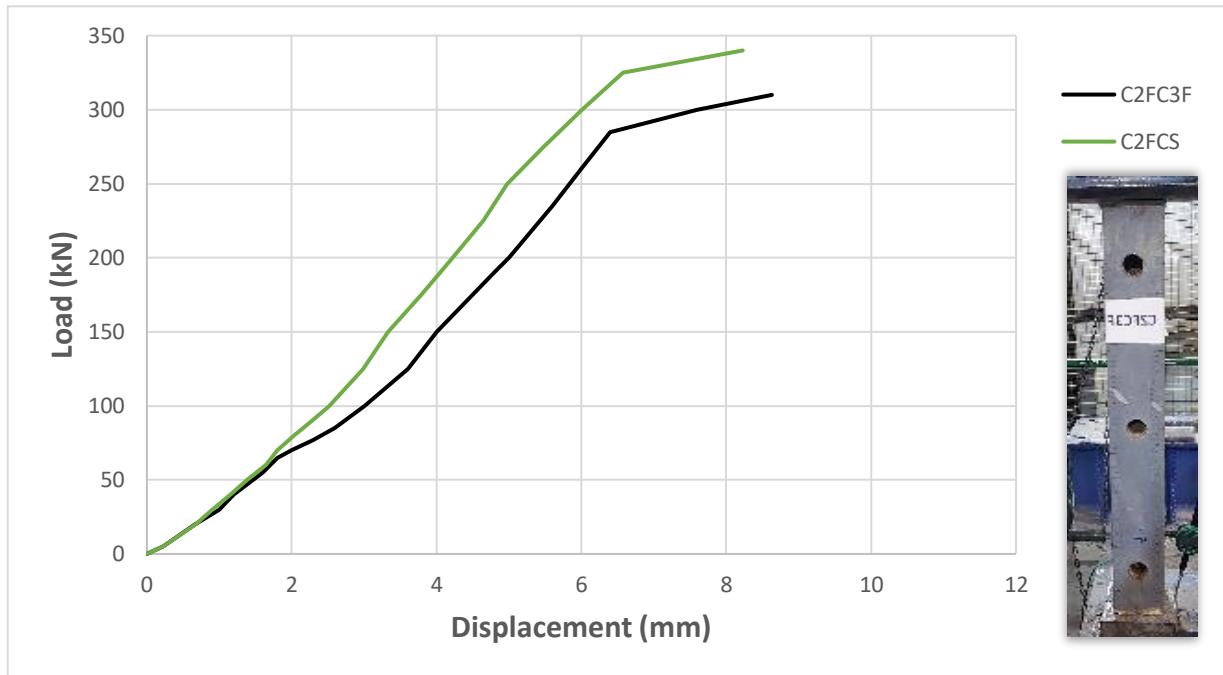
Figure 4-37: The load-displacement curve - C2FCS&C2FC3F columns

4.3.٦   Columns with openings on two opposite sides

This group includes three columns, as shown in Figure (4-38)

Figure 4-38: Columns with openings on opposite sides

4.3.6.1 C2FC1F1R Column

This column specimen has a opening through opposite sides of 35 mm diameter. The column is filled with plastic fiber concrete. The load is gradually loaded, as shown in Figure (4-39), until the column fails, as shown in Figure (4-40).

The model failed at 310 kN; the maximum displacement achieved was 8.25 mm. When comparing these results with the results of the standard column (C2FCS), it was found that the bearing capacity of this column decreased by 8.82%. It is almost identical to column (C2FC1F1R), which resulted in 8.47%.

Figure (4-41) presented a comparison of the load-displacement curve of the column (C2FC1F1R) and the standard column (C2FCS).

Figure 4-39: Load column gradually

Figure 4-40: Column fails
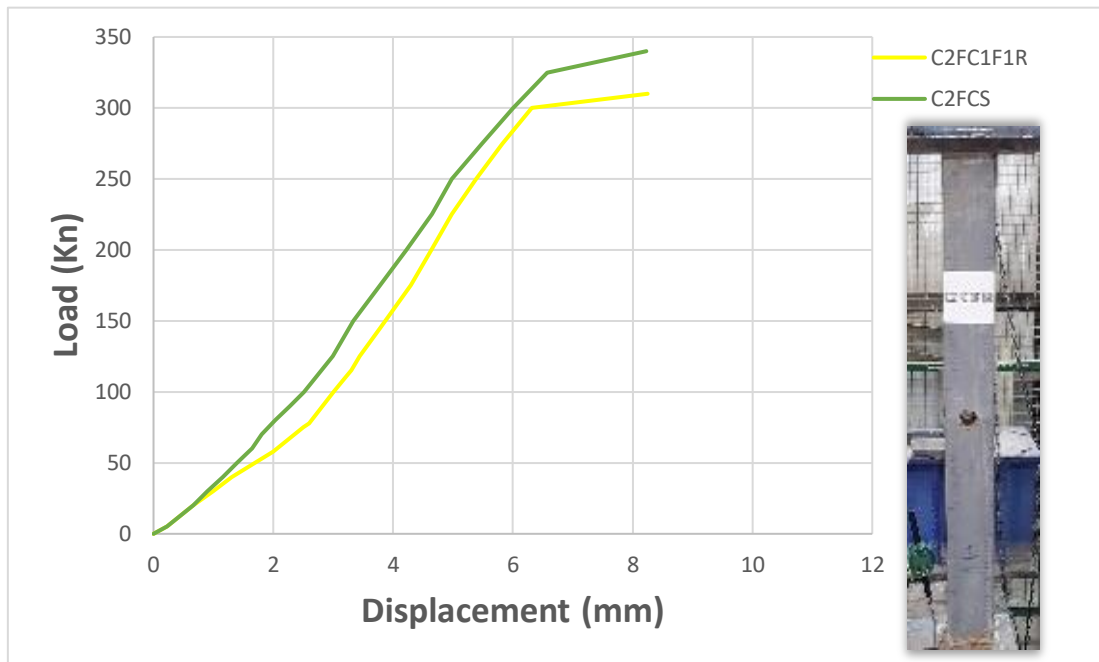
Figure 4-41: Load-displacement curve - C2FCS&C2FC1F1R columns

4.3.6.2 C2FC2F2R Column

This column specimen has two openings on opposite sides; each opening diameter is 35 mm. The column is filled with normal concrete.

The load is loaded gradually, as shown in Figure (4-42) until the column fails, as shown in Figure (4-43). The model failed at 320 kN; the maximum displacement was 12.00 mm. When comparing these results with the results of the standard column (C2FCS), it was found that the bearing capacity of this column decreased by 5.88%.

Figure (4-44) presented a comparison of the load-displacement curve of the column (C2FC2F2R) and the standard column (C2FCS).

Figure 4-42: Load column gradually

Figure 4-43: Column fails
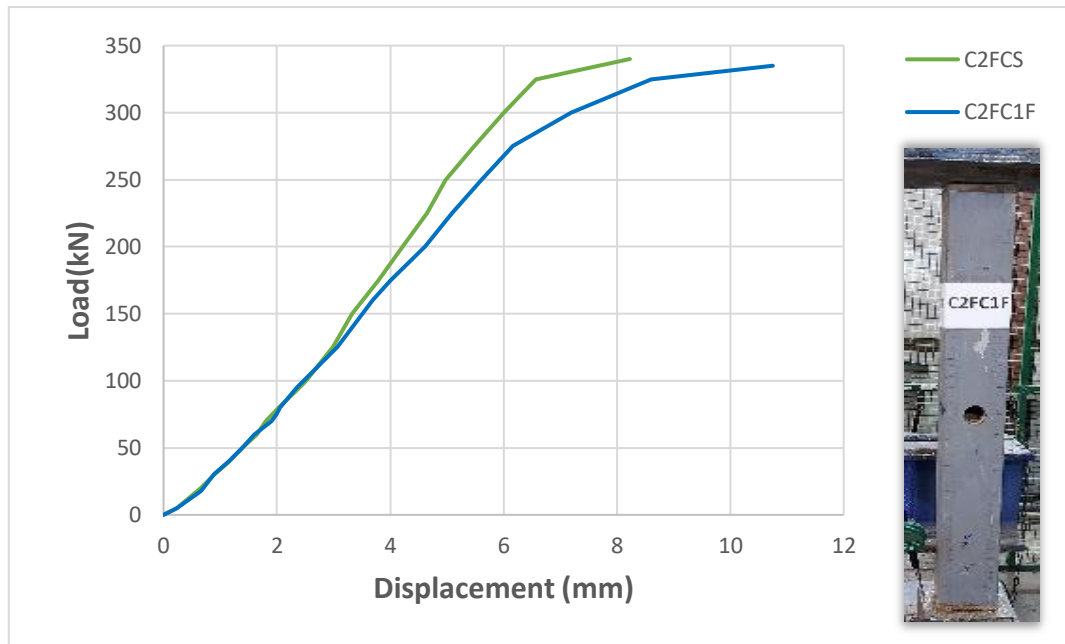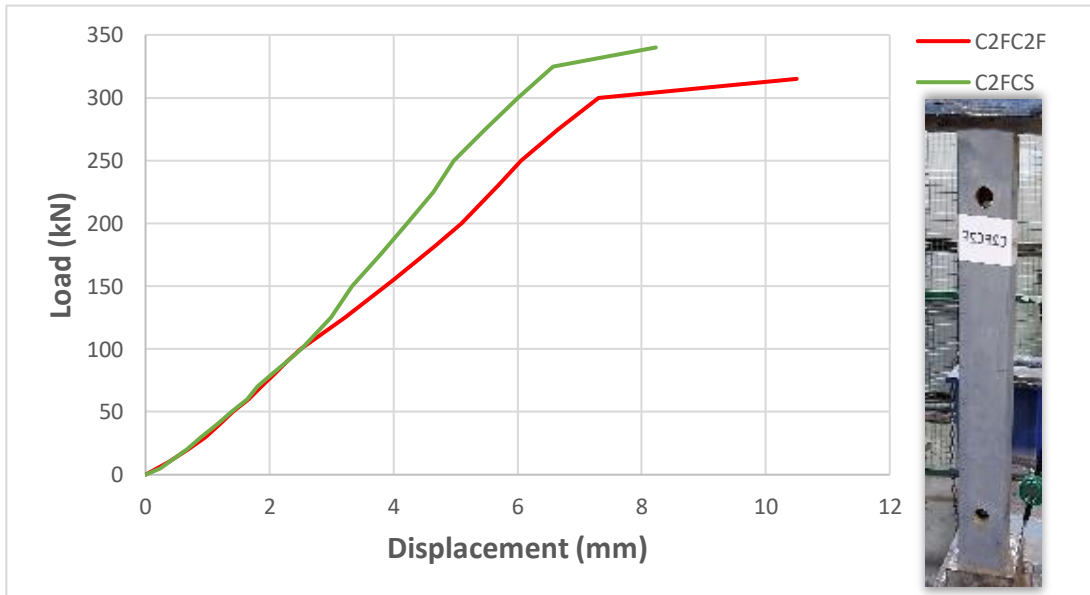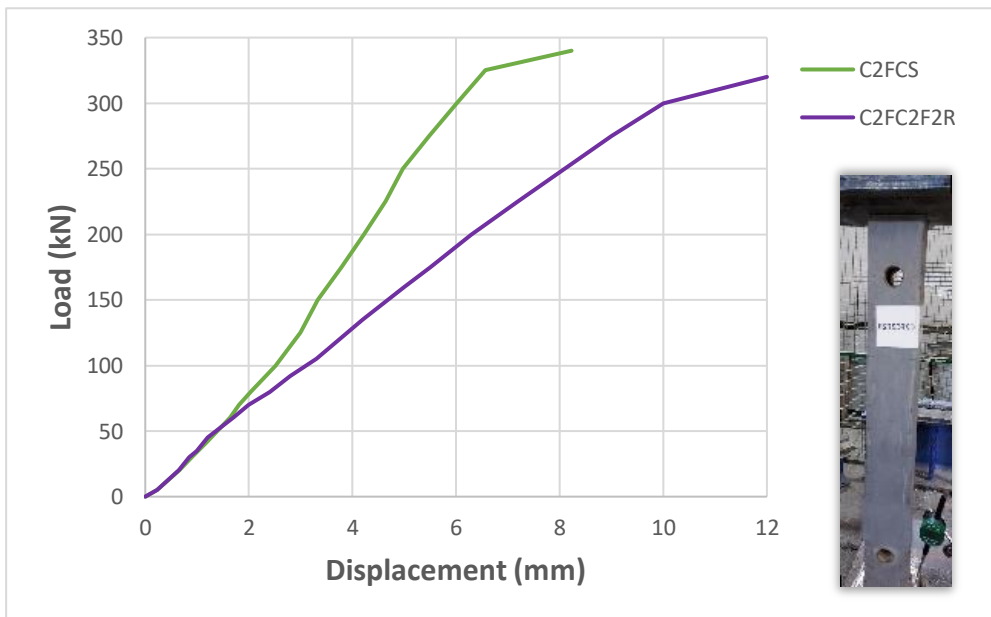

Figure 4-44: Load-displacement curve - C2FCS&C2FC2F2R columns

4.3.6.3 C2FC3F3R Column

This column specimen has three openings on opposite sides; each opening diameter is 35 mm. The column is filled with normal concrete.

The load is loaded gradually as shown in Figure (4-45), until the column fails, as shown in the Figure (4-46). After a practical check, the model failed at 285 kN; the maximum displacement was 8.13 mm. When comparing these results with the results of the standard column (C2FCS), The bearing capacity of the column (C2FC3F3R) is significantly reduced, due to the increase in openings to six (three on each side), which makes the column weaker than the previous model (C2FC2F2R).

Figure (4-47) presents a comparison of the load-displacement curve of the column (C2FC3F3R) and the standard column (C2FCS).

Figure 4-45:   Load column gradually

Figure 4-46:   Column fails
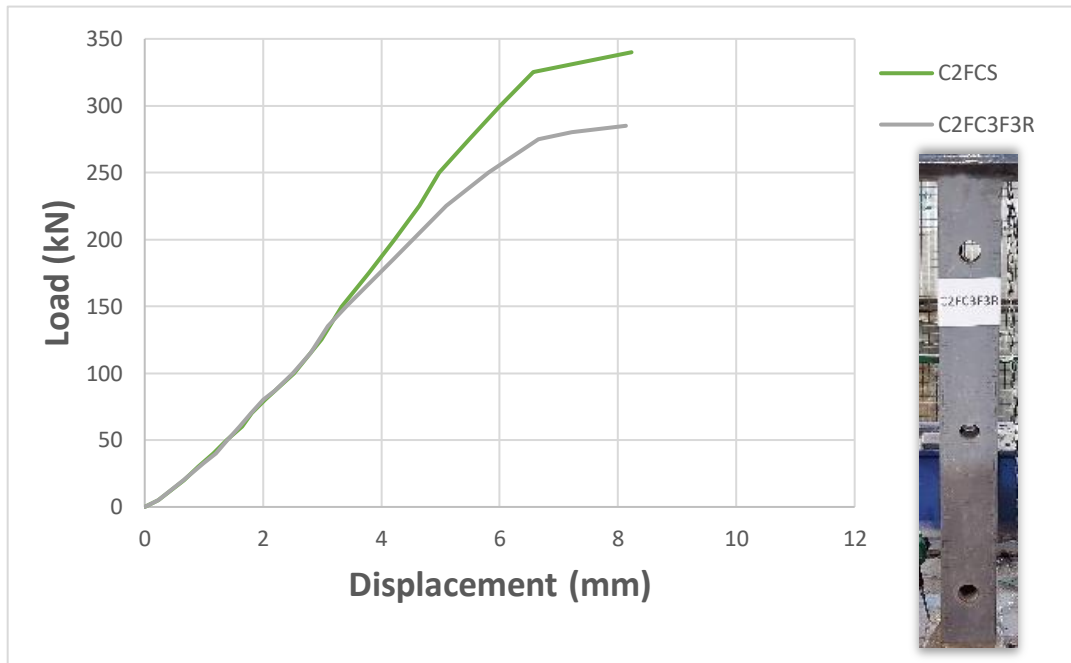
Figure 4-47: Load-displacement curve - C2FCS&C2FC3F3R columns

4.3.6.4 Load-Displacement Curve for All Group Two

Figure (4-48) represents a combined case of the load-displacement curve for group two.

4.4 Effect of Experimental Parametric Studies on Bearing Capacity of (CFDST) Columns with Various Openings.

Some of the variables were experimentally tested during the application of axial stress when testing the composite Concrete-filled double skin steel tubular (CFDST)). These parameters significantly impact the bearing capacity and the amount of displacement. The main parameters that were studied in this study are as follows:

1. The type of concrete used to fill the column (Normal concrete or Plastic fiber concrete).

2. The number of openings in the (CFDST) columns.

3. Number of sides with openings in (CFDST) columns (one or two opposite sides).

4.4.1 The type of concrete used to fill the column (The normal concrete or the plastic fiber concrete)

Changing the type of concrete that fills the tested models from the normal concrete to the plastic fiber concrete contributed to enhancing the load-bearing capacity and increasing the rigidity of a concrete-filled double-skin steel tubular column (CFDST).

The performance of the (PFC) models was better than the normal concrete models, as the high compressive strength of the(PFC) (about 40 MPa) helped give it better strength. In addition, the plastic fibers provide the cohesion strength between the concrete parts, and this gives better durability.

The number of openings also plays an important role in influencing the bearing capacity, as it is noted that the greater their number, the less the bearing capacity of the column, and this effect is more pronounced in (NC) models than in concrete models made of (PFC) because of the strength of the latter and thus the lack of impact of openings.

Table (4-1) shows the load-bearing capacity of tested models and the amount of difference when using the two types of concrete for the same tested model.
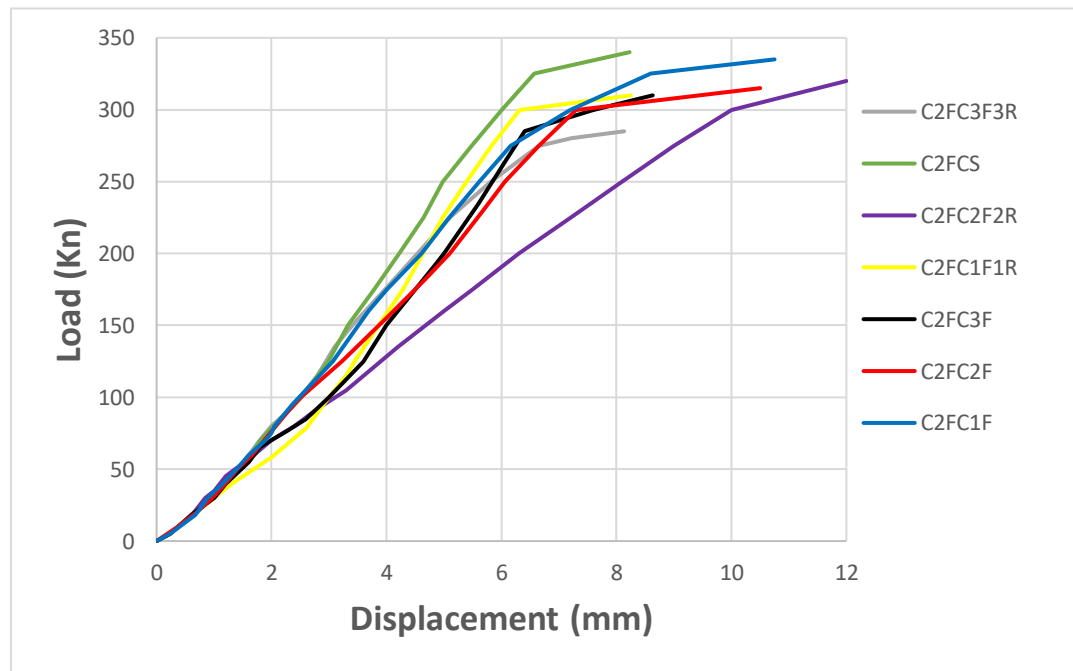
Figure 4-48: The load-displacement curve- all group two.

Table 4-1: The difference in the results of two types of concrete and for the same
tested models

No. of specimen	Specimen name	Ultimate load Pu (Kn)	Differ. P* (%)	Failure type
1	C1PCS	295	+15.25%	Local buckling(at the top area)
	C2FCS	340		Local buckling (in the middle)
2	C1PC1F	285	+14. 03%	Local buckling(at the top area)
	C2FC1F	325		Local buckling(at the top area)
3	C1PC2F	275	+14.54%	Local buckling(at the top openong area)
	C2FC2F	315		Local buckling(at the top openong area)
4	C1PC3F	260	+19.23%	Local buckling(at the top area)
	C2FC3F	310		Local buckling(at the top opening area)
5	C1PC1F1R	270	+14.81%	Local buckling(at the top area)

No. of specimen	Specimen name	Ultimate load Pu (Kn)	Differ. P* (%)	Failure type
	C2FC1F1R	310		Local buckling (in the middle opening region)
6	C1PC2F2R	250	+28.00%	Local buckling(at the top openong area)
	C2FC2F2R	320		Local buckling(at the down openong area)
7	C1PC3F3R	240	+18.75%	Local buckling(at the top area)
	C2FC3F3R	285		Local buckling(at the down openong area)

Difference P= $(\frac{PFC-NC}{NC})$ *100

Table (4.3) shows that plastic fiber concrete has increased the Maximum load by 14.03 to 28.00% and at a rate of 17.80%. This means that PFC has significantly improved the performance of this type of columns..

4.4.2 The number of openings in the concrete-filled double skin steel tubular (CFDST).

Table (4.2) below shows the effect of the number of openings in the column (openings on one side) on the load-bearing capacity. For the same type of concrete, the first group filled with normal concrete was relied upon, and the second group filled with plastic fiber concrete

for comparison, as the comparison was made with the standard column for each type of concrete.

It was noticed from the below table that the increase the number of openings, the lower of bearing capacity, and this ranged between -3.34 to -11.86 % and an average -7.32 for normal concrete columns, while for the concrete made of PFC , the ratio was -4.41 to -8.82% and average of -6.62, This means that the bearing capacity of the columns is inversely proportional to the openings, as the bearing capacity decreases with the increase in the number of openings. This is logical because the column becomes weaker as the number of openingsin it increases. These results are considered good and acceptable for this type of effect.

Table 4- 2: Effect of openings on the bearing capacity of normal concrete columns and plastic fiber concrete columns

Groupe name	*Specimen name (S.N)*	*Ultimate load (Pu) (kN)*	*Differ. (P) (%)*
	Normal Concrete		
Group (1)	C1PCS	295	0%
	C1PC1F	285	-3.34%
	C1PC2F	275	-6.78%
	C1PC3F	260	-11.86%
	Plastic Fiber Concrete		
Group (2)	C2FCS	340	0%
	C2FC1F	325	-4.41%
	C2FC2F	315	-7.35%
	C2FC3F	310	-8.82%

4.4.3 Number of sides with openings in concrete-filled double skin tube (CFDST)

Table (4-3) below shows the effect of the number of sides on which the openings are located (one side or two opposite sides) on the load bearing capacity. For the same type of concrete, the first group filled with normal concrete and the second group filled with plastic fiber concrete was used for comparison, and the comparison was made with the standard column for each type of concrete.

It was noted from the above table that the increase the number of openings (on both sides of the studied model), the lower the bearing capacity, and this ratio ranged between -8.74 and -18.64% and an average of 14.12% for normal concrete columns, while for PFC it ranged between -5.88 and -16.17% and an average of -10.29%.

Through the above results, it was found that the achieved rate in the normal concrete models (14.12%), in the plastic fiber concrete models, the average was (10.29%.) meaning that there is a difference of (03.83%.) in favor of the (PFC) models, meaning that the (PFC) has improved the performance of these columns by (03.83%), which is expected given that the compressive strength of the plastic fiber concrete was higher than the normal concrete .

Table 4- 3: Effect of the number of perforated sides (one side or two opposite sides) on the load-bearing capacity

Groupe name	Specimen name	Ultimate load Pu (kN)	Differ. P** (%)
	Normal Concrete		
Group (1)	C1PCS	295	0%
	C1PC1F1R	270	-8.474%
	C1PC2F2R	250	-15.25%
	C1PC3F3R	240	-18.64%
	Plastic Fiber Concrete		
Group (2)	C2FCS	340	0%
	C2FC1F1R	310	-8.82%
	C2FC2F2R	320*	-5.88%
	C2FC3F3R	285	-16.17%

* The reason for the higher bearing capacity of this column(C2FC2F2R) is higher than the previous one is due to the fact that its openings do not fall in the weak area of the column, i.e. in the middle of the model.

CHAPTER FIVE: FINITE ELEMENT ANALYSIS

Chapter Five

Finite Element Analysis

5.1 General

Abaqus Version 2019 software was used to represent and analyze the behavior of CFDST complex column models using a finite element package(Kim et al., 2021) .

This chapter of the study describes the limits of the models of the elements adopted in the research. Numerical models were adopted to analyze the studied column models, consisting of seven CFDST composite columns of normal concrete and seven CFDST composite columns of plastic fiber concrete. Linear analysis was used to solve these models (Ahmed et al., 2020).

The acceptance of the results of the samples obtained by finite element analysis is checked by comparing these results with the results of practical samples obtained from the laboratory (Li et al., 2013) . Using the theoretical data of the program, the approved models are verified. The deformation load curve was also discussed, and its results were compared with the experimental results of each model.

5.2 Test Electronic Forms for Columns (CFDST)

Fourteen samples represent the total number of composite columns tested in this study. Seven samples of CFDST composite columns of normal concrete, divided to one column without openings, three columns with different openings on one side, and three columns with multiple openings on both sides. Seven samples of CFDST composite columns of plastic fiber concrete were divided into one column without openings, three columns with different openings on one side, and three columns with different openings on both sides. These 14 samples were used to verify the numerical analysis on which the Abaqus software is based.

5.3 Finite Element Modeling

Analyzing the concrete in the Abaqus program, it relied on analyzing the behavior of concrete using concrete damage plasticity (Huang et al., 2010).

The analysis of the steel model relied on the Von Mises theory of failure.

All this requires providing the program with some information and engineering details of tested models in terms of:

1- Types of elements and the nature of their mesh.

2 - The nature of the interaction between the materials of the tested elements.

3- Engineering properties of materials for the tested elements.

The steel tubes were represented using three-dimensional models consisting of 8 nodes (C3D8), while the concrete was represented by models consisting of 4 nodes (C4 R). Surface-to-surface contact in the program interface studs was used as a connector to connect the concrete and the two steel pipes (inner and outer). As shown in Figures (5-1) and (5-2) a coefficient of friction between concrete and steel of (0.٦٥) was (Rabbat & Russell, 1985).
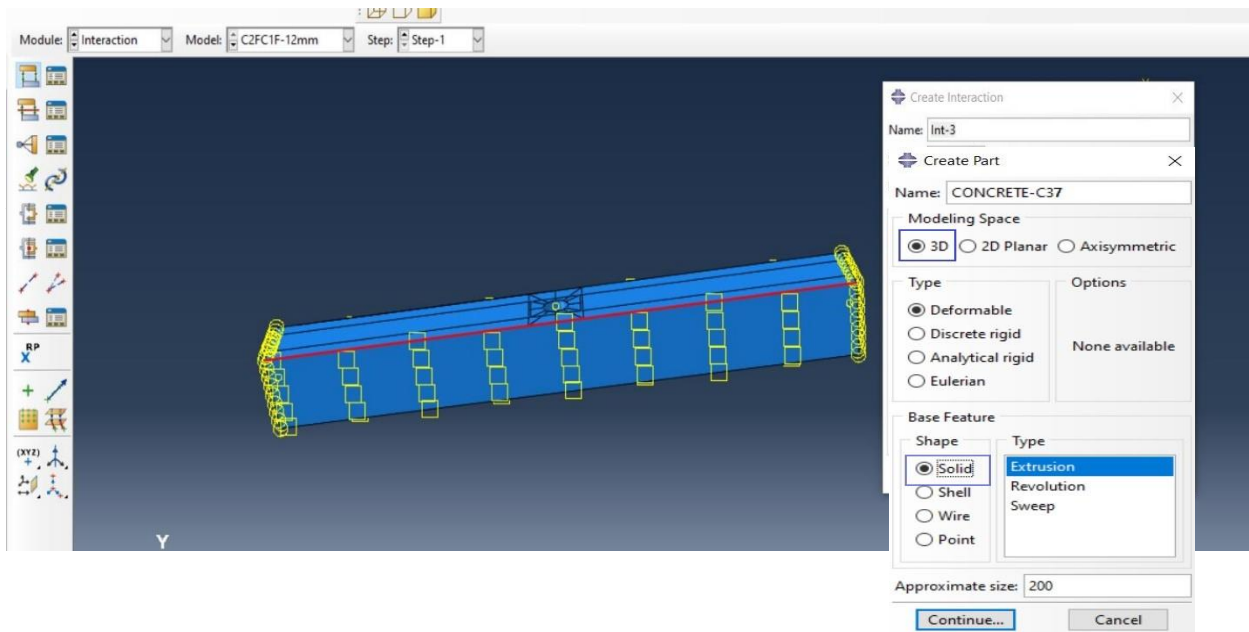
Figure 5-1: Surface-to-surface contact
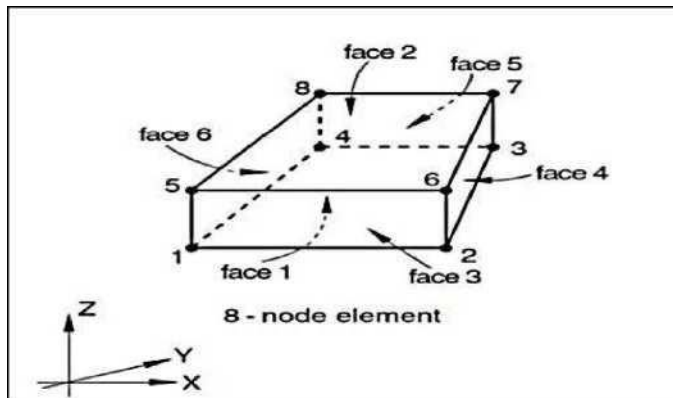
*Figure 5-2: Solid element (**Punshi, 2003***)*

Since the steel tube (inner and outer) has a small thickness (2mm) compared to the other dimensions, a three-dimensional four-knotted element S4R (Shell) of third-degree was used for each node, as shown in Figure (5-3**).**
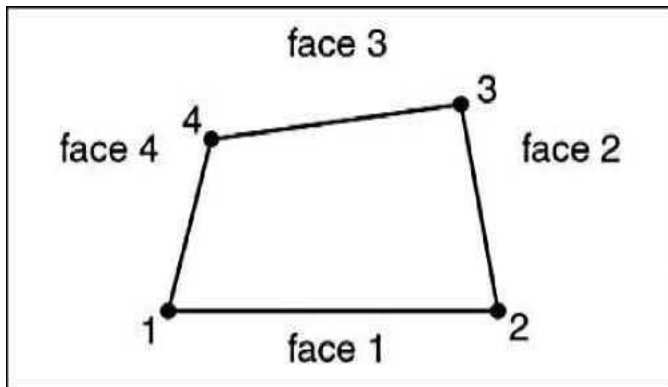
*Figure 5-3: Shell element (**Punshi, 2003***)*
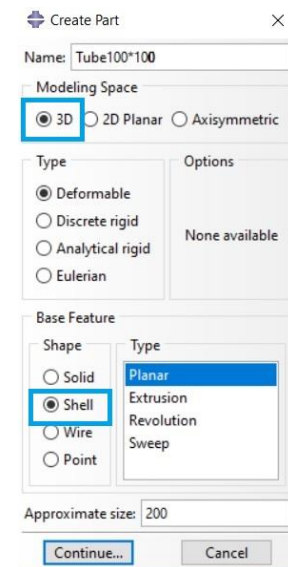
5.3.1 Parts and assembly

The results of the tests (tensile strength of steel and pressure of concrete) described in this study's third chapter were used to provide the program with the engineering information necessary to complete the models shown in Figure (5-4).

Steel is a homogeneous material, so the tensile strength listed in the laboratory test is approximately equal to the compressive strength.

Concrete is a brittle material whose tensile strength is much lower than the compressive strength obtained from laboratory testing. The properties of its constituent materials are listed in Appendix B.

(1) C1PCS-C2FCS

(2) C1PC1F-C2FC1F   (3) C1PC2F-C2FC2F   (4) C1PC٣F-C2FC٣F

(5)C1PC1F1R-C2FC1F1R   (6)   C1PC2F2R-   (7) C1PC3F3R-C2FC3F3R
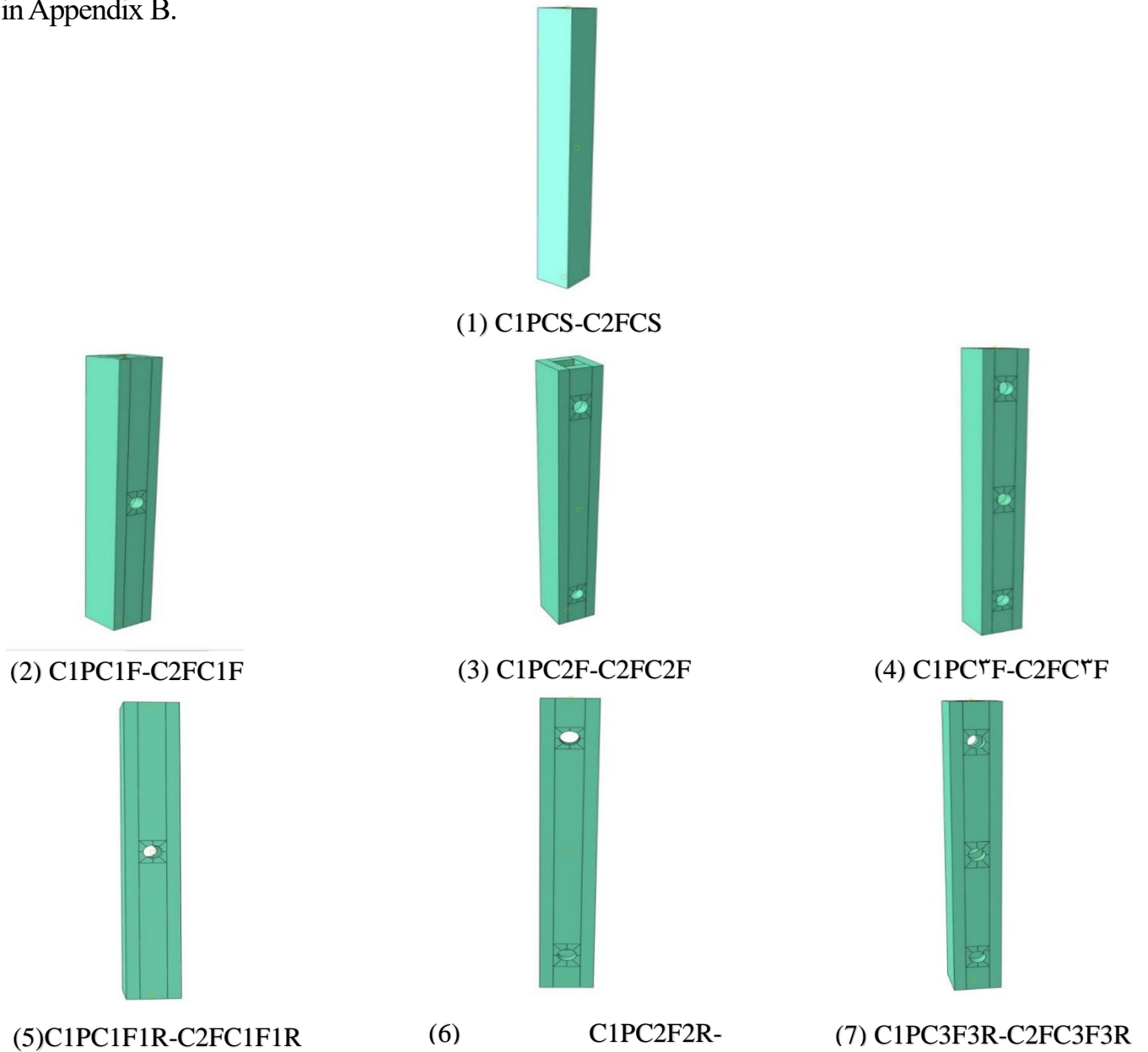
Figure 5-4: Approved Forms in Abaqus

5.3.2 The dimensions of the mesh elements used

Choosing an appropriate mesh size for finite element model analysis is an important step in avoiding the influence of mesh size on the analysis results. Four variable mesh sizes were adopted for pattern analysis (12.5, 15, 20, 25) mm. They are evident in Figure (5-5), and it is noted in Figure (5-6) how convergent the load and displacement curves of the C1PCS column sample are using the mesh sizes (12.5, 15, 20, 25) mm, so it was chosen that the measurement of the mesh used in the analysis be 12.5 mm to ensure the highest accuracy.
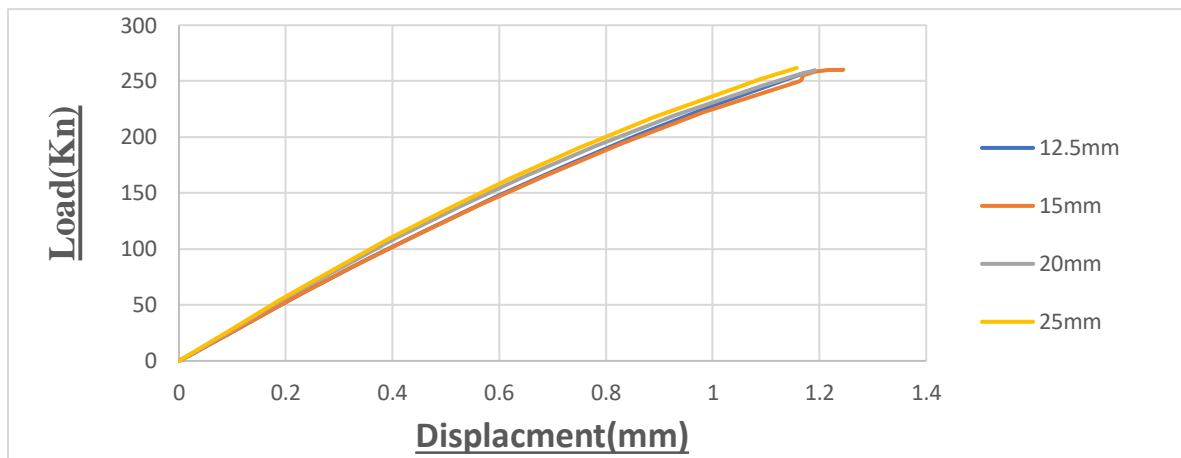
Figure 5-5: Effect of mesh size in the Load- Displacement relationship of C1PCS column

| Case1: Mesh 12.5mm | Case2: Mesh 15mm | Case2: Mesh 20mm | Case2: Mesh 25mm |
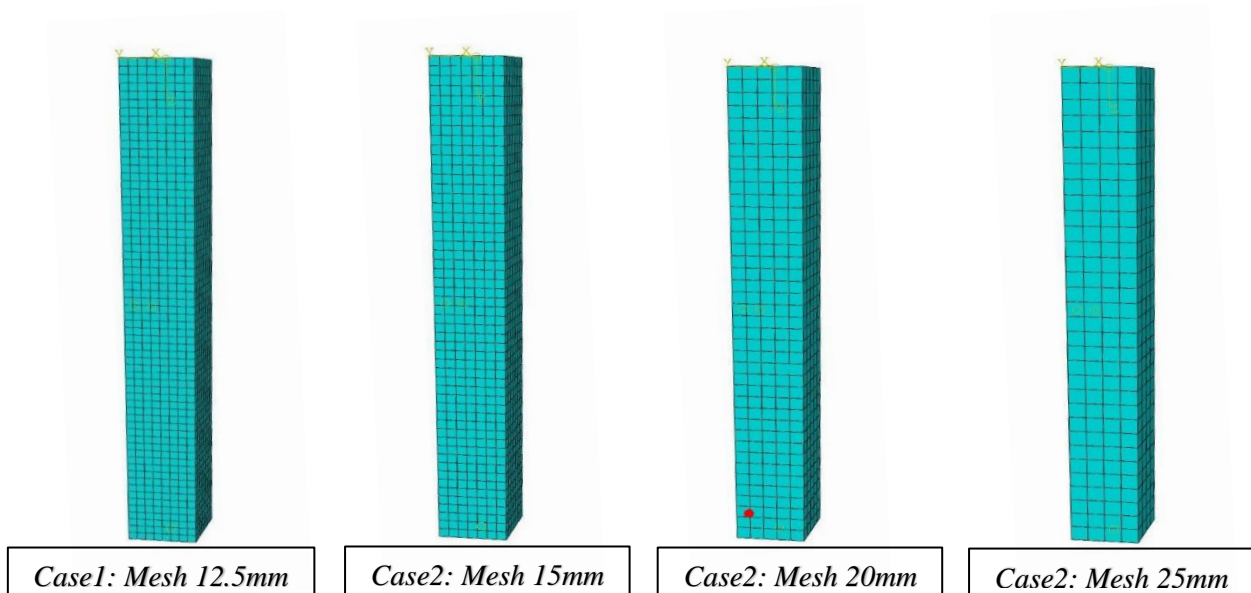
Figure 5-6: C1PCS Columns-different mesh size

5.3.3 Loading and Boundary Conditions

Figure (5-7) shows that the lower surfaces of the tested columns are constrained by all degrees of freedom

Figure 5-7: Support conditions

On the top of the test specimen, a load is applied, a square steel plate (120*120*20) mm distributes this load evenly over the entire top surface and, similar to that found in a laboratory, using a displacement control pattern on top of the specimen axial pressure loads were simulated. Due to the number of models analyzed in this study, and to accurately calculate the resulting load, the following steps were followed:

1- The upper surface of the upper steel plate is selected and then the distributed load is applied to it as shown in the Figures (5-8) and (5-9).
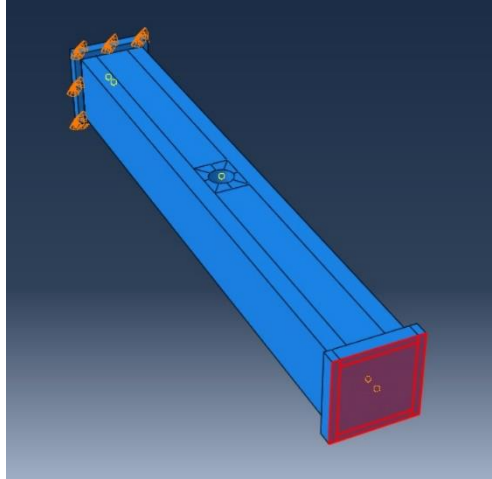
Figure 5-8: Selection of the upper surface of the upper steel plate
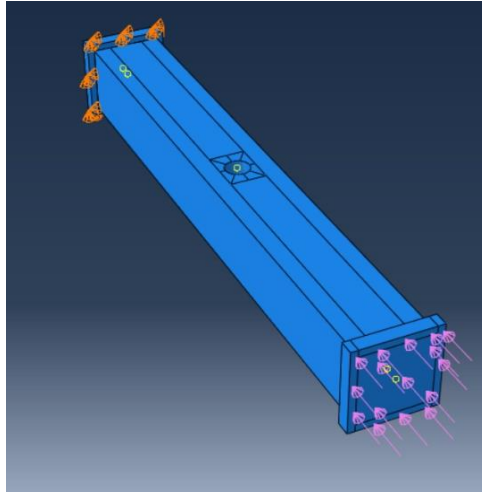
Figure 5-9: Load application

2- Using sit in assembly, the points of the upper surface of the column model are chosen and we call them the bearing surface, as shown in Figure (5-10).
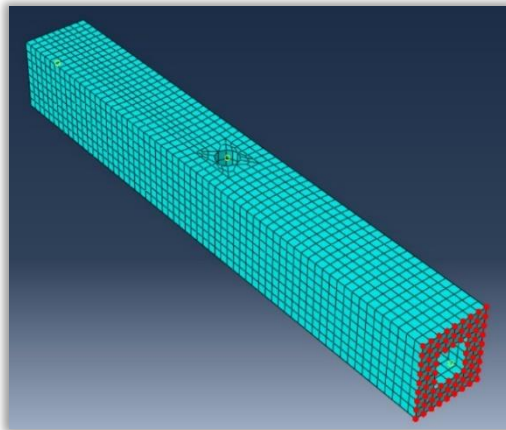
Figure 5-10: Choosing a column top loading surface

85

3- Using the tie option in the reaction menu, the lower surface of the upper steel plate mentioned in 1 above is connected to the upper points of the column (the load surface mentioned in paragraph 2 above), as shown in Figures (5-11) and (5-12). Thus, the load is transferred from the steel plate to the inspection column model, similar to the process in the laboratory.
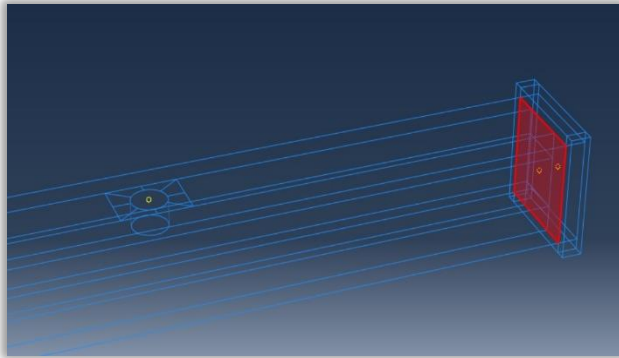
Figure 5- ١١: Choosing the bottom surface of the top steel plate
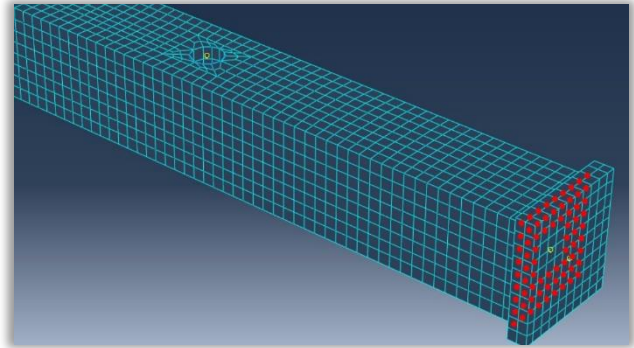
Figure 5- ١٢: Choosing a column top loading surface

5.3.4 Modelling Analysis

- Abaqus has two structural solvers for solving mechanical and structural problems.

- Abaqus/ implicit: implicit techniques are used to solve linear and nonlinear problems.

- Abaqus/ explicit: explicit techniques are used to solve linear and nonlinear problems.

Probably it can be said that the static general step is Abaqus's most famous and practical step (2019). It is one of the available steps of Abaqus/standard solver. It is developed for simulating linear and nonlinear static and quasi-static problems.

This step considers hyperplastic materials' rate-dependent effect and hysterical behavior while ignoring the time-dependent effects of materials such as creep, swelling, and viscoelasticity .

Figure (5-13) shows the use of static general steps in analyzing the tested models.
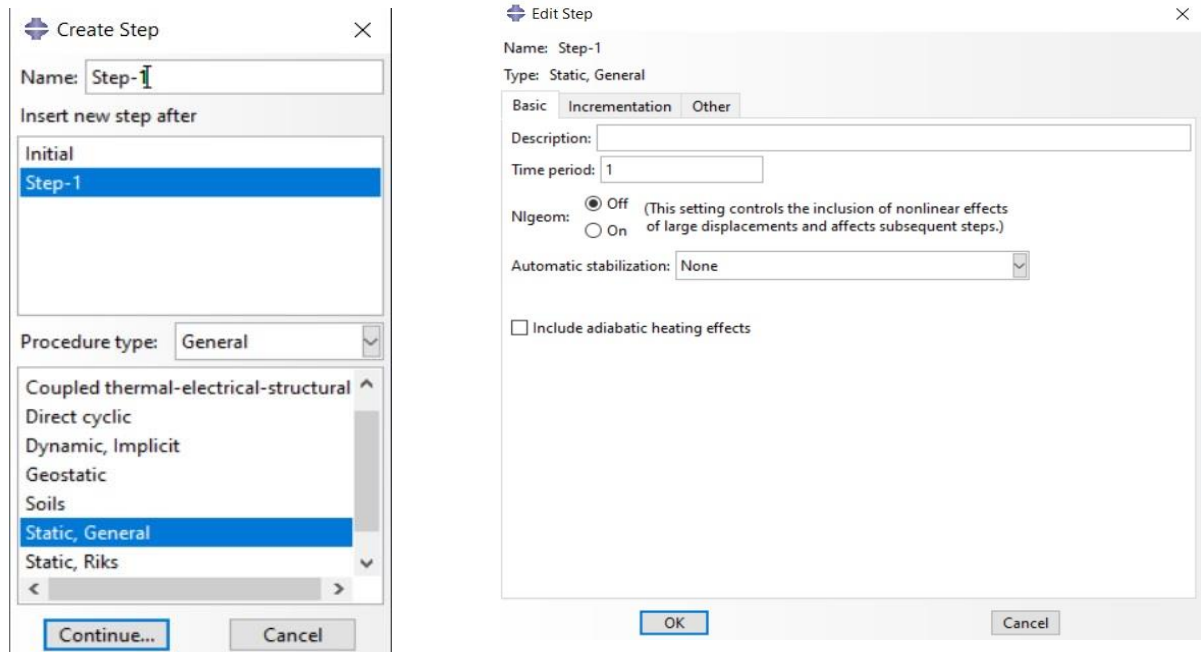
Figure 5-13: Static general step

5.4 Verification of Modeling Results

All (CFDST) samples were analyzed using the finite element method in the Abaqus software.

The analysis was conducted on fourteen samples, as shown in Figure (5-14), and it relied on a (12.5 mm) mesh scale, as mentioned in paragraph 5.3.2 above.
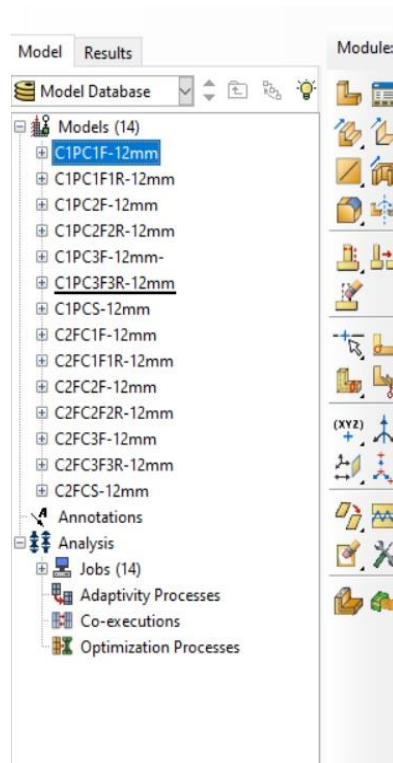
Figure 5-14: Fourteen model analysis

5.4.1 Modelling Verification of Circular Section

Verifying the results of the practical program with the numerical data of fourteen computer models and comparing their results with the results of the fourteen laboratory samples, each according to the corresponding computer model.

By observing the resulting numbers, it can be concluded that the results of FE have good agreement with the results of experimental work.

By comparing the results in Table (5-1) and Figure (5-15), it was found that they indicate a good agreement in terms of maximum resistance values and relative displacement between practical and theoretical values, where the highest difference was (-12.7%) for maximum resistance and (-28.57%) for displacement. These estimates are considered good and reasonable.

Table 5- 1 The differences between the FEM results and the results of the experimental work

of the fourteen models

Specimen	Ultimate load Pu (Kn)		Differ.P * (%)	Displacement at the ultimate load (mm)		Diff. Dis. ** (%)
	FEM	Exp.		FEM	Exp.	
Group 1 (Normal Concrete)						
C1PCS	295	295	0	٣,٩٢	٤,٣٧	-١٠.٢٩
C1PC1F	267	285	-6.30	9.6	7.84	+22.00
C1PC2F	260	275	-5.45	8.4	8.7	-3.45
C1PC3F	240	260	-7.69	٧.٣	٦.411	+١٣.٨٨
C1PC1F1R	237	270	-12.22	٥,١	6.731	-23.88
C1PC2F2R	231	250	-7.60	6.4	8.67	-26.18
C1PC3F3R	210	240	-7.50	6.85	8.4	-18.45
Group 2 (Plastic Fiber Concrete)						
C2FCS	310	340	-8.60	6.3	8.228	-23.43
C2FC1F	300	325	-7.70	8.2	10.75	-23.72
C2FC2F	297	315	-8.80	7.5	10.5	-28.57
C2FC3F	306	310	-1.29	6.9	8.63	-20.00
C2FC1F1R	298	310	-3.87	7.2	8.25	-12.72
C2FC2F2R	313	320	-2.20	9.1	12	-24.16
C2FC3F3R	255	285	-10.52	6.4	8.188	-21.84

➢ **Difference P=** $\frac{FEM-Exp.}{\text{Exp.}}$ ***100**

➢ **Difference Dis.** $= \frac{FEM-Exp.}{Exp.}$ ***100**

Figure (5-15) compares the load-displacement curve for the FEM models and the fourteen laboratory models, each according to their equivalents (Continued).
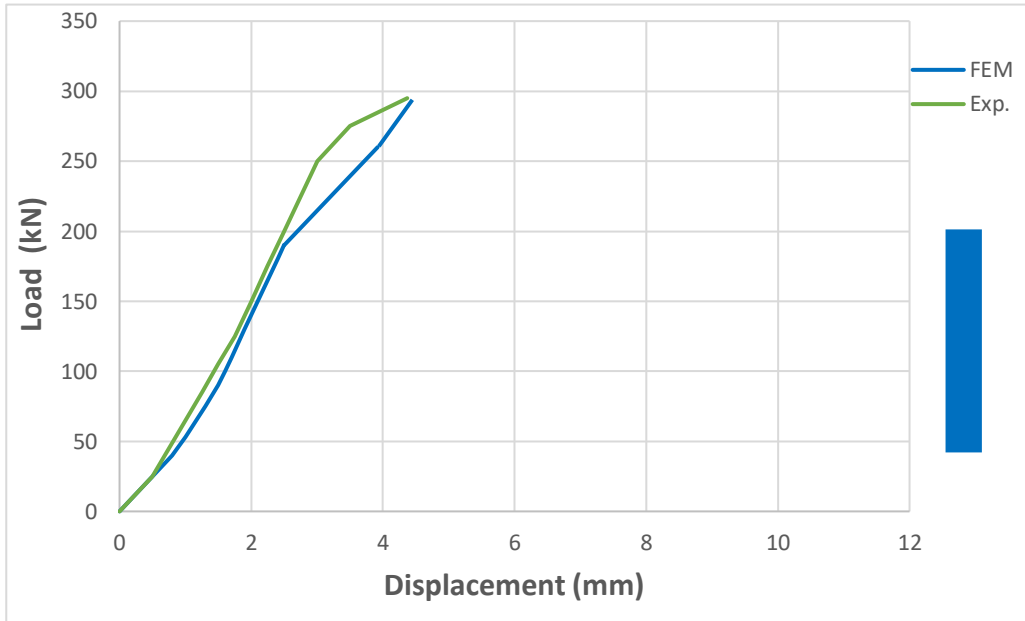
Load-Displacement curve for (C1PCS) column
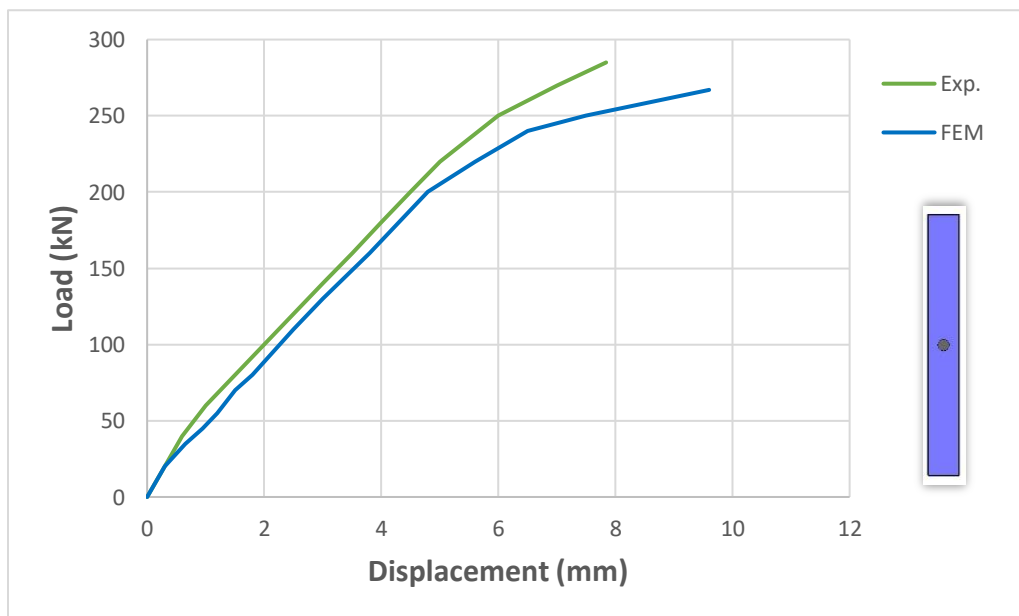
Load-Displacement curve for (C1PC1F) column
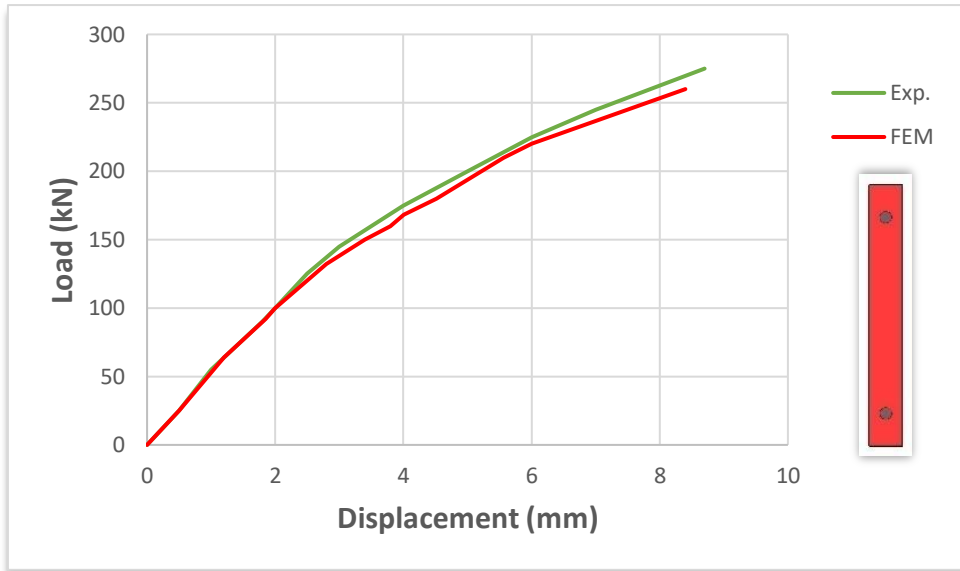
Cont.

Load-Displacement curve for (C1PC2F) column
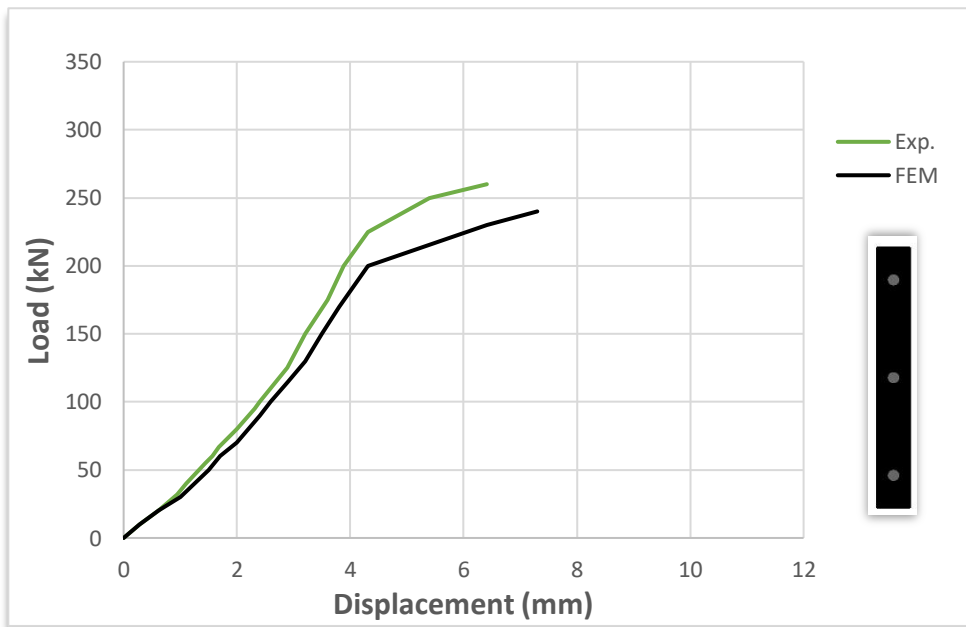
Load-Displacement curve for (C1PC٣F) column
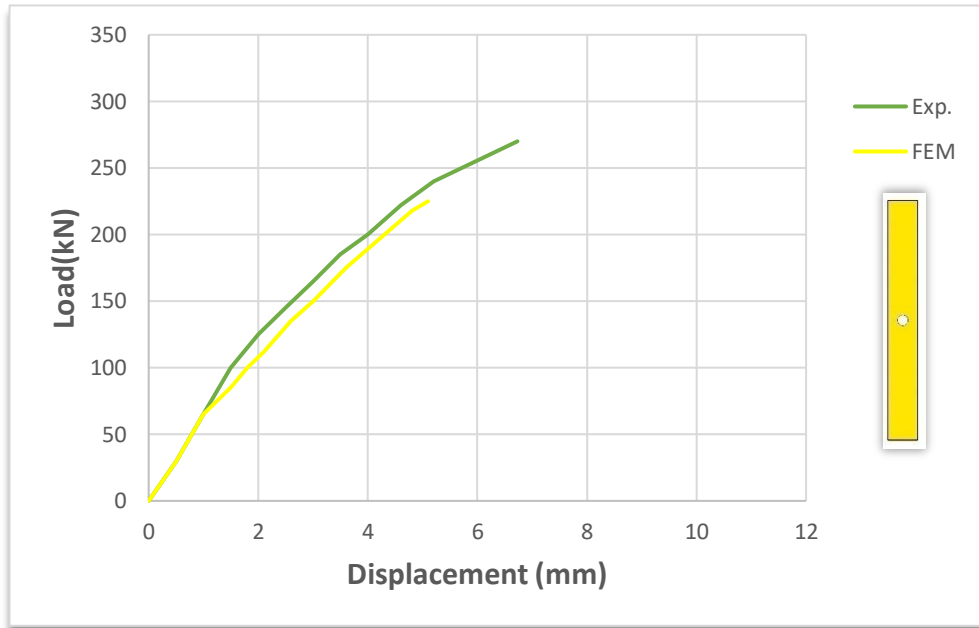
Cont.

Load-Displacement curve for (C1PC1F1R) column
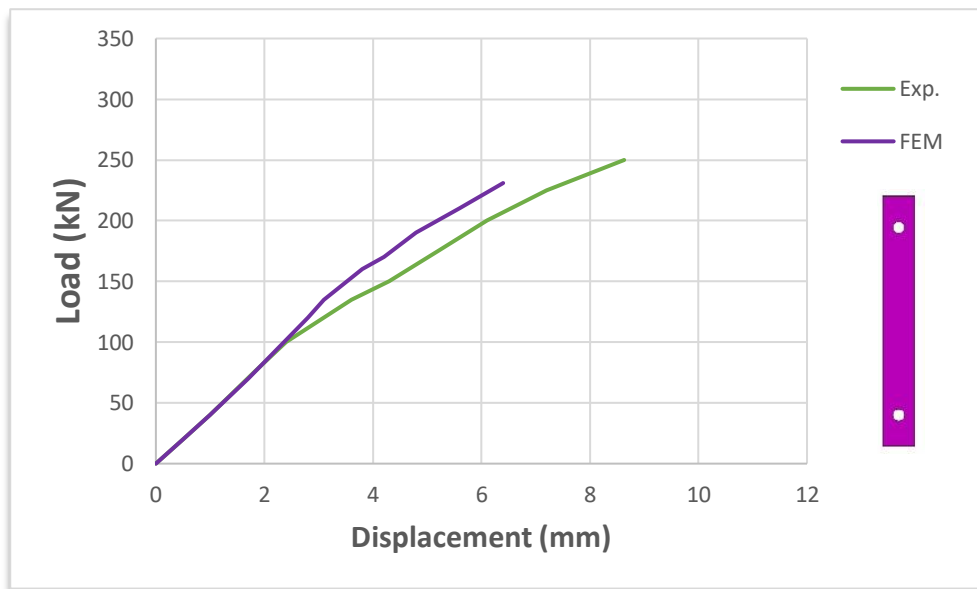
Load-Displacement curve for (C1PC2F2R) column

Cont.
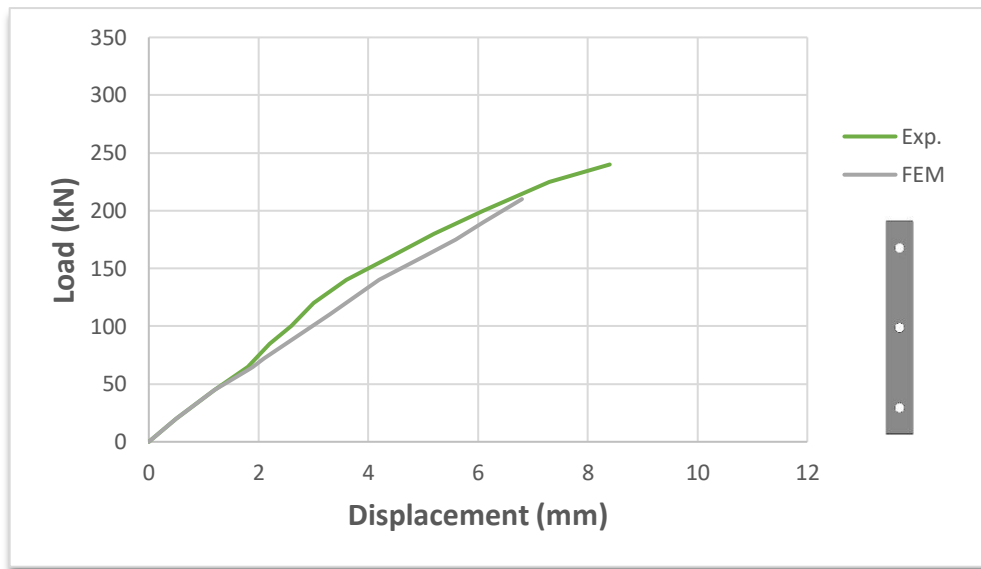
Load-Displacement curve for (C1PC3F3R) column
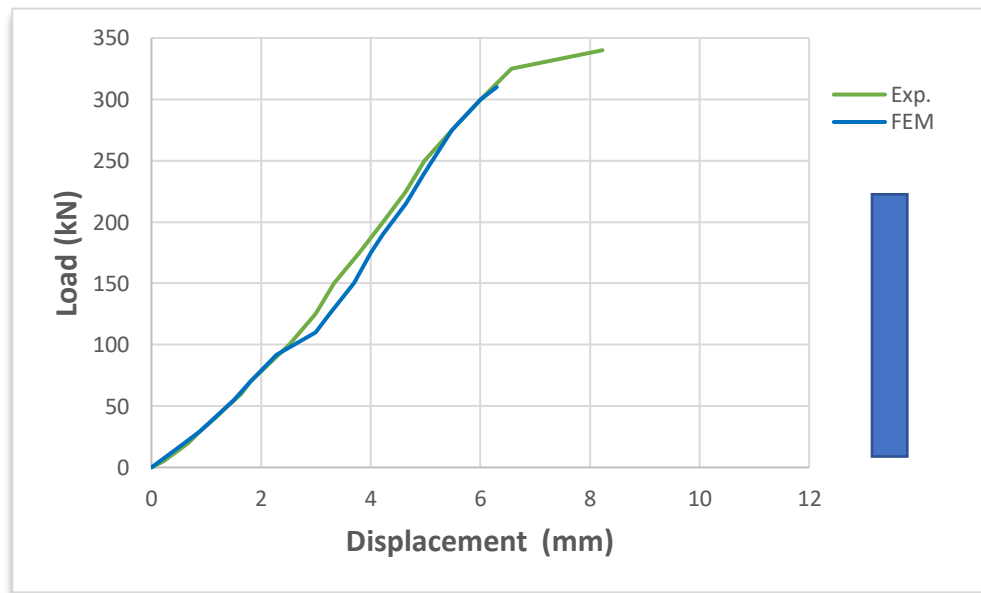
Load-Displacement curve for (C2FCS) column

Cont.
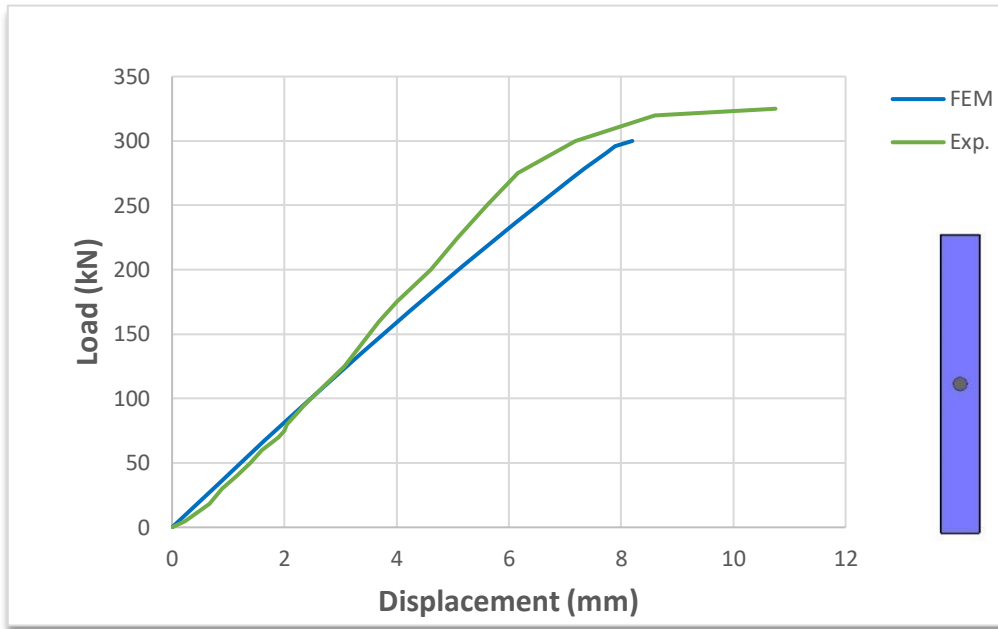
Load-Displacement curve for (C2FC1F) column
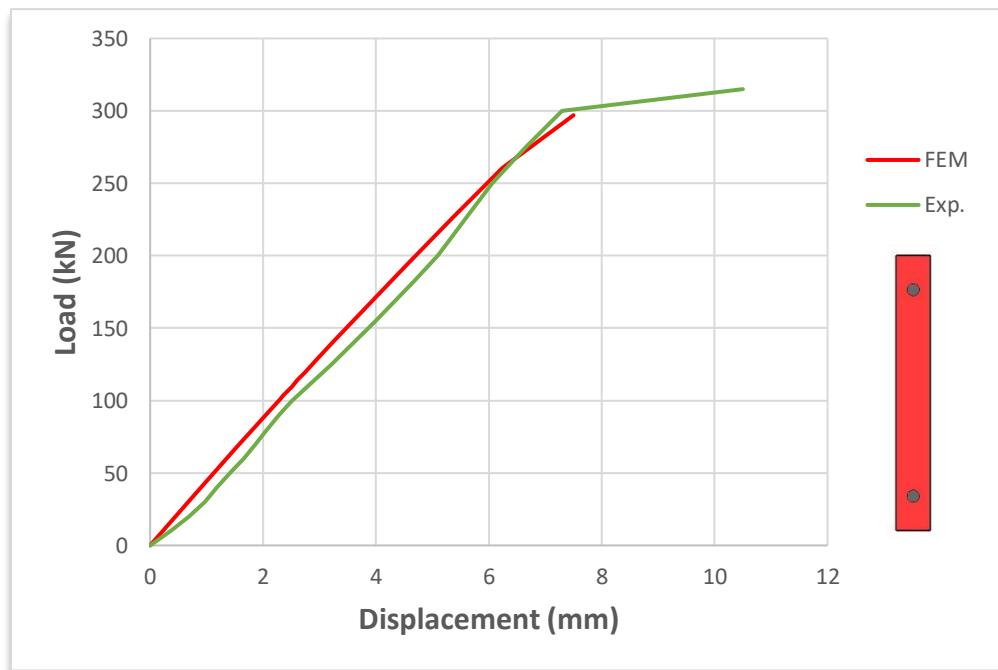
Load-Displacement curve for (C2FC2F) column

Cont.
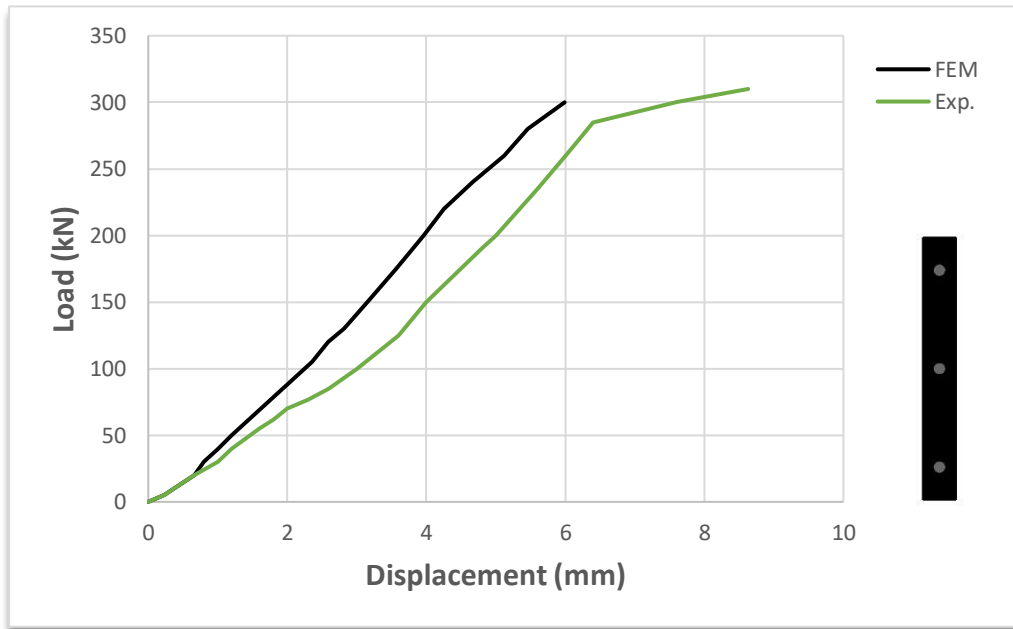
Load-Displacement curve for (C2FC3F) column
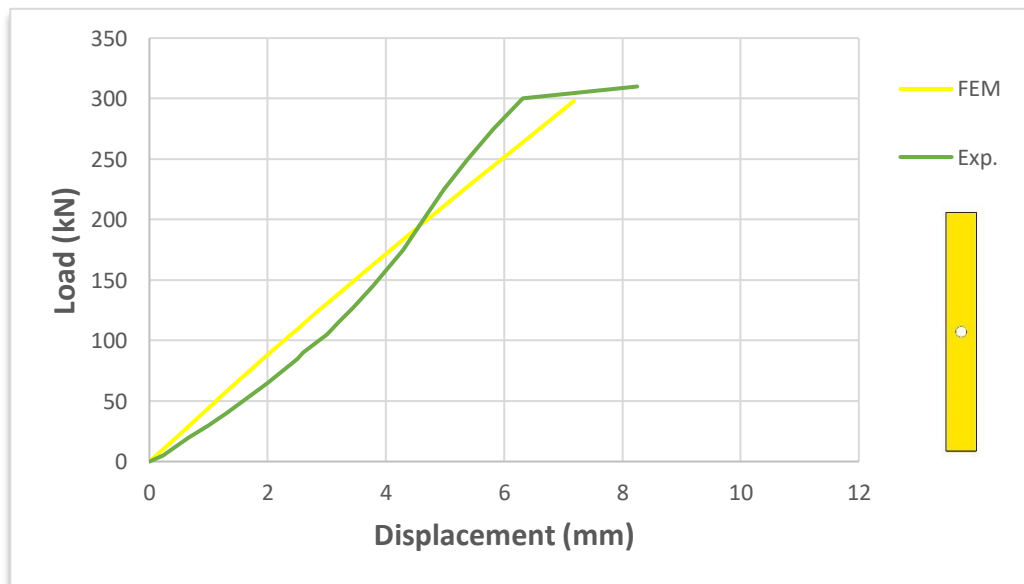
Load-Displacement curve for (G2FC ۲F1R) column
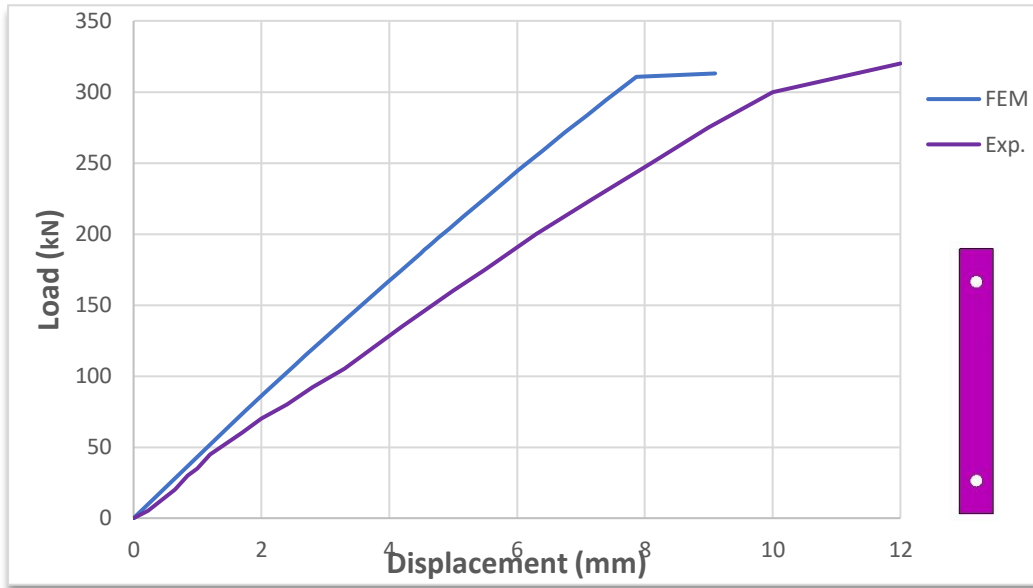
Load-Displacement curve for (C2FC2F2R) column
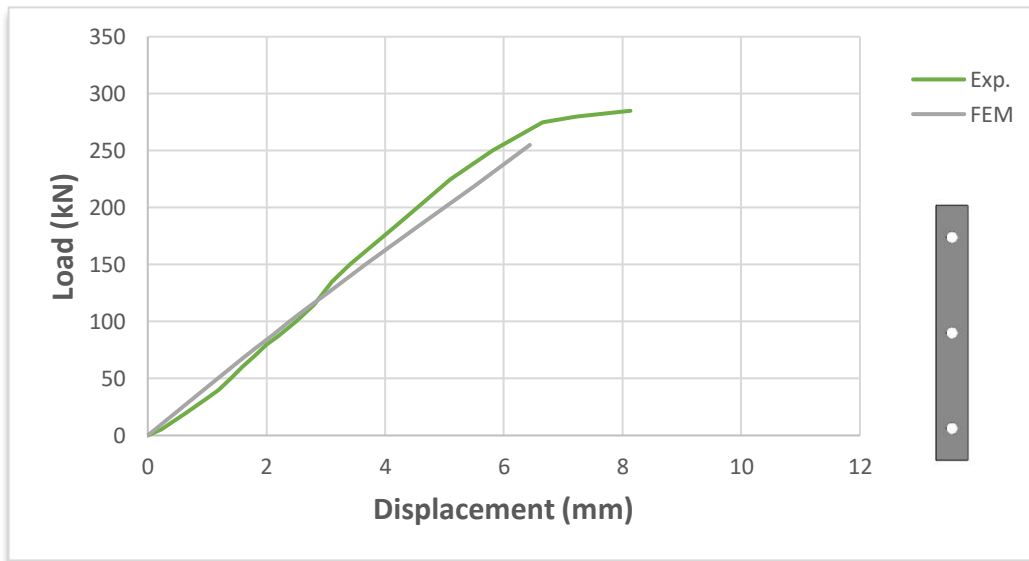
Load-Displacement curve for (C2FC3F3R) column

That most of the theoretical results are in agreement with the operation of the two tested models, but in the two (C2FC3F) (C2FC1F1R) models there was some difference from the previous models, due to the effect of the opening in the middle in these two models. This is the weakest part of the column and therefore some variation occurred.

5.5 Effect of Experimental Parametric Studies on Bearing Capacity Of (CFDST) Columns with Various Openings

This section of the study will discuss the impact of the following variables on the carrying capacity of the studied electronic models. These variables are:

1. Effect of the type of concrete filling.

2. Effect of the number of openings in the model.

3. Effect of whether the openings are from This section of the study will discuss the impact of the following variables on the carrying capacity of the studied electronic models. These variables are: one or two opposite sides in the study models.

5.5.1 Type of Concrete Filling

The properties of the normal concrete material as well as the properties of the plastic fiber concrete were entered into the Abaqus program. Table (5-٢) shows the results obtained from the Abaqus program using the method of finite element analysis.

The program results were close to the results obtained from the experimantal models, where the program rate was 20.25%. In comparison, in the experimantal models (the fourth chapter), it was 17.80%, which indicates the credibility of the results obtained using the program and its reliability in such barometric variables.

Table 5- 2: The difference between the results of the two types of concrete and the same tested models.

No. of specimen	Specimen name (FEM)	Ultimate load Pu (Kn)	Differ. P* (%)
1	C1PCS	295	+5.10%
	C2FCS	310	
2	C1PC1F	267	+12.35 %
	C2FC1F	300	
3	C1PC2F	260	+14.23%
	C2FC2F	297	
4	C1PC3F	240	+27.50%
	C2FC3F	306	
5	C1PC1F1R	237	+25.73%
	C2FC1F1R	298	
6	C1PC2F2R	231	+35.49%
	C2FC2F2R	313	
7	C1PC3F3R	210	+21.43%
	C2FC3F3R	255	

Difference P= ($\frac{PFC-NC}{NC}$)*100

Table (5-2) shows that plastic fiber concrete has increased the ultimate load by 5.1to 35.49 %.

5.5.2 The Number of Openings in The Concrete-Filled Double Skin Tube (CFDST)

In this numerical analysis program, two models were used. The first group used regular concrete, and the second used plastic fiber concrete; each column was compared with a column similar to the other type of concrete.

It was found from table (5-3) that the models of normal concrete columns analyzed in the program show that their load-bearing capacity decreases with the increase in the openings. This percentage ranged between -9.45 and -18.64% and an average of -13.33%. For the electronic models of the plastic fiber concrete columns, their performance was better in bearing capacity percentage ranged between -1.29 and -3.22% and an average of -2.90% for the plastic fiber concrete columns.

Through the results of the above program, it was found that these results were documented, good and acceptable with this type of barometric variable.

Table 5- 3: Effect of openings on bearing capacity (normal concrete columns and plastic fiber concrete columns)

Groupe name	Specimen name	Ultimate load Pu (Kn)	Differ. P** (%)
	Normal Concrete		
Group (1)	C1PCS	295	--------
	C1PC1F	267	-9.49%
	C1PC2F	260	-11.86%
	C1PC3F	240	-18.64%
Group (2)	C2FCS	310	------------
	C2FC1F	300	-3.22%
	C2FC2F	297	-4.20%
	C2FC3F	306	-1.29%

٥.٥.3 Number of Sides With Openings in Concrete-Filled Double Skin Tube (CFDST) (One Side or Two Opposite Sides)

Table (5-4) below shows the effect of the number of sides on which the openings are located (one side) on the load-bearing capacity of electronic models. The first group filled with normal concrete and the second group filled with plastic fiber concrete were used for

comparison with the standard column model for each concrete. It was noticed from the above table that the higher the number of openings, the lower the bearing capacity, and this ratio ranged between -09.49 and-18.64% and an average 13.33% for normal concrete columns, while it ranged between -01.29 and -03.22% and an average 2.90% plastic fiber concrete column models.

Table (5-5) below shows the same effect, but for two-sided openings, as it is noted from this table that the greater the number of openings, the lower the bearing capacity, and this percentage ranged between -19.66 and -28.81% and an average of 23.38% for normal concrete columns, while it ranged between -03.87 and plastic fiber concrete column models with a percentage of 17.74% and an average of 06.91%.

The results of electronic models of plastic fiber concrete columns were better than those of normal concrete. These results are considered good and acceptable for this type of barometric effect.

Table 5- 4: Effect of the number of openings in the examined column models on the bearing capacity of these columns(one side)

Groupe name	Specimen name	Ultimate load Pu (kN)	Differ. P (%)
	Normal Concrete		
	C1PCS	295	------
Group (1)	C1PC1F	267	-09.49%
	C1PC2F	260	-11.86%
	C1PC3F	240	-18.64%
	Plastic Fiber Concrete		
	C2FCS	310	------
Group (2)	C2FC1F	300	-3.22%
	C2FC2F	297	-4.20%
	C2FC3F	306	-01.29%

Table 5- 5: Effect of the number of openings in the examined column models on the bearing capacity of these columns(two side)

Groupe name	Specimen name	Ultimate load Pu (kN)	Differ. P (%)
	Normal Concrete		
Group (1)	C1PCS	295	------
	C1PC1F1R	237	-19.66%
	C1PC2F2R	231	-21.69%
	C1PC3F3R	210	-28.81%
	Plastic Fiber Concrete		
Group (2)	C2FCS	310	------
	C2FC1F1R	298	-3.87%
	C2FC2F2R	313	+0.97%
	C2FC3F3R	255	-17.74%

Chapter Six: Conclusions and Recommendations

Chapter Six

Conclusions and Recommendations

6.1 General

In this study, the effect of openings on (CFDST) columns was studied by studying the behavior of these columns when subjected to axial load. The program consists of manufacturing fourteen (CFDST) column models; These 14 models are divided into two parts:

• The first group consists of seven columns (CFDST) filled with normal concrete.

• The second group consists of seven columns (CFDST) filled with plastic fibres concrete.

The dimensions of the 14 models are all equal and were of dimensions (100 * 100) mm and length (800) mm to facilitate the examination process.

This study showed several important engineering properties of CFDST columns. Based on the tests performed on CFDST columns and the results obtained from these tests, several points can deduce shown below.

6.2 Conclusions

The most important points that were concluded in this study can be abstract as follows:

1- The predominant characteristic of failure in all examined samples was local buckling. Samples with normal concrete showed a more pronounced external buckling, especially in the area of the openings.

2- The models of columns filled with plastic fiber concrete showed an increase in bearing capacity than that of normal concrete models, and this increase ranged from 14.03% -28.00%. This difference in bearing capacity means that (PFC) effectively increases the bearing capacity of columns (CFDST), and tubular columns filled with plastic fiber concrete can achieve high compressive potential but are very brittle after crossing the maximum load.

3- The final results of the tested column models showed that the final capacity of the column models (CFDST) decreases with the increase in the number of openings in these models. The final capacity is higher in the tested column models where the openings are on one side of them when the openings are on two sides, whether for laboratory or electronic models.

4- The failure of the tested column models is of the type of local deflection in all models, with the difference that such inflection occurs on one or several sides.

6.3 Recommendation for Future Studies

1- It is necessary to study the effect of other types of concrete with high compressive strength (60,70,80 MPa) and compare it with plastic fiber concrete and its effect on the bearing capacity of CFDST columns.

2- Studying the effect of the percentages of plastic fibers in the concrete mixture and their effect on the bearing capacity of CFDST columns.

3- Conducting additional studies showing the advantages and disadvantages of CFDST columns in terms of manufacturing and installation.

4- It is recommended that further tests be carried out on CFDST columns using multiple thicknesses of steel tubes and their effect on the bearing capacity of CFDST columns containing openings.

5-It is recommended to conduct more tests on CFDST columns using openings of different diameters and shapes and their effect on the bearing capacity of the load in this type of column.

6-Conducting more tests on the mid-column area, as it is the most dangerous area, using openings of different diameters, and measuring the effect of this on the bearing capacity of the column.

7-Conducting research on the age of structures built with these structural elements compared to their counterparts of ordinary concrete structures

References

Ahmed, M., Liang, Q. Q., Patel, V. I., & Hadi, M. N. (2020). Experimental and numerical investigations of eccentrically loaded rectangular concrete-filled double steel tubular columns. *Journal of Constructional Steel Research*, *167*, 105949.

Alhalaby, M., & Wang, Y. (2017). 18.05: Second-order effects of cantilever concrete filled double skin tube (CFDST) transmission towers. *ce/papers*, *1*(2-3), 4390-4399.

Ayough, P., Sulong, N. R., Ibrahim, Z., & Hsiao, P.-C. (2020). Nonlinear analysis of square concrete-filled double-skin steel tubular columns under axial compression. *Engineering Structures*, *216*, 110678.

Bhatia, S., & Tiwary, A. K. (2022). Analytical Behavior of Concrete-Filled Single-Skin and Double-Skin Tube Columns Subjected to Axial Loading. In *Advances in Construction Materials and Sustainable Environment* (pp. 809-821). Springer.

Cai, J., Pan, J., & Li, X. (2018). Behavior of ECC-encased CFST columns under axial compression. *Engineering Structures*, *171*, 1-9.

Ci, J., Jia, H., Ahmed, M., Chen, S., Zhou, D., & Hou, L. (2021). Experimental and numerical analysis of circular concrete-filled double steel tubular stub columns with inner square hollow section. *Engineering Structures*, *227*, 111400.

Dey, P., Gupta, R., & Laskar, A. (2019). Numerical and experimental investigations of different cross-sectional configuration of plain concrete and CFST short columns under axial compression. *International Journal of Civil Engineering*, *17*(10), 1585-1601.

Ekmekyapar, T., & Hasan, H. G. (2019). The influence of the inner steel tube on the compression behaviour of the concrete filled double skin steel tube (CFDST) columns. *Marine Structures*, *66*, 197-212.

Fang, Y., Wang, Y., Hou, C., & Lu, B. (2020). CFDST stub columns with galvanized corrugated steel tubes: Concept and axial behaviour. *Thin-Walled Structures*, *157*, 107116.

Farajpourbonab, E. (2017). Effective parameters on the behavior of CFDST columns. *Journal of Applied Engineering Science*, *15*(1).

Gupta, A., Mohan, R., Bisht, H., & Sharma, A. (2022). Experimental testing and numerical modelling of CFST columns under axial compressive load. *Asian Journal of Civil Engineering*, *23*(3), 415-424.

Han, L.-H., Lam, D., & Nethercot, D. A. (2018). *Design guide for concrete-filled double skin steel tubular structures*. CRC Press.

Han, L.-H., Li, W., & Bjorhovde, R. (2014). Developments and advanced applications of concrete-filled steel tubular (CFST) structures: Members. *Journal of Constructional Steel Research*, *100*, 211-228.

Han, L.-H., Ma, D.-Y., & Zhou, K. (2018). Concrete-encased CFST structures: behaviour and application. Proceedings of the 12th International Conference on Advances in Steel-Concrete Composite Structures. ASCCS 2018,

Hassan, A., & Bhat, J. A. (2021). Behaviour of CFDST and RCC member hybrid frames. *Asian Journal of Civil Engineering*, *22*(6), 1045-1058.

Hassanein, M., Elchalakani, M., Karrech, A., Patel, V., & Yang, B. (2018). Behaviour of concrete-filled double-skin short columns under compression through finite element modelling: SHS outer and SHS inner tubes. Structures,

Hossain, K., & Chu, K. (2019). Confinement of six different concretes in CFST columns having different shapes and slenderness. *International Journal of Advanced Structural Engineering*, *11*(2), 255-270.

Huang, H., Han, L.-H., Tao, Z., & Zhao, X.-L. (2010). Analytical behaviour of concrete-filled double skin steel tubular (CFDST) stub columns. *Journal of Constructional Steel Research*, *66*(4), 542-555.

Ibanez, C., Hernández-Figueirido, D., & Piquer, A. (2021). Effect of steel tube thickness on the behaviour of CFST columns: Experimental tests and design assessment. *Engineering Structures*, *230*, 111687.

Imani, R., Mosqueda, G., & Bruneau, M. (2015). Experimental study on post-earthquake fire resistance of ductile concrete-filled double-skin tube columns. *J. Struct. Eng*, *141*(8), 04014192.

Ipek, S., & Güneyisi, E. (2019). Ultimate axial strength of concrete-filled double skin steel tubular column sections. *Advances in Civil Engineering*, *2019*.

Ipek, S., & Guneyisi, E. M. (2021). Nonlinear analysis of concrete-filled single and double skin steel tubular tapered columns under axial loading. *Smart Structures and Systems*, *27*(4), 571-592.

Kalemi, B. (2016). Numerical modeling and assessment of circular concrete-filled steel tubular members. *Master in Science Thesis. Istituto Universitario di Studi Superiori di Pavia*.

Kim, S.-E., Papazafeiropoulos, G., Truong, V.-H., Nguyen, P.-C., Kong, Z., Duong, N.-T., Pham, V.-T., & Vu, Q.-V. (2021). Finite element simulation of normal–Strength CFDST members with shear connectors under bending loading. *Engineering Structures*, *238*, 112011.

Kothari, S., Singh, D. K., & Chamoli, P. (2022). Comparative Analysis of CFST Columns and RC Columns Under Uniaxial Compressive Loads. In *Smart Technologies for Energy, Environment and Sustainable Development, Vol 2* (pp. 135-144). Springer.

Li, N., Lu, Y., Li, S., & Gao, D. (2020). Axial compressive behaviour of steel fibre reinforced self-stressing and self-compacting concrete-filled steel tube columns. *Engineering Structures*, *222*, 111108.

Li, W., Han, L.-H., & Chan, T.-M. (2014). Tensile behaviour of concrete-filled double-skin steel tubular members. *Journal of Constructional Steel Research*, *99*, 35-46.

Li, X. H., Lei, J. P., & Wang, R. (2013). Finite element analysis of concrete-filled double skin steel tubes with simply supported under lateral impact. Applied Mechanics and Materials,

Nguyen, T.-T., Thai, H.-T., Ngo, T., Uy, B., & Li, D. (2021). Behaviour and design of high strength CFST columns with slender sections. *Journal of Constructional Steel Research*, *182*, 106645.

Ou, Z. J. (2013). The practice of concrete filled steel tube piers to bridges: A review. *Applied Mechanics and Materials*, *405*, 1602-1605.

Ouyang, Y., & Kwan, A. (2018a). Finite element analysis of square concrete-filled steel tube (CFST) columns under axial compressive load. *Engineering Structures*, *156*, 443-459.

Ouyang, Y., & Kwan, A. (2018b). Use of analytical lateral-axial strain relation in FE analysis of axially loaded rectangular CFST columns. *Engineering Structures*, *166*, 142-151.

Punshi, V. D. (2003). *Non-linear analysis of circular FRP-confined concrete columns using finite element methods*.

Qian, W.-W., Li, W., Han, L.-H., & Zhao, X.-L. (2016). Analytical behavior of concrete-encased CFST columns under cyclic lateral loading. *Journal of Constructional Steel Research*, *120*, 206-220.

Rabbat, B., & Russell, H. (1985). Friction coefficient of steel on concrete or grout. *Journal of Structural Engineering*, *111*(3), 505-515.

Salim, N. M., & Al-Khekany, A. M. (2021). Effect of geometrical properties on slenderness ratio of concrete filled multi-skins steel tube column. Journal of Physics: Conference Series,

Wang, Y., Chen, P., Liu, C., & Zhang, Y. (2017). Size effect of circular concrete-filled steel tubular short columns subjected to axial compression. *Thin-Walled Structures*, *120*, 397-407.

Wang, Y., Yang, L., Yang, H., & Liu, C. (2019). Behaviour of concrete-filled corrugated steel tubes under axial compression. *Engineering Structures*, *183*, 475-495.

Wang, Z.-B., Tao, Z., Han, L.-H., Uy, B., Lam, D., & Kang, W.-H. (2017). Strength, stiffness and ductility of concrete-filled steel columns under axial compression. *Engineering Structures*, *135*, 209-221.

Witteck, D., Winkler, R., & Knobloch, M. (2022). Experimental Investigation of Concrete-Filled Double Steel Tube Columns (CFDST) with High Performance Materials Under Monotonic and Cyclic Loading. International Conference on the Behaviour of Steel Structures in Seismic Areas,

Xiong, Q., Chen, Z., Zhang, W., Du, Y., Zhou, T., & Kang, J. (2017). Compressive behaviour and design of L-shaped columns fabricated using concrete-filled steel tubes. *Engineering Structures*, *152*, 758-770.

Yan, X.-F., Zhao, Y.-G., & Lin, S. (2021). Compressive behaviour of circular CFDST short columns with high-and ultrahigh-strength concrete. *Thin-Walled Structures*, *164*, 107898.

Yan, Y., Liang, H., Lu, Y., & Huang, Y. (2021). Behaviour of concrete-filled steel-tube columns strengthened with high-strength CFRP textile grid-reinforced high-ductility engineered cementitious composites. *Construction and Building Materials*, *269*, 121283.

Yang, B., Wang, W., Yang, L., Sun, G., & Liu, S. (2020). Study on Stressing State and Failure Criterion of Concrete-Filled Stainless Steel and Steel Tubular Column. *Advances in Civil Engineering*, *2020*.

Yang, Y.-F., Fu, F., Bie, X.-M., & Dai, X.-H. (2021). Axial compressive behaviour of CFDST stub columns with large void ratio. *Journal of Constructional Steel Research*, *186*, 106892.

Zhang, S., Li, X., Chen, X., & Chen, J. (2022). Behavior of circular-steel-tube-confined square CFST short columns under axial compression. *Journal of Building Engineering*, *51*, 104372.

Zhang, T., Lyu, X., Liu, H., Zhang, L., Wang, J., & Gao, S. (2020). Axial performance degradation of squared CFST stubs in severe cold and acid rain area. *Construction and Building Materials*, *262*, 120612.

Appendix –A:Materials properties

Appendix –A

Materials properties

A.1 Properties of Cement

Table (A-1) Cement's Test Results

Chemical Specifications	Result	Boundary according to IQS No. 5/1984	
		Ordinary	Resistant to Sulphate
(1) CaO (%)	62.02	—-	
(2) SiO_2 (%)	22.05	—-	
(3) Al_2O_3 (%)	4.56	—-	
(4) Fe_2O_3 (%)	4.7	—-	
(5) MgO (%)	2.6	<5%	
(6) SO_3 (%)			
- If C_3A < 5%	2.16	< 2.5%	
- If $C3A$ > 5%	...	< 2.8%	< 2.5%
(7) Ignition's Loss (%)	2.86	<4%	
The residue of Insoluble (%)	1.35	< 1.5%	
L.S.F.	0.852	0.66 -1.02	
C_3S (%)	35.88	—-	—-
C_2S (%)	38.1	—-	—-
C_3A (%)	1.853	—-	—-

C4AF (%)	14.302	—-	—-
Total = (1+2+3+4+5+6+7)	99.44	—-	—-
Physical Properties	**Test Result**	**Limit according to IQS No. 5/1984**	
Setting Time - Initial setting time (min) - Final setting time (hrs)	95 4.92	≥ 45 min < 10 hrs.	
Fineness (%)	5	...	
Compressive Strength (MPa) - 3 days - 7 days	17.73 31.6	> 15 MPa > 23 MPa	

A.2 Properties of Fine Aggregate

Table (A-2-1) Grading of Fine Aggregate Used Throughout This Work

Sieve size (mm)	Passing (%)	Limit according to IQS No. 45M984 Zone (2)
10	100	100
4.75	92.6	90 -100
2.36	76.3	75 -100
1.18	64.7	55-90
0.6	37.6	35- 59
0.3	21.8	8-30

Sieve size (mm)	Passing (%)	Limit according to IQS No. 45M984 Zone (2)
0.15	4.7	0-10
SO3	0.27	< 0.5 %

Table (A-2-2) Physical Properties of Fine Aggregate

Physical properties	Test results	Limits of Iraqi specification No.45/1984
Specific gravity	2.64	—
Fineness modulus	3.04	—
Sulfate content %	0.10	<0.5
Absorption %	0.77	—

A.3 Properties of Coarse Aggregate

Table (A-3-1) Grading of Crushed Aggregate Used Throughout This Work

Sieve size (mm)	Passing (%)	Limit according to IQS No. 45\1984 Zone (3) (5 -14) mm
37.5	100	------------
20	100	100
14	100	90 -100
10	79.6	50-80
5	9.5	0-10
2.36	0.5	0-5
SO3	0.39	< 0.5 %

Table (A-3-2) Physical Properties of Coarse Aggregate

Physical properties	Test results	Limits of Iraqi specification No.45/1984
Specific gravity	2.66	—
Sulfate content %	0.04%	<0.1
Absorption %	0.06%	< 3%
Clay content	0.2%	< 2%

Appendix(B): Material properties in finite element models

Appendix(B)

Material properties in finite element models

B.1 Introduction

The current work examines the structural behavior of CFDST columns with axial load using the finite element method using Abaqus program 2019.

Abaqus is a suite of powerful engineering simulation software based on the finite element method that can solve problems ranging from relatively simple linear analyzes to the most challenging nonlinear simulation.

In Abaqus, there are three constitutive models for defining the inelastic behaviour of concrete, including the concrete smeared cracking model (CSCM) in Abaqus/Standard, concrete damaged plasticity (CDP) model in both Abaqus/Standard and Abaqus/Explicit and brittle cracking concrete (BCC) model in Abaqus/Explicit.

During the modelling of specimens, the concrete material models, and material parameters were discussed in detail.

The following paragraphs describe the program's inputs for the materials used in the models of this study.

As for the modulus of elasticity (Ec) for concrete, it was calculated according to the American code ACI and according to the equation:

$$\mathbf{E}c=4700 \sqrt{Fc'} \qquad \text{--} \quad \text{Eq.(B-1)}$$

B.2 Concrete Damage Plasticity Definition

The CDP model requires defining five parameters to solve the Drucker-Prager plastic; These parameters include shape factor, eccentricity, bi-axial compressive stress ratio, dilation angle, and viscosity. The shape of the state of stress utilized in

the CDP model is represented as a three-dimensional cone. The states of stress corresponding to material failure are located on the surface of the cone, and the states of stress corresponding to safe material behavior are located inside the cone.

1-Kc: The Drucker-Prager strength hypothesis assumed that the cross-section of the failure cone is a circle Figure (B.1). However, the crosssection of the cone was not an actual circle but rather defined by a shape factor, K Figure (B.2). The K factor is the ratio of the distances between the hydrostatic axis, the compression meridian, and the tension meridian. This factor expresses the shape of the yield surface in the deviatory plane. The default value is 2/3.

Figure (B-1): Drucker-Prager boundary surface
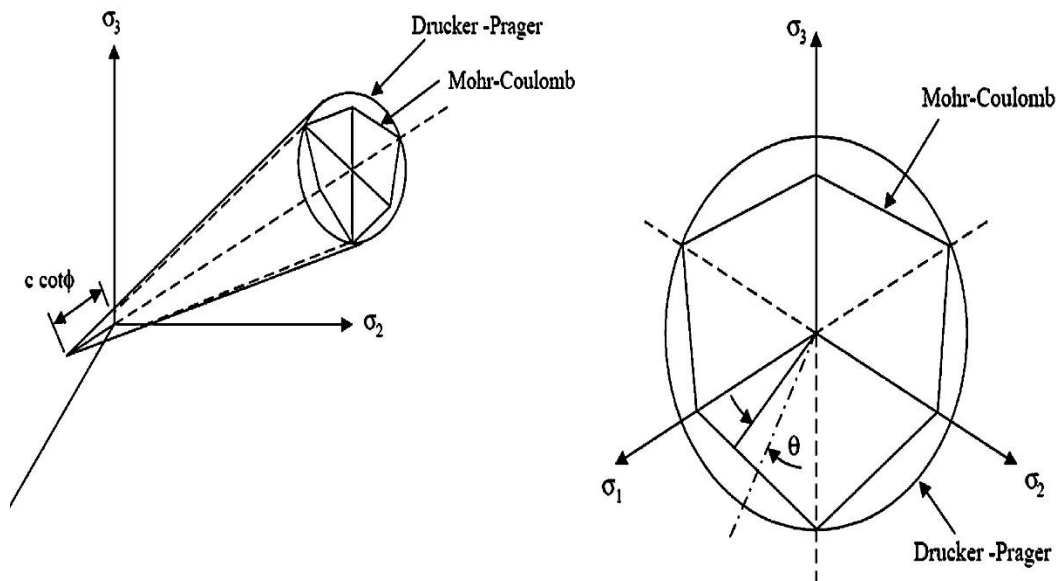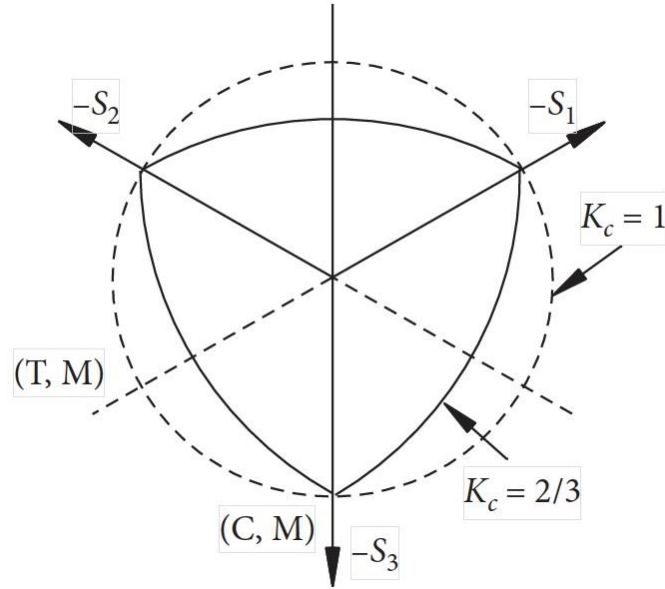
Figure (B-2): Deviatoric cross-section of failure surface in CDP model

2-Eccentricity: The shape of the compression and tension meridians is not constant but rather assumes the form of a hyperbola. The rate of change of these meridians to their asymptote is known as eccentricity. Figure (B.3)The default value in Abaqus
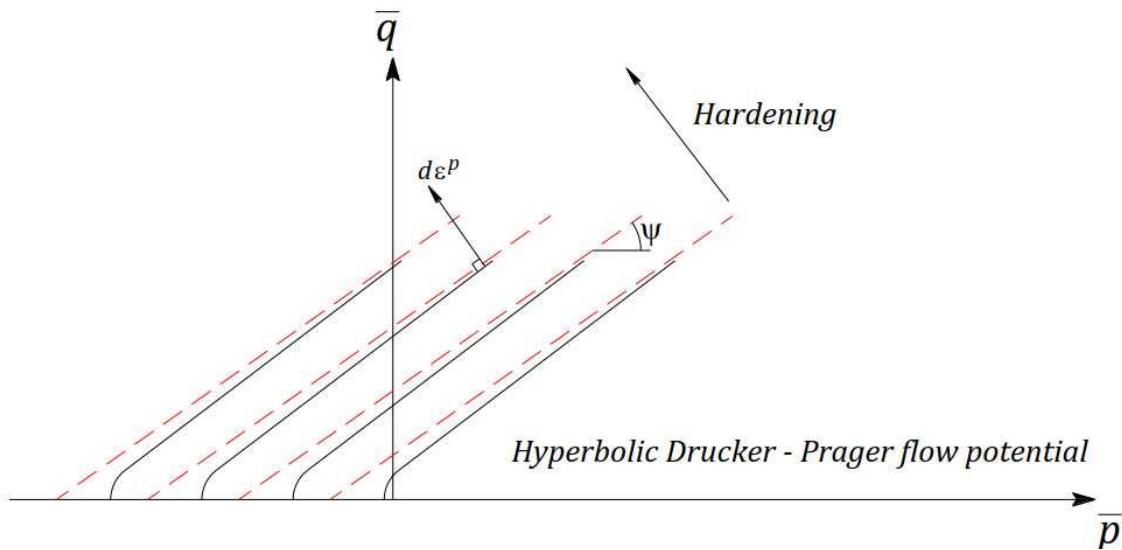

Figure (B-3): Hyperbolic Plastic Flow Rule

3-fb0/fc0: the uniaxial concrete compressive strength ratio to its tensile strength. To fully define the Drucker-Prager yield function, the ratio of biaxial compressive stress to uniaxial compressive stress needs to be expressed. The default value is 1.16.

4-E: is the dilation angle, measured in a p-q plane and should be defined to calculate the inclination of the plastic flow potential in high confining pressures, Figure (B.3).The dilation angle is equal to the friction angle in low stresses. The maximum value is ψ max $= 56.3°$, and the minimum value is close to $0°$. Upper values represent a more ductile behavior, and lower values show a more brittle behavior. In this study, its value was assumed to be $36°$.

5-μ: is viscosity parameter, used for the visco-plastic regularization of the concrete constitutive equations in ABAQUS/Standard analysess.This parameter is ignored in ABAQUS/Explicit. The default value is 0.0.

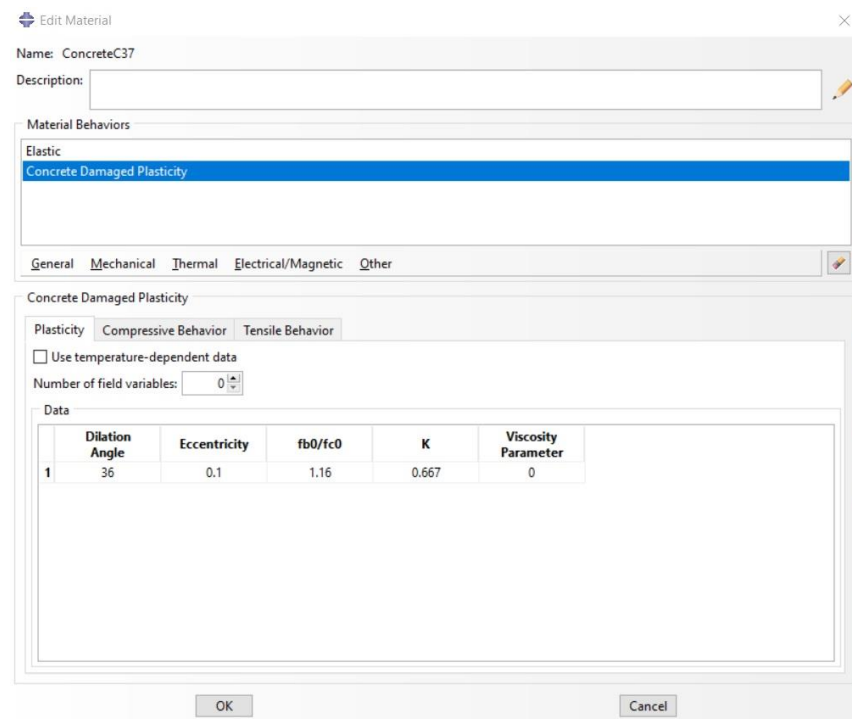Figure (B-4) shows the inclusion of the above point values in the Abaqus program

Figure (B-4): Values CDP entered

B.3 Enter The Properties of The Materials Used in This Study

Table (B-1) elastic properties of concrete

Normal Concrete

Compressive strength (MPa)	Young's modulus (MPa)	Poisson's ratio
36.95	26000	٠,١٨

Plastic Fiber concrete

Compressive strength (MPa)	Young's modulus (MPa)	Poisson's ratio
39.66	٢٨587	٠,١٨

Table (B-2) Plastic properties of concrete (NC&PFC)

Dilation angle	Eccentricity	Fb0/fc0	K	parameter Viscosity
50	0.1	0.16	2/3	0

Table (B-3-1) Stress-displacement relationship

(Tensile behavior of normal concrete specimens)

Yielding stress	*Cracking strain*
2.390981781	*0*
1.717787005	*0.000121899*
1.436950518	*0.000231035*
1.270651607	*0.000336445*
1.156726844	*0.000440151*
1.072054713	*0.000542905*
0.906917121	*0.000848277*
0.80629908	*0.00115155*
0.736339159	*0.001453826*
0.683865334	*0.001755533*

Table (B-3-2) Stress-displacement relationship

(Tensile behavior of plastic fiber concrete specimens)

Yielding stress	*Cracking strain*
2.56496392	*0*
1.86200964	*0.000122333*
1.562204275	*0.000231858*
1.383342594	*0.000337541*
1.260341119	*0.000441448*
1.168708264	*0.00054436*
0.989546167	*0.000850052*
0.880138456	*0.001153528*
0.803976821	*0.001455947*
0.746809205	*0.001757764*

Table (B-4-1) stress-Strain Relationship

(Compressive behaviour of normal concrete specimens)

Yielding stress	*Inelastic strain*
6.350228546	*0*
11.83811268	*3.63234E-05*
16.51929328	*9.47536E-05*
20.44472521	*0.000177768*
23.66116043	*0.000283847*
26.21157263	*0.000411592*
28.13553129	*0.000559715*

29.46953226	*0.00072703*
30.2472905	*0.000912439*
30.5000	*0.001114928*
30.36861148	*0.001273623*
29.98145376	*0.001440638*
29.34862363	*0.001615645*
28.47969331	*0.001798332*
27.38374415	*0.001988404*

Table (B-4- ٢) stress-Strain Relationship

(Compressive behaviour of plastic fiber concrete specimens)

Yielding stress	*Inelastic strain*
6.678839484	*0*
12.5163345	*3.27692E-05*
17.54994462	*8.80585E-05*
21.81493819	*0.000167767*
25.34455018	*0.000270839*
28.17012671	*0.000396279*
30.32125731	*0.000543146*
31.82589629	*0.000710552*
32.71047414	*0.000897658*
33.00000000	*0.001103669*
32.86685288	*0.001255509*
32.47223379	*0.001415656*
31.82318144	*0.001583887*
30.92648415	*0.001759985*
29.78869085	*0.001943743*

Table (B5) Plastic properties of steel materials

Stress	Strain
٣٧٥	0
٤٢٥	٠,٢

الخلاصة

أدى التطور في تصميمات المنشآت وزيادة ارتفاعاتها إلى الحاجة في تطوير علم البناء لمواكبة هذا التطور. تعتبر الأعمدة الأنبوبية المزدوجة المملوءة بالخرسانة (CFDST) مثالاً على هذا التطور في العشرين عامًا الماضية.

تتمتع أعمدة CFDST بالعديد من المزايا ، مثل قدرة التحمل العالية (أعلى من تلك الموجودة في أعمدة الخرسانة المسلحة (RCC)) بالإضافة إلى مقاومة أعلى للحريق وسرعة في الإنجاز.

في هذا البحث تم أخذ العوامل التالية بعين الاعتبار: نوع الخرسانة المستخدمة في هذا النوع من الأعمدة ، هل هي خرسانة العادية (NC) ام خرسانة الياف بلاستيكية (PFC) ،وعدد الفتحات في نموذج واحد ، وما إذا كانت هذه الفتحات من جانب واحد أو جانبين متقابلين.

تم عمل (١٤) نموذجًا ، (٧) نماذج منها تكون مملوءة بالخرسانة العادية و (٧) نماذج بخرسانة ألالياف البلاستيكية وتقارن النتائج العملية لـ (١٤) نموذجًا مع نتائج نماذج العناصر المحدودة المماثلة التي تم الحصول عليها من برنامج Abaqus للتأكد من دقتها.

ان خصائص الخرسانة العادية وخرسانة الألياف البلاستيكية ضرورية للدراسة العددية لتوفير ظروف عمل مماثلة للمختبرات.

تم اختبار نماذج الأعمدة باستخدام الحمل المركزي ، حيث تم تطبيق الحمل المحوري بشكل تدريجي.

من خلال نتائج الاختبارات تبين أن استخدام (PFC) يعطي نتائج تحمل أعلى للعمود من استخدام (NC) وكان معدل الزيادة هو(٬۱۷،۸۰) ، كما تبين انه كلما زاد عدد الفتحات في العمود من جانب واحد تقل قدرة تحمل العمود وتتراوح النسبة بين (٬۱٤،۰۳ - ۱۹،۲۳).

علاوة على ذلك ، فان الفتحات نافذة من جهتين متقابلتين يمكن ان يضعف الأعمدة بنسبة تتراوح بين (٬۱٤،۸۱ الى ٬۲۸،۰۰).

عند استخدام العناصر المحددة كانت النتائج أقل من تلك الموجودة في الدراسة التجريبية حيث تراوحت النسبة في النماذج الخرسانية العادية (٬۰-۱۲،۲۲) بينما كانت في خرسانة الألياف البلاستيكية (٬۱،۲۹-۱۰،۵۲). كانت نتائج الدراسة العددية جيدة ومقبولة وقريبة من نتائج البحث التجريبي. لذلك من الممكن الاعتماد على العناصر المحددة لتشكيل نماذج أكثر تعقيدًا.

جمهورية العراق

وزارة التعليم العالي و البحث العلمي

جامعة كربلاء

كلية الهندسة

قسم الهندسة المدنية

سلوك العمود الفولاذي المزدوج المقطع ذو الثقوب تحت التحميل المركزي

رسالة مقدمة الى مجلس كلية الهندسة / جامعة كربلاء وهي جزء من متطلبات نيل درجة الماجستير

في علوم الهندسة المدنية

كتبت بواسطة:

ليث غانم مهدي

(بكالوريوس في الهندسة المدنية ـ الجامعة التكنولوجية ـ ٢٠٠١)

باشراف :

أ..د .سجاد عامر حمزه

<table>
<tr><td>رجب ـ ١٤٤٣</td><td>شباط ـ ٢٠٢٢</td></tr>
</table>